Functional role and top-down control of alpha oscillations

Maxime Ferez

THESE de DOCTORAT
DE L'UNIVERSITE CLAUDE BERNARD LYON 1

Ecole Doctorale N° 476 - NSCO
ECOLE DOCTORALE NEUROSCIENCE ET COGNITION

Discipline :
Neurosciences

Soutenue publiquement le 27/10/2022, par :
Maxime Ferez

ROLE FONCTIONNEL ET TOP-DOWN CONTROLE DES OSCILLATIONS ALPHA
/
FUNCTIONAL ROLE AND TOP-DOWN CONTROL OF ALPHA OSCILLATIONS

Devant le jury composé de :

Présidente : George Nathalie

Bénar Christian, Directeur de recherche, INSERM Marseille	Rapporteur
George Nathalie, Directrice de recherche, CNRS Paris	Rapporteure et présidente
Cristofori Irene, Maître de conférences HDR, Université de Lyon	Examinatrice
Vidal Juan R., Enseignant Chercheur, Université catholique de Lyon	Examinateur
Bertrand Olivier, Directeur de recherche, INSERM Lyon	Directeur de thèse
Bonnefond Mathilde, Chargée de recherche, INSERM	Co-directrice de thèse

Université Claude Bernard – LYON 1

Président de l'Université	M. Frédéric FLEURY
Président du Conseil Académique	M. Hamda BEN HADID
Vice-Président du Conseil d'Administration	M. Didier REVEL
Vice-Président du Conseil des Etudes et de la Vie Universitaire	Mme Céline BROCHIER
Vice-Président de la Commission de Recherche	M. Petru MIRONESCU
Directeur Général des Services	M. Pierre ROLLAND

COMPOSANTES SANTE

Département de Formation et Centre de Recherche en Biologie Humaine	Directrice : Mme Anne-Marie SCHOTT
Faculté d'Odontologie	Doyenne : Mme Dominique SEUX
Faculté de Médecine et Maïeutique Lyon Sud - Charles Mérieux	Doyenne : Mme Carole BURILLON
Faculté de Médecine Lyon-Est	Doyen : M. Gilles RODE
Institut des Sciences et Techniques de la Réadaptation (ISTR)	Directeur : M. Xavier PERROT
Institut des Sciences Pharmaceutiques et Biologiques (ISBP)	Directeur : M. Claude DUSSART

COMPOSANTES & DEPARTEMENTS DE SCIENCES & TECHNOLOGIE

Département Génie Electrique et des Procédés (GEP)	Directrice : Mme Rosaria FERRIGNO
Département Informatique	Directeur : M. Behzad SHARIAT
Département Mécanique	Directeur M. Marc BUFFAT
Ecole Supérieure de Chimie, Physique, Electronique (CPE Lyon)	Directeur : Gérard PIGNAULT
Institut de Science Financière et d'Assurances (ISFA)	Directeur : M. Nicolas LEBOISNE
Institut National du Professorat et de l'Education	Directeur : M. Pierre CHAREYRON
Institut Universitaire de Technologie de Lyon 1	Directeur : M. Christophe VITON
Observatoire de Lyon	Directrice : Mme Isabelle DANIEL
Polytechnique Lyon	Directeur : Emmanuel PERRIN
UFR Biosciences	Administratrice provisoire : Mme Kathrin GIESELER
UFR des Sciences et Techniques des Activités Physiques et Sportives (STAPS)	Directeur : M. Yannick VANPOULLE
UFR Faculté des Sciences	Directeur : M. Bruno ANDRIOLETTI

Table of contents

Remerciements

Je tiens à exprimer ma gratitude aux membres de mon jury. Merci à Nathalie George et Christian Bénar d'avoir accepté d'examiner ma thèse. Je remercie également Irène Cristofori et Juan R. Vidal d'avoir accepté d'être présents lors de la soutenance. Votre avis d'expert est essentiel pour l'évaluation de mon travail.

Mathilde, merci pour tout. Pour la confiance que tu m'as accordée lors de ton retour en France. Pour le fait de m'avoir fait grandir en tant que « chercheur », de m'avoir aiguillé pour affiner ma réflexion scientifique au cours de nos nombreux échanges. Pour ta bienveillance, ta gentillesse et tes encouragements tout au long de notre collaboration. Et enfin, pour ton aide afin de pouvoir réaliser cette thèse.

Olivier je voudrais te remercier pour ta bien vaillance et ton aide au cours de cette thèse que ce soit scientifiquement ou administrativement pour que je puisse atteindre mon objectif concrétisé par ce manuscrit.

A toutes les personnes passées par l'équipe, Tommy, Rasa, Anne, Fardin, Julia, Melinda et tous les stagiaires merci pour votre générosité. Par extension je voudrai remercier toutes l'équipe Cophy (Jérémie, Christina, Nicole, Romain …) pour ces échanges que ce soit lors des réunions ou de discussion.

Merci aux équipes du CERMEP. Danielle et Franck à l'IRM pour leur gentillesse, leur patience et leur aide notamment avec les problèmes d'eyetracker. Sébastien et Denis également pour leur gentillesse, leur dévouement et pour les nombreuses heures passées ensemble que ce soit pour l'élaboration du Headcast ou les acquisitions MEG/EEG.

Merci à toutes les personnes qui ont fait ou qui font toujours partie des équipes du bâtiment Dycog. La liste est très longue donc je ne pourrais pas citer tous les noms, mais merci à vous pour tous ces moments de discussion scientifique et moins scientifique lors des repas ou des TGIFs. Donc merci à Florian, Jérémie, Benjamin, Benoit, Alex, Agathe, Rémi, Salomé, Lou, Pierre, Loic, Mélodie, Gaëtan, … Merci à l'équipe informatique, Thibaut, Hervé et PierreM pour leur aide notamment pour mes débuts sur le cluster de calcul. Je voulais aussi remercier Martine, la meilleure secrétaire qui existe au monde, qui trouve toujours la solution à tout et nous enlève un sacré poids administratif. Ton départ à la retraite va faire un grand vide dans le labo.

Je remercie les membres de mon CSID Nadine et Andrea pour leurs conseils et leurs retours avisés. Remerciement particulier pour toi, Nadine, car tu étais déjà là lors de mon stage de M2 à me transmettre ton savoir et qui par la suite m'a mis en relation avec Mathilde lors de son retour en France (pour la suite que l'on connait).

Que dire de la Team Harvard, Benoit et Anaëlle (et Harvard bien sûr). Benoit depuis les bancs de la fac de médecine dans l'amphi Herman en passant par la collocation voilà plus de 10 ans qu'on se connait. Difficile donc de résumé tous ces bons moments en seulement

quelques lignes donc tout simplement merci. Anaëlle merci pour tout lors de ces nombreuses années notamment dans la coloc du 333.

Merci pour tous ces moments de détentes à Antoine, Cassandre, Thomas, Margaux, Pauline, Amedé, Flo et Ester. Que ce soit autour d'un bon repas, d'un jeu de société ou une soirée. Chaque moment n'est que du bonheur avec vous.

Merci à toutes les personnes que j'ai côtoyées à l'ISC : Felipe, Maeva,Rémi(bis), Sébastien, Marie, Valentin, Maciek, Alice, Etienne… Mais également les « diner franglais » où l'on parlait surtout anglais avec Holly et Jimmy.

Les années fac n'auraient pu être meilleures qu'avec ce groupe : Rémi, Aurélie, Nadia, Baptiste, Inès, Alexia et bien sûr Mathilda (mais tu auras droit à un paragraphe rien qu'à toi). Ce groupe qui nous a emmené au fin fond de l'Amazonie d'Equateur et avec qui maintenant, malgré la distance, chaque retrouvaille se passe comme si on n'avait jamais quitté les bancs de la fac.

Merci à mes parents et mes frères qui m'ont toujours soutenu dans mes choix et qui m'ont apporté toute l'aide qu'ils pouvaient ce qui m'a permis de franchir les étapes une à une pour en arriver là aujourd'hui. Merci à Anaïs, Léon et Marcel pour tous les moments en famille.

Mathilda, voilà enfin le paragraphe qui t'es consacré. Je ne saurais comment décrire le bonheur de vivre avec toi au quotidien. Depuis toutes ces années à mes côtés dans les bons comme les mauvais moments tu as toujours su restée souriante et déterminée pour continuer à avancer. Si j'en suis là aujourd'hui tu y es pour beaucoup. Vivement qu'on parte en vacances que tous les deux.

Summary

Humans evolve in a complex environment. At each moment of the day, the brain processes a lot of information allowing us to make decisions. Information to consider can be external, i.e., coming from the environment and processed by the brain through our senses, or coming from internal sources like e.g., proprioception or memory. Whether we focus on external, or internal information, ignoring the irrelevant information might be as important as optimizing the processing of relevant information. The main goal of this thesis is to probe the neural mechanisms underlying these processes. The suppression of the irrelevant information has often been linked with Alpha oscillations (7-14 Hz). However, the role of alpha oscillations in protecting perceptual and higher-level processes from distractors is still unclear. Here, I used magnetoencephalography (MEG) to further investigate this question.

In the first study (**Chapter 1**), using a cue-based modified Stroop task, I did not find the expected effect of an increase in alpha oscillations over sensory regions, while processing the distractors. However, I have observed modulations in the activity of the ventral attention network (VAN) and the default mode network (DMN). Both networks have been shown to be inhibited during goal-driven tasks and linked with attention capture by external information VAN and internal focus DMN. In line with suggested inhibitory role of alpha oscillations (and higher frequencies), during our task, we found an increase in power in Alpha and Beta frequency bands in previously mentioned networks. In addition, we found stronger theta (4 Hz) power in anticipation and during stimulus processing over the cognitive control network.

In my second study (**Chapter 2**), to create a more challenging task we developed a novel version of a Stroop like task with more salient distractors. Instead of colors and word-color names we have used faces and names. I have observed a higher alpha power over high-order visual regions, namely the visual word form area (VWFA), when participants had to ignore names. Results confirmed inhibitory role of Alpha band activity. We also observed an increase of delta oscillation activity over the left occipitotemporal and parietal cortices.

In my last study (**Chapter 3**), we used a reasoning task requiring to overcome a perceptual bias, thus inhibiting certain visual information. When participants had to overcome such bias, I have found a power increase in the alpha band located over the left temporal cortex, and the VAN.

To sum up, presented results show the role of alpha (but also delta, theta and, beta) band activity might be involved in functional inhibition of a long-range network. However, the modulation of the sensory areas might be dependent on task parameters like task difficulty or distractor salience.

Keywords: alpha oscillation, inhibition, ventral attention network (VAN), visual area, MEG, human

Résumé

L'être humain évolue dans un environnement complexe. À chaque instant de la journée, le cerveau traite un grand nombre d'informations afin de prendre des décisions. Ces informations peuvent être externes, c'est-à-dire provenir de l'environnement et être traitées par l'intermédiaire de nos sens, ou provenir de sources internes comme, la mémoire. Que nous nous concentrions sur les informations externes ou internes, ignorer les informations non pertinentes peut être aussi important que d'optimiser le traitement des informations pertinentes. L'objectif principal de cette thèse est de sonder les mécanismes neuronaux qui sous-tendent ces processus. La suppression des informations non pertinentes a souvent été liée aux oscillations Alpha (7-14 Hz). Cependant, le rôle de ces oscillations dans la protection des processus perceptifs et de plus haut niveau contre les distracteurs n'est toujours pas clair. J'ai utilisé la magnétoencéphalographie (MEG) pour approfondir cette question.

Dans la première étude (**chapitre 1**), utilisant une tâche modifier de Stroop, je n'ai pas trouvé l'effet attendu d'une augmentation des oscillations alpha dans les régions sensorielles, lors du traitement des distracteurs. Cependant, j'ai observé des modulations dans l'activité du réseau d'attention ventral (VAN) et du réseau du mode par défaut (DMN). Ces deux réseaux sont inhibés pendant les tâches orientées vers un but et ils sont liés à la capture de l'attention par des informations externes (VAN) et à la concentration interne (DMN). Le rôle inhibiteur suggéré des oscillations alpha (et des fréquences plus élevées), pendant notre tâche, nous avons trouvé une augmentation de la puissance dans les bandes Alpha et Beta dans les deux réseaux précèdent. Nous avons trouvé une puissance thêta plus forte dans l'anticipation et lors du traitement du stimulus dans le réseau de contrôle cognitif.

Dans ma deuxième étude (**chapitre 2**), nous avons utilisé une version de la tâche Stroop avec des distracteurs plus saillants, des visages et des noms. J'ai observé une puissance alpha plus élevée sur les régions visuelles d'ordre supérieur, à savoir l'aire visuelle de la forme du mot (VWFA), lorsque les participants devaient ignorer les noms. Les résultats ont confirmé le rôle inhibiteur de l'activité de la bande Alpha. Nous avons aussi observé une augmentation de l'activité des oscillations delta dans les cortex occipito-temporaux et pariétaux gauches.

Dans ma dernière étude (**chapitre 3**), nous avons utilisé une tâche de raisonnement nécessitant de surmonter un biais perceptuel. Lorsque les participants devaient surmonter un tel biais, j'ai constaté une augmentation de puissance dans la bande alpha située sur le cortex temporal gauche, et le VAN.

En résumé, les résultats présentés montrent que l'activité de la bande alpha (mais aussi delta, thêta et bêta) pourrait être impliquée dans l'inhibition fonctionnelle. Cependant, la modulation des zones sensorielles pourrait dépendre de paramètres de la tâche tels que la difficulté de la tâche ou la saillance des distracteurs.

Mots clés : oscillation alpha, inhibition, réseau d'attention ventral (VAN), aire visuelle, MEG, humain

Abbreviations

ACC: anterior cingulate cortex

CNN: 'cognitive control network'

DAN: dorsal attention network

DICS: dynamic Imaging of Coherent Sources

DLPFC: dorsolateral prefrontal cortex

DMN: default mode network

EcoG: electrocorticography

EEG: electroencephalography

ERF: event-related field

FEF: frontal eye field

FFA: fusiform face area

FFT: fast Fourier transform

fMRI: functional magnetic resonance imaging

IFG: inferior frontal gyrus

GC: granger causality

LCMV: the Linearly Constrained Minimum Variance

LFPs: local field potentials

LGN: lateral geniculate nucleus

LIP: lateral intraparietal

LOT: left occipitotemporal cortex

MEG: magnetoencephalography

MFG: middle frontal gyrus

mPFC: medial superior prefrontal cortex

MPRAGE: magnetization-prepared rapid gradient-echo

PPC: posterior cingulate cortex / cuneus

REM: rapid eye movement stage of sleep

RT: response time

SMA: supplementary motor area

TE: echo time

TEO: temporo-occipital area

TFR: time-frequency representation

TI: inversion time

TMS: transcranial magnetic stimulation

TPJ: temporoparietal junction

TR: repetition time

V1: primary visual area

VAN: ventral attention network

VWFA: visual word form area

Background and experimental questions

Humans evolve in a complex environment. At any time of the day, the brain processes huge amounts of information, allowing us to navigate the environment. The source of the information can be either **external**, i.e., from the environment and transmitted to the brain through our senses, or **internal,** like proprioception or memory. For example, when you drive your car in traffic, you must pay attention to many important things such as the color of the traffic lights, pedestrians on the crosswalks, or the car leaving its parking space without using an indicator. In this everyday example, we can see the necessity to flexibly adjust our attention to the environment. To make the optimal decision in the shortest possible time we need to select the important information and suppress the irrelevant. On the opposite side of the spectrum, some situations require you to concentrate on the internal information. For example, when you need to choose an answer on a test, it requires you to ignore the external distractors and suppress competing information in your memory.

External information is initially processed in early sensory regions and transferred to areas responsible for increasingly abstract processing. For example, in the visual system, the light reflected off the stimulus arrives on the retina. Photoreceptor cells convert photons from the incoming light into electrical signals that are transmitted by the optic nerve to the lateral geniculate nucleus (LGN). The next step of the information transfer is a primary visual area V1 (see **figure 1A** for an example during reading). Subsequently the more complex aspects of visual information are split between two major cortical processing streams.

First discovered in monkeys: a ventral stream that extends to the temporal lobe, and a dorsal stream that projects to the parietal lobe (Mishkin & Ungerleider, 1983). Each streams has a different functional role (Logothetis & Sheinberg, 1996). In this review, the authors showed that the primary function of the ventral stream would be to facilitate the conscious perception, recognition, and identification of objects by processing their "intrinsic" visual characteristics, such as form, color, etc. The dorsal stream's suggested primary goal was to maintain the control of visuomotor behavior by processing their "extrinsic" characteristics essential for grasp, such as spatial location, orientation, or size. Different kind of information can be processed by partially overlapping groups of neurons in higher-order regions, creating a hierarchical bottleneck (**Figure 1B**). It is therefore crucial that the processing of information is organized with clear prioritization of relevant information regarding the current goal of the agent**.** It has been suggested that ignoring irrelevant information is also crucial for specifically selecting relevant information (Lavie, 2005; **figure 1B**).

Internal processes such as reasoning involve higher order regions such as the prefrontal cortex (PFC; Krawczyk et al., 2011) and might involve ignoring any external stimulation. Many studies have shown that the PFC exerts top-down control over visual regions (for a review see Paneri & Gregoriou, 2017) that could allow the implementation of such a mechanism (**Figure 1C**).

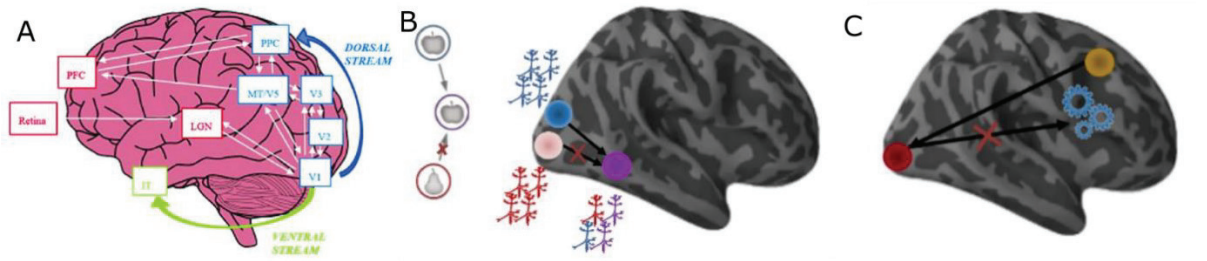

***Figure 1**. **(A)** Processing of visual stimulation. Left: pathways associated with visual processing during reading highlighting the cortical hierarchy (lateral geniculate nucleus: LGN; visual cortex: V1, V2, V3, V4, MT/V5; posterior parietal cortex PPC; pre-frontal cortex: PFC; inferior temporal cortex: ITC; adapted from Archer et al., 2020). **(B)** Illustration of the bottleneck issue resulting from the hierarchical organization of visual processing. A pear and an apple simultaneously presented might be processed by partially overlapping groups of neurons in high-order visual areas potentially creating spurious feature binding. The blue (next to the blue circle) and the red (next to the red circle) neurons in the V1 process respectively the apple and the pear. Some neurons in ITC (purple circle) process specifically the apple and the pear (blue and red neurons) but some other neurons are involved in the processing of both stimuli (purple neurons). Attention would allow us to prioritize processing the most relevant stimulus at a given time, e.g., the apple, and avoid potential spurious binding. Oscillations could allow for the implementation of such specific selection. **(C)** Protection of internal processes such as problem-solving would involve an inhibitory top-down control from the prefrontal cortex. In order to solve the problem, the activity of the regions involved (represented here by gears) must not be disturbed by external information. the prefrontal regions (yellow circle) must inhibit the primary visual areas (red circle)*

Whether we focus on external or internal information, it is clear that we need to ignore irrelevant information. However, the mechanism behind this process is not clear? Precisely, how is the relevant information prioritized and transferred through relevant brain networks?

It has been proposed that oscillations, in particular in the alpha frequency band (7-13Hz, i.e., between 7 and 13 cycles per second) could play a role in mechanisms of information selection. Oscillations reflect rhythmical changes in the excitability of the population of neurons which potentially can organize the processing of information. This idea will be further expended below.

I will first briefly define oscillations and the techniques used to detect them. Then I will focus on alpha oscillations and their functional role. Finally, I will present the different experiments that I conducted during my thesis.

1. Oscillations: broad definition, brain recording techniques, and main frequency bands

1.1 Definition of oscillations

Neural oscillations originate from the rhythmical fluctuation of the excitability of populations of neurons. They can be generated spontaneously or in response to a stimulus and detected using several techniques. In closer details, the excitation of a neuron leads to the release of neurotransmitters by the synapse which will bind to receptors on the dendrite that will cause the opening of ion channels. Charged particles flow between the intra- and extra-cellular mediums. The movement of particles produces an electric current, and all currents generate a magnetic field around them. The so-called "source" or "primary" current corresponds to the intracellular current. To maintain the charge balance, cell generates extracellular currents called "secondary" or "volumic". Oscillations are detected when such flow is rhythmical for a given duration.

Oscillations can be described by following parameters: the frequency, the amplitude, and the phase at a given time (**Figure 4A**). First, frequency is the number of cycles per unit of time (a second) and is expressed in Hertz (Hz). In the literature, specific labels have been proposed for different frequency bands: e.g., delta (below 4Hz), theta (4-7 Hz), alpha (7-13 Hz), beta (15-30 Hz), low-gamma (30-80 Hz) and high-gamma (80-150 Hz). The amplitude corresponds to the difference between the peak and the trough of an oscillation. The amplitude squared gives the power of the oscillation, which means the energy in the corresponding frequency band. Finally, the phase is the position along the sine wave (or cosine wave that is 90 degrees out of phase with the sine wave) at any given time and is measured in radians or degrees.

1.2 Recording techniques

There are several ways to record brain activity developed over the years. Each method has its advantages and disadvantages, mostly associated with how directly the neural activity is measured. Depending on the method, certain experimental questions can or cannot be answered. Thus, to appropriately answer the scientific question at hand, the specific method of recording brain activity has to be chosen. Two criteria are important to consider: the temporal and the spatial precision of the recording (**Figure 2**).

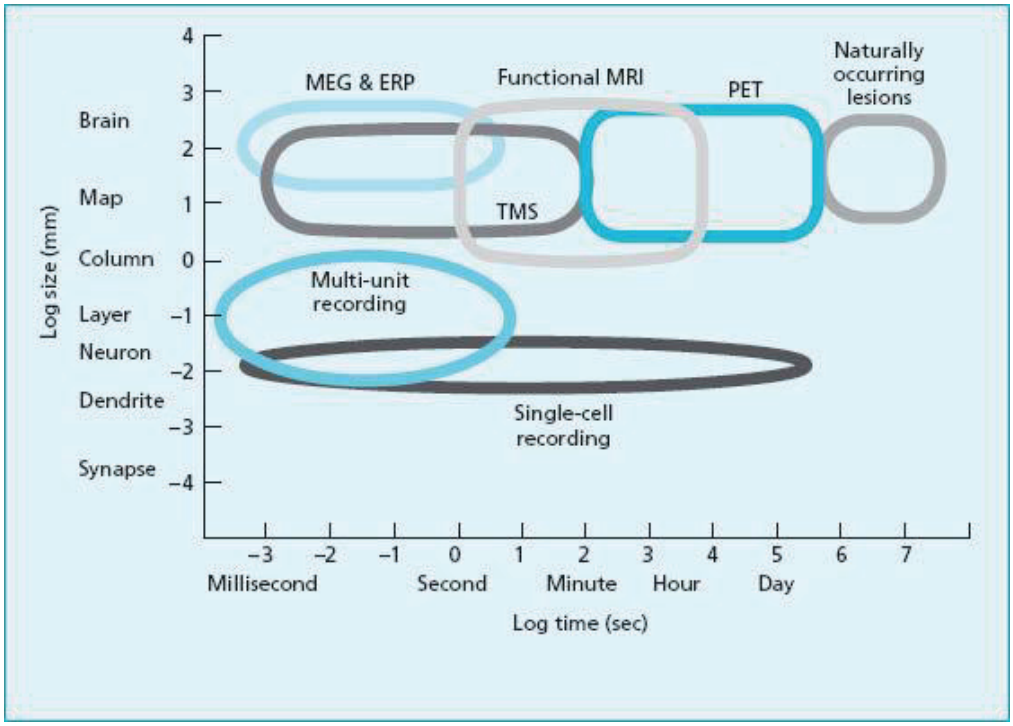

***Figure 2**: Methods of Cognitive Neuroscience. Cognitive neuroscience techniques can be categorized according to their spatial and temporal resolution. (Adapted from Churchland and Sejnowski, 1988)*

One of the most popular techniques is the functional magnetic resonance imaging (fMRI). It indirectly measures the brain activity by detecting changes associated with blood flow (Huettel et al., 2008). The general principle of an fMRI study is to analyze the BOLD (Blood Oxygen Level Dependent) signal which translates the increase of oxygen influx in the activated brain regions. But this phenomenon is not instantaneous as we can see in **Figure 2**, and it takes a few seconds to observe it.

However, to detect oscillations and their fast and transient aspects, other techniques are more suitable.

Two non-invasive techniques allow to record the brain oscillations in humans. Electroencephalography (EEG) measures the brain's electric fields with electrodes placed on the scalp. The potential differences measured between two electrodes in EEG are due to the current lines flowing on the surface of the scalp, and thus to the volume currents. The Magnetoencephalography (MEG) is measuring the magnetic field resulting from the primary electric current that is produced by postsynaptic potentials (Cohen, 1968; Hämäläinen et al., 1993; Hansen et al., 2010). In addition, the measurable currents (for EEG) and magnetic field (for MEG) on the surface of the head must result from the synchronization in time and space of an assembly of neurons (10^5 neurons). These assemblies are typically contained in functional macrocolumns of about 3 mm in radius and 3 mm in depth. The currents resulting

from the activity of a macrocolumn are modeled by a current dipole whose direction is given by the principal orientation of the dendrites. We can distinguish several types of dipoles based on this orientation. Radial dipole, perpendicular to the scalp, corresponds to the activity in the gyri and tangential dipole corresponds to the dipole in the sulcus of the cortex, tangential to the scalp (**Figure 3**). MEG and EEG do not have the same sensitivity to the orientation of the sources. The activity of the radial dipoles is better detected by EEG, whereas the magnetic field produced by such dipoles is expected to be poorly detected by MEG. Regardless of the orientation of the sensor, radial dipoles are unable to generate an external magnetic field outside of a volume conductor that is spherically symmetric (Baillet et al., 2001). Another important difference between EEG and MEG is the electrical current is more affected by the different tissues separating the source and the electrode because they all have distinct conductance while their magnetic field is much less affected by skin, bone, and cerebrospinal fluid. As a results, a topography of the sources is more diffused in EEG.

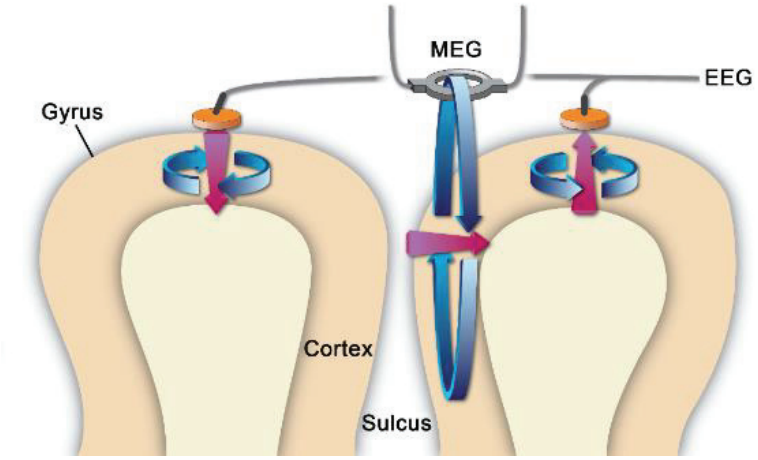

***Figure 3**: Definition of radial and tangential dipoles. Dipoles with a radial direction concerning the skull surface are produced in the gyri of the cortex, whereas dipoles with a tangential direction are emitted by the sulci. Pink arrows represent electric dipoles and blue arrows represent the magnetic field. EEG electrodes can detect radial and tangential electric dipoles, however, the MEG sensors detect magnetic fields from dipoles directed tangentially to the cortical surface (adapted from Peitz et al., 2021).*

MEG is a noninvasive, external measurement technique with specific magnetometers, also known as Superconducting QUantum Interference Devices (SQUIDs). SQUIDs are cooled down by a liquid helium to achieve a super-conductance at very low temperatures (**Figure 4B**), turning into highly responsive magnetic field sensors. Magnetic fields recorded by MEG are extremely small. Around a magnitude of a femtotesla, which is a 1^{-15} of the magnetic field of the earth. Magnetically shielded environment is necessary to reduce environmental

electromagnetic noise while recording. MEG was used in all the studies presented in this thesis.

In some specific cases, another technique can be used, the intracranial electrodes. They are considered invasive and are mostly used in animal models such as monkeys or rats. In specific cases, patients with pharmacoresistant epilepsy are implanted with such electrodes to localize the epileptic source before surgery. This creates a unique opportunity to use this technique on humans. Intracranial electrodes enable recording activity of a single neurons, or the activity of a group of neurons around the electrode. The latter is called a local field potential (LFP).

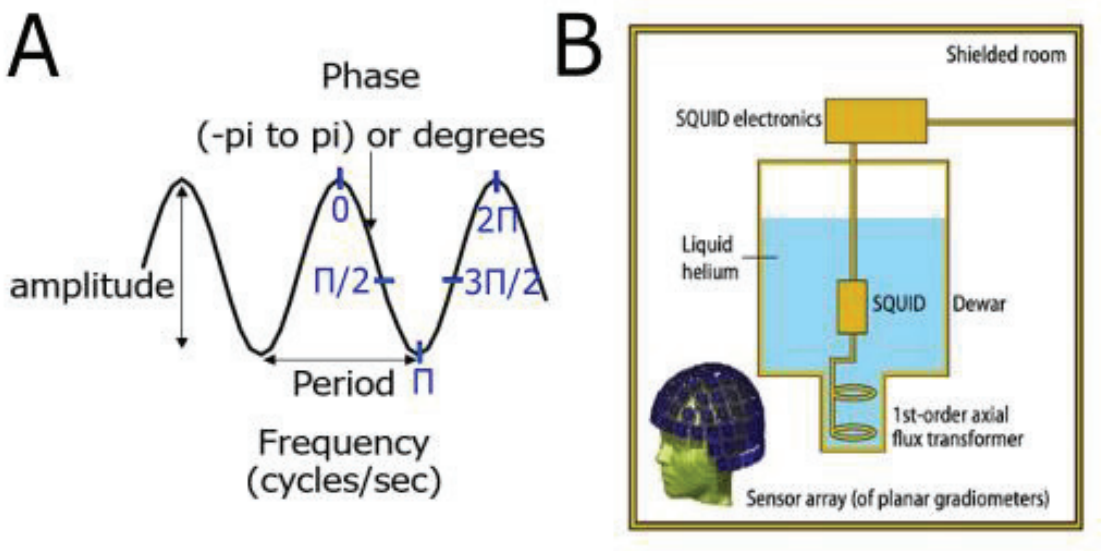

***Figure 4**: **(A)**The three parameters used to define an oscillation: phase, amplitude, and frequency. **(B)** Schema of a SQUID in liquid helium*

1.3 Brief overview of the role of oscillations at different frequencies

To put the Alpha oscillations, the focus of this thesis, in the broader context, I will briefly introduce the other frequency bands observed in brain recordings.

1.3.1 Delta activity

Delta band was among the first pattern of brain activity recorded during sleep from the human scalp (Davis et al., 1937), named “slow waves”. The reason behind the analysis of the delta rhythm was for a long time focused on sleep and still is used as an index of deep

sleep state (Steriade, 2006). It was shown that delta oscillation (or slow-wave oscillation, 0.5-4.5 Hz) characterizes the non-rapid eye movement (NREM) stage in rodents' sleep and during the N3 stage in human sleep (Adamantidis et al., 2019). Given the strong link between sleep, memory consolidation and forgetting, the research was directed to establish the mechanism of delta oscillations in memory during sleep (Kim et al., 2019). The authors showed that delta waves mediate the weakening of memory reactivations and contribute to forgetting. The role of delta oscillations was studied in cognitive processes other than sleep and memory. An increase of delta activity was shown following the target presentation in an oddball paradigm (Başar-Eroglu et al., 1992). I was hypothesized that the increase in delta power band could be involved in signal matching, decision-making, and surprise. Delta oscillations may also play a role in active attentional selection (Lakatos et al., 2008; Schroeder & Lakatos, 2009). Lakatos et al (2008; see **Figure 5**) used an oddball task with simultaneously presented bimodal stimuli (visual and auditory). Monkeys were aware of the block modality by a cue (indicating to pay attention to visual or auditory stimuli) to detect oddballs in that modality. Task related delta-band oscillations in the primary visual cortex entrained to the rhythm of the stream, and this entrainment increased response gain for task-relevant events and shortened the reaction times. Authors have proposed that a major mechanism of selective attention to rhythmic auditory or visual input streams is the entrainment of cortical delta oscillations.

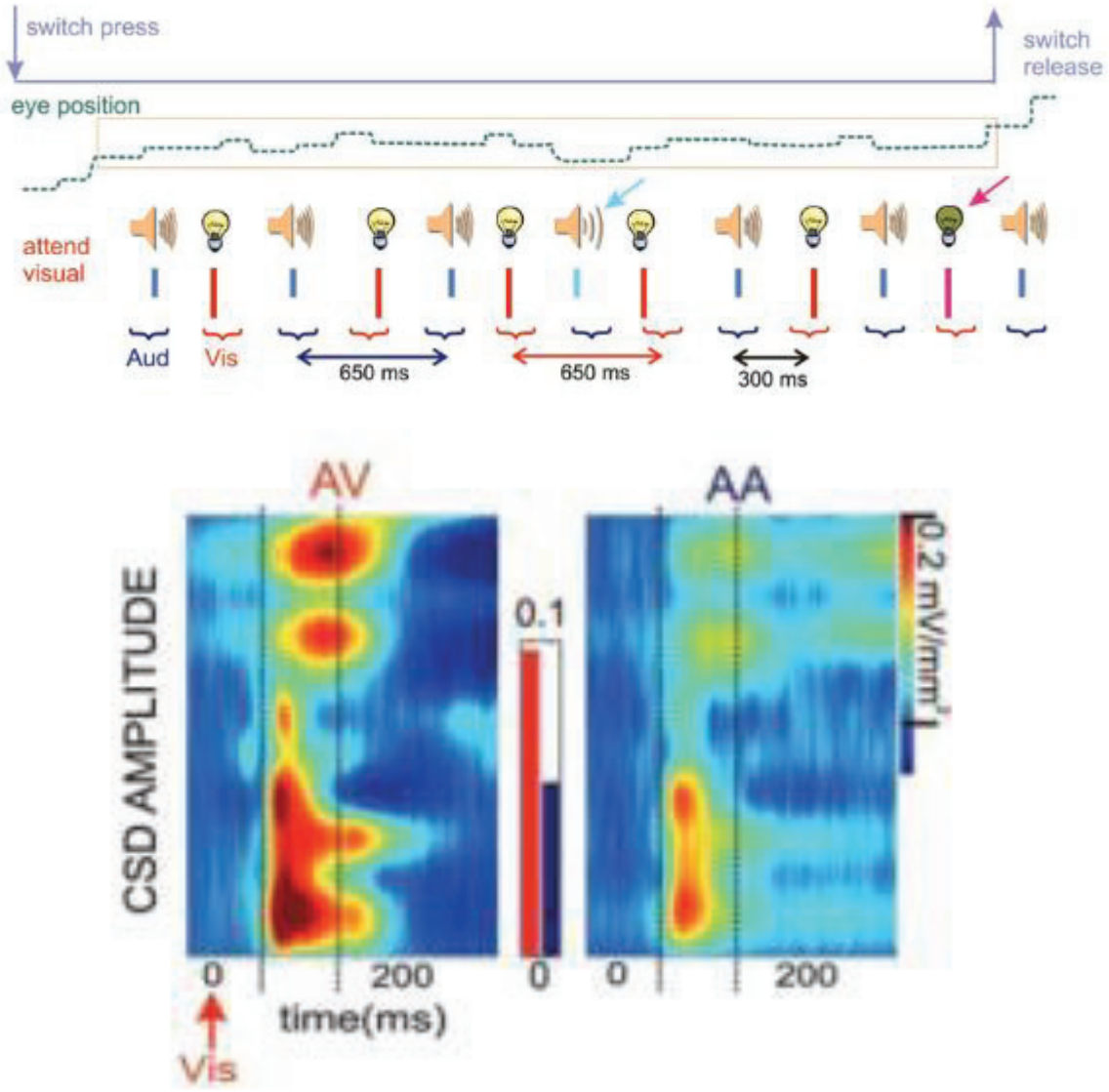

***Figure 5**: task requiring intermodal selective attention. **Top**: In the mixed sensory stream, lightbulbs and speakers stand in for both visual and audio inputs. Arrows in light blue and red, respectively, are used to identify visual and aural deviations. The stimulus onset asynchronies (SOA) for each modality were jittered (650ms; Gaussian distribution). The average SOA between modalities was 300ms. **Bottom**: Time-frequency graphs. Prestimulus delta phase and the impact on the reaction to a visual event. Laminar CSD profiles were produced in a sample experiment using conventional visual stimuli. Response amplitudes over the 50 to 135 ms period under the AV and AA conditions, respectively, are shown as red and blue bars between the color maps (adapted from Lakatos et al., 2008).*

1.3.2 Theta activity

Theta band is often defined as the "hippocampal rhythm" because it was found for the first time in this structure in freely moving rodents (Winson, 1974) or during spatial

navigation tasks (Watrous et al., 2013). In the hippocampus, place cells are group of cells that activate when the animal is in a receptive field associated with it. From an experimental point of view, these neurons are identified by recording them in an animal that freely walks through space. The activity of these cells is peaking when the animal is at a specific location in the field. These activations are modulated by the theta rhythm (O'Keefe & Recce, 1993). This rhythm is also characteristic of the rapid eye movement (REM) stage of sleep. It is associated with consolidation of memory during sleep (Montgomery et al., 2008). Theta oscillations are also implicated in memory during awakening. It was suggested that theta rhythm could play a role during memory encoding and retrieval in animals (Seager et al., 2002; Vertes et al., 2001). This rhythm has also been observed in the hippocampus during task involving episodic memory in humans (Lega et al., 2012). The involvement of theta oscillations has also been shown in short term memory task, e.g., the Sternberg working memory task (Raghavachari et al., 2001). This task consisted of a list of consonants presented successively that the subject had to memorize, followed by a probe and the subject's response. Raghavachari et al. (2001) showed sustained theta activity from the beginning of the test to the appearance of the probe. There is evidence for a role of Theta rhythm in attentional sampling over multiple visuospatial positions (Fiebelkorn et al., 2018). A spatial attention task was used to probe the attentional processes. Monkeys had to monitor three different locations because the cue was not reliable, and to detect the presence of a close-to-threshold target, which appeared at varying cue-target-intervals. LFP data was collected from the frontal eye field (FEF) and lateral intraparietal (LIP), two important nodes of the frontoparietal network. With a spectral maximum around 4 Hz, the monkeys' capacity to recognize the target varied rhythmically as a function of the time delay between the cue and the target. Similar rhythm has been found in many behavioral and electrophysiological experiments (Brookshire, 2022; Landau et al., 2015; Landau & Fries, 2012; Senoussi et al., 2019).

Finally, this type of oscillation is thought to be implicated in conflict resolution. More specifically, theta power over midfrontal and dorsolateral regions was correlated with the magnitude of the conflict (Cohen & Donner, 2013). Subjects were simultaneously presented with visual stimulus (left or right side of the visual field) and an auditory stimulus presented to the side congruent or incongruent with visual stimuli. The subject had to answer with the right hand if the stimulus was presented in the right hemifield and the left hand if it was located in the left hemifield. The conflict occurred when the presented orientation of the visual and auditory stimuli was incongruent. Ongoing theta-band oscillations occurred during the decision process. A recent study further revealed that the anticipation of conflict was associated with increased frontal theta and posterior alpha decrease and that these two measures were associated with faster conflict resolution (Kaiser et al., 2022)

1.3.3 Beta activity

Beta oscillations have been mainly observed during sensorimotor processing (Pfurtscheller & Lopes da Silva, 1999). However, it has been recently shown that beta-band activity would be expressed in transient bursts instead of sustained oscillations. This transient

activity in the sensorimotor plays a role in movement control (Little et al., 2019). The beta rhythm has also been seen in tasks that did not involve either planning or executing motor actions. For example, an increased phase synchronization in the beta band during attentional activities reflects communications across task-relevant areas (Gross et al., 2004). In the task of this article, capital white letters were visually displayed in a rapid serial visual presentation for each experimental trial, and the subject have to detect the target letter among all those presented. Several types of trials were possible, notably two targets separated by one distractor, and two targets separated by five distractors. It was shown that the ability to report the second target is reduced if the delay between the two is lower than 500ms (case here when there is one distractor), but this prevents only conscious reporting of missing target stimuli, not their perceptual processing. Subjects were instructed to report all targets in the proper order after each stream presentation. The results showed a communication within the fronto-parieto-temporal attentional network. More precisely, for trials with five distractors, a stronger synchronization for the second target and desynchronization for the distractor compared to trials with one distractor. It was further shown that a number of variables that affect the regulation of cognitive control are reflected in beta oscillations in a trial-and-error task of searching for which target was rewarded from a choice of 4 (Stoll et al., 2016).In this intracranial study in monkeys, Stoll and collaborators showed the functional importance of frontal beta-band oscillations in top-down control processes. They observed more top-down signaling accounted by the enhanced functional connectivity between visual and frontal regions. Moreover, the attentional modulation of feedback-related beta oscillations in the visual system has been documented in an EcoG study (Bastos et al., 2015). The authors analyzed the activity of eight macaque visual regions and discovered that across the several inter-areal projections, granger causality measures (reflecting the strength of effective connectivity) in the beta band were stronger in the feedback than in the feedforward direction while the opposite was observed in the theta and gamma band.

Moreover, a human EcoG study using a semi-predictable sequence of sounds to force subjects to continuously update their predictions, provided evidence that beta-band oscillations are involved in updating the content of sensory predictions (Sedley et al., 2016). In line with this result, the beta activity observed in Bastos et al. 2015 might represent the transfer of predictions to lower-order regions (see also Bastos et al., 2012).

Finally, it was shown that alpha/beta oscillations (12-20 Hz) were found during a goal-driven task (Solís-Vivanco et al., 2021). The authors observed, following a signal suggesting the modality to attend, a power increase of alpha/beta oscillations in the ventral attention network (VAN; for details on VAN see section 2.1.5.1). Stronger VAN power increases were related to better task performance. Given the activation of the VAN has been associated with the capture of attention by unattended, not relevant, stimuli, these results suggest that the suppression of the activity of the VAN prevents the capture of attention by the unattended stimulus.

1.3.4 Gamma activity

Gamma oscillations have been associated with a wide range of cognitive processes. For example, gamma band signal has been associated with sensory perception, memory, and decision-making (for a review see Fries, 2009). More precisely, gamma activity was shown to be associated with stimulus processing in visual perception (Fries et al., 2008). It has been shown to be induced by visual stimuli and transferred in the feedforward direction (e.g. Michalareas et al., 2016; van Kerkoerle et al., 2014). Regarding working memory, it was shown in two implanted epileptic patients that gamma oscillations increased in a quasi-linear way with the memory load (Howard, 2003). The task was a Sternberg task, i.e., letters were presented successively to the subjects who had to retain them. After a retention period, probes were presented, and the subjects had to say if it were part of the dataset. Gamma activity remained high during the retention period and returned to a base level when the information was no longer needed. The gamma rhythm was also modulated by attentional processes (Taylor et al., 2005). In this study of monkeys implanted in visual area V4, the authors found that attention strongly increased oscillatory activity in the gamma frequency range. Gamma frequency found in V4 LPF recording, was modulated by the attention processes. This was interpreted as increased neuronal synchronization within the population of V4 neurons representing the attended stimulus by the monkey. A change in gamma frequency with attention was found in other studies (e.g., Bosman et al., 2012).

The mechanism behind most oscillations observed in the brain is not clearly known. It has been suggested that gamma oscillations can emerge from the interaction between excitatory pyramidal cells and inhibitory interneurons (Buzsáki & Wang, 2012).

Discussing in detail the potential role and origin of each frequency band would require an entire thesis. As mentioned above, this thesis presents experiments testing hypotheses regarding the general role of alpha oscillations in prioritizing information in different contexts.

2. Alpha oscillations

2.1.Functional Role

2.1.1. Background and main theoretical frameworks

Historically, alpha oscillations were discovered by Hans Berger using EEG in 1929. These oscillations are particularly strong over the occipital region when subjects close their eyes. As a consequence, they were first considered as reflecting the idling state of the human brain (Pfurtscheller et al., 1996). Quickly, new hypotheses on the role of alpha oscillations were developed because it has been observed that alpha has a distributed activity in the human brain. Implications for various brain functions including sensory, motor, and memory processes have been investigated (for reviews see Başar et al., 1997, 1999). For example, prior to successful cognitive tasks, they saw consistent, 10Hz activity, phase-ordered pre-stimulus EEG oscillations that frequently form repetitive patterns. Moreover, during a memory task,

Başar et al (1997) showed that during retrieval, for the analysis of alpha amplitude, alpha desynchronization is more pronounced for bad performers than for good performers. Thereafter, new frameworks regarding the role of alpha oscillations have emerged following interesting experimental works that questioned this view on alpha oscillations. It has been proposed that alpha oscillations reflect functional inhibition (Jensen & Mazaheri, 2010; Klimesch et al., 2007; Palva & Palva, 2007). More precisely, it was proposed that alpha could be associated with an increase of inhibition every ~100ms (Mathewson et al., 2011). Importantly, unlike gamma oscillations, alpha oscillations would travel in the feedback direction and would be considered as internally controlled (Michalareas et al., 2016; van Kerkoerle et al., 2014).

To explain the role of alpha oscillations, a theory was developed, i.e., the "gating by inhibition" theory (Jensen & Mazaheri, 2010; **Figure 6**). Jensen & Mazaheri (2010) hypothesized that the relevant information sent from one region to another is guided by the functional blocking of the pathway that is not relevant to the task. As we saw at the beginning of this manuscript, with the example of the visual processing of an apple and not a pear, there is a convergence of information in the visual hierarchy (see **Figure 1B**). It is therefore important to be able to prioritize the relevant information.

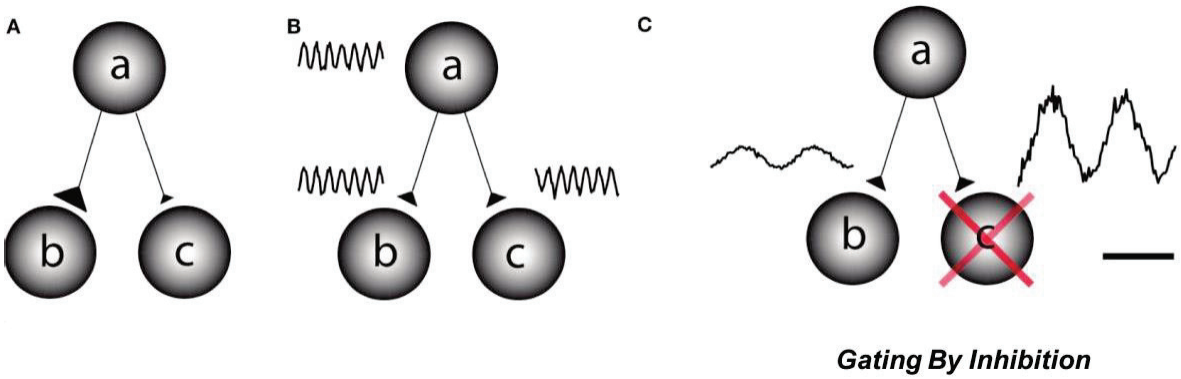

Figure 6*: In the context of the information is supposed to be routed from node a to node b but not to node c.* ***A.*** *One theory is that, on a short time scale, the synaptic connections between nodes a and b are strengthened, while those between nodes a and c are decreased. This would need a synaptic plasticity mechanism that operates quickly.* ***B.*** *Information might be gated through neuronal phase-synchronization between nodes a and c. The information flow from node a to c is blocked by adjusting the phase difference.* ***C****. Gating by inhibition. Functional inhibition actively suppresses node c. This controls the flow of information from point a to point b. The 9–13 Hz alpha band reflects the functional inhibition (Adapted from Jensen & Mazaheri, 2010).*

It is to explain this phenomenon that the theory of gating by inhibition was proposed and subsequently the nested oscillations framework (Bonnefond et al., 2017). This framework reconciles the gating by inhibition theory view with the communication through coherence framework (Fries, 2005, 2015; see **Figure 7**) in which synchronized gamma oscillations between regions allow to set up of specific communication, in order to allow internally controlled flexible communication. More precisely, in the communication through coherence framework, communication between transmitting and receiving neural pools depends on their gamma-band phase synchronization, or, more specifically, on whether the gamma oscillatory activity between the two neuronal pools is coherent. Therefore, signal transmission across neural connections would be controlled by the coherent phase of gamma oscillations (Fries, 2005). This might be achieved by the sending neuronal pool entraining the gamma phase in the receiving pool thus rendering their interconnection more powerful (Fries, 2009)

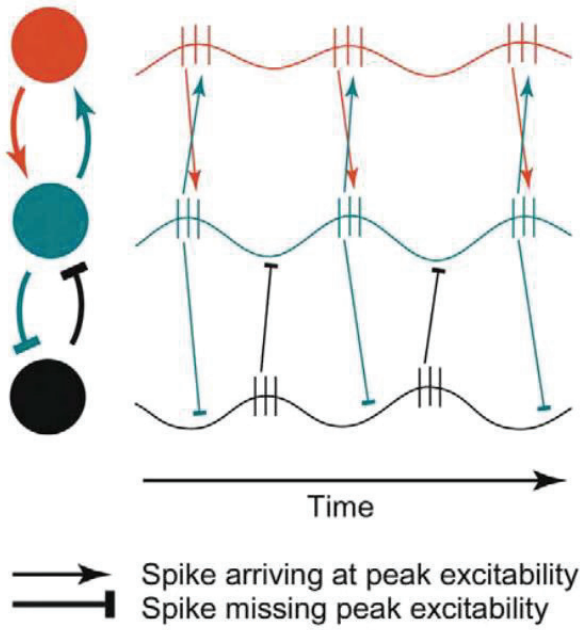

***Figure 7**: A sending neural group is represented by red-filled circles and a receiving neuronal group by green-filled circles. Action potentials of the neurons in the two groups are depicted by the thin vertical lines, and their motion is shown by the arrows along the connecting axons. Spikes that arrive at excitability peaks of the receiving neuronal group have pointed arrowheads. The arrowheads of spikes that miss excitability peaks are blunt. Coherent excitability changes between the red and green neural groups enable effective communication between them. However, the black neuronal group experiences excitability changes that are incoherent with the green neuronal group, which prevents communication between the two groups (Adapted from Fries, 2005).*

Bonnefond et al.(2017; **Figure 8**) suggested that brain communication would be set up by (1) a top-down controlled low alpha power in relevant and communicating regions and (2) an optimal alignment of the phase of alpha oscillations (see also Palva & Palva, 2007) between these regions (as proposed in the gamma band by Fries et al., 2005, 2015) (3) an increase of alpha power in irrelevant brain regions possibly associated with an anti-phase alignment with relevant regions. This setting would allow gamma oscillations, induced by stimuli, and locally controlled by alpha oscillations, i.e., they could occur only during the excitable phase of alpha oscillations, to be specifically transferred between relevant regions. As for the *"gating by inhibition"* theory, functional inhibition of irrelevant brain regions is also crucial in this framework.

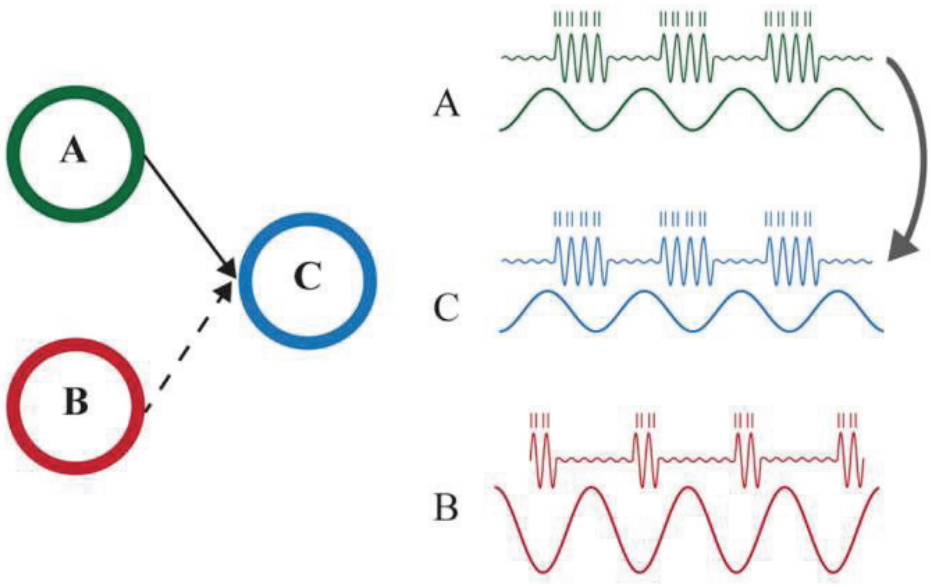

***Figure 8**: The functional connection between A and C is established by the synchronization in the alpha-band. This allows for representational specific neuronal firing reflected by the gamma band activity to flow to region C. High alpha power in B and an asynchrony between B and C could be used to block communication between B and C. Information is thereby routed between regions based on both changes in alpha-band power, as in gating by inhibition, and phase synchronization between the regions, as in the communication through coherence. (Adapted from Bonnefond et al, 2017).*

Below, I present experimental works showing a link between alpha oscillations and perception and how they are modulated by attention. More specifically, I present the evidence in favor of and against a link between, top-down controlled, alpha oscillations and functional inhibition in particular to protect perceptual and memory processes from distractors.

2.1.2. Alpha power influences perception and is modulated by attention

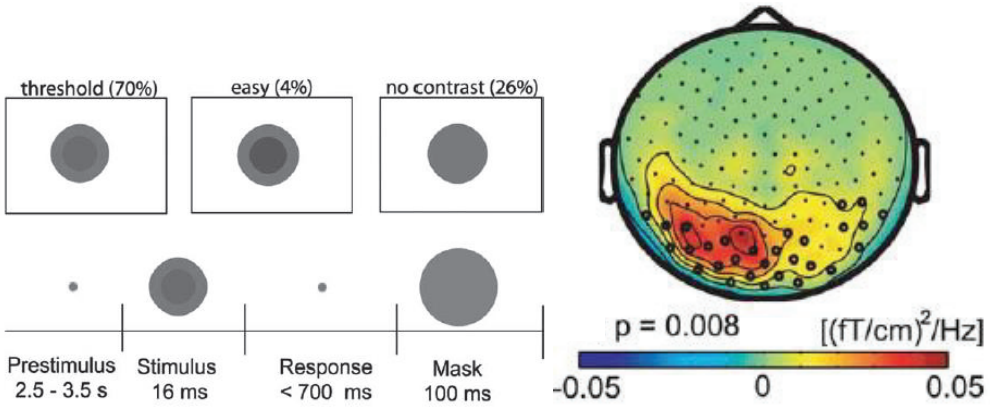

***Figure 9**: **Left**, the design of a detection task. **Right**, the topography of power of alpha band before stimulus presentation in the detection task. Stronger posterior alpha power was observed for misses than hits trials (adapted from van Dijk et al., 2008)*

Many studies have focused on how alpha power is related to visual perception. They hypothesized that if alpha oscillations are related to functional inhibition, low alpha power should be associated with higher cortical excitability than high alpha power (Romei et al., 2008; Sauseng et al., 2009).

In a detection task, it was shown that higher pre-stimulus alpha power, in the parieto-occipital sulcus, was associated with a decrease of the likelihood of reporting a near-threshold stimulus (van Dijk et al., 2008; ***Figure 9***). In this study, a smaller disc superimposed on a larger disc with different contrasts (gray levels) were shown to subjects. If there was a small variation in the gray levels between the two discs, subjects had to report it. Authors discovered that when prestimulus alpha power increased, visual discrimination ability decreased. Additionally, when alpha power is low, people have a higher likelihood of reporting TMS-induced phosphenes (Romei et al., 2008) or visual stimuli even in the absence of any visual stimulation (an increase of the False alarm rate; Iemi et al., 2017). Alpha modulations have therefore been proposed to be specifically associated with changes of the criterion parameters, i.e., the amount of sensory evidence needed to make a 'signal present' decision, as defined in the signal detection theory (Iemi et al., 2017; see Samaha et al., 2020 for a review). Signal detection theory (Emmerich, 1967; Macmillan & Creelman, 2005) quantifies the ability to differentiate a stimulus from noise - or by extension to differentiate between two stimuli. Signal detection theory allows us to know whether a change in performance is related to a change in perceptual sensitivity or in the response criterion. Overall, these studies indicate that alpha power could impact the likelihood of reporting the presence of (near-threshold or absent) stimuli by changing the excitability of visual areas.

Furthermore, many studies have shown that alpha oscillations can be internally (top-down) controlled. Most of these studies manipulated spatial attention. In the Oxford dictionary, attention is defined as "the act of listening to, looking at or thinking about

something/somebody carefully; an interest that people show in somebody/something". The attentional system operates in two dimensions: (1) the spatial dimension, by allowing the selection of relevant information to be processed, and (2) the temporal dimension by maintaining the resources to process such information. We can define two subtypes of spatial attention. The first subtype of spatial attention is the overt attention which is associated with eyes movement toward the attended stimulus. In contrast, in the covert attention, eyes are fixed on a different spatial location than the attended stimulus. Only the so-called attention spotlight is on the attended stimulus.

In sensory regions, as in the primary visual cortex, it was shown that alpha oscillations are modulated by covert spatial attention in anticipation of stimuli (Fries et al., 2008; Worden et al., 2000; Wyart & Tallon-Baudry, 2008, 2009). The alpha decrease was observed contralateral to the attended stimulus (Capilla et al., 2014; Thut, 2006; Worden et al., 2000) while the alpha increase was observed in some studies contralateral to the unattended side, in particular when distractors were presented (Gutteling et al., 2021; Haegens et al., 2012; Kelly et al., 2006; Rihs et al., 2009). Worden et al. (2000) developed a cued attention task using an arrow to indicate to the participants the side they should attend in each trial. If the stimulus, i.e., moving dots, appeared on the attended side, they had to indicate the motion direction. They had to ignore the stimulus when it was presented on the other side. They showed, using EEG, a posterior increase of alpha power before the stimulus contralateral to the side-to-ignore. This result was supported by several other studies using different paradigms (Gould et al., 2011; Händel et al., 2011; Kelly et al., 2006), including during stimulus presentation when a relevant change was expected to occur on the stimulus (Bauer et al., 2014; see also Händel et al., 2011). All previous studies focused on visual areas, but similar results were found over somatosensory areas (e.g. Haegens et al., 2012) and over auditory areas (Wöstmann et al., 2019). Overall, these studies show a role of alpha power increase in functional inhibition or, in other terms, a disengagement of irrelevant areas that may decrease distractors processing.

An alpha increase has also been observed over posterior regions to protect working memory from distracters (Jensen & Tesche, 2002; Jokisch & Jensen, 2007). Bonnefond and Jensen, in 2012, developed a working memory task in which each trial consisted of a set of four consonants to memorize followed by a retention period (see **Figure 10**). Then a probe was presented, and the subjects had to determine whether it was part of the memory set or not. A distractor was systematically presented during the retention period, 1.1s after the last consonant letter of the memory set. Two types of distractors, a "strong" one which was a consonant, i.e., it could be incorporated into working memory, and a "weak" one which was a symbol. These types of distractors were presented in different blocks, so the participants could anticipate which kind of distractor would be presented in each trial. The authors reported that alpha power over the occipitotemporal cortex was higher in anticipation of the distractor onset, of strong distractors than in anticipation of weak distractors. Furthermore, a stronger alpha power before strong distractors was associated with faster reaction times to

the probe (Bonnefond & Jensen, 2012, 2013; see also Payne et al., 2013). The authors interpreted these results as indicating that, a top-down controlled, alpha power increase would protect working memory against distractors.

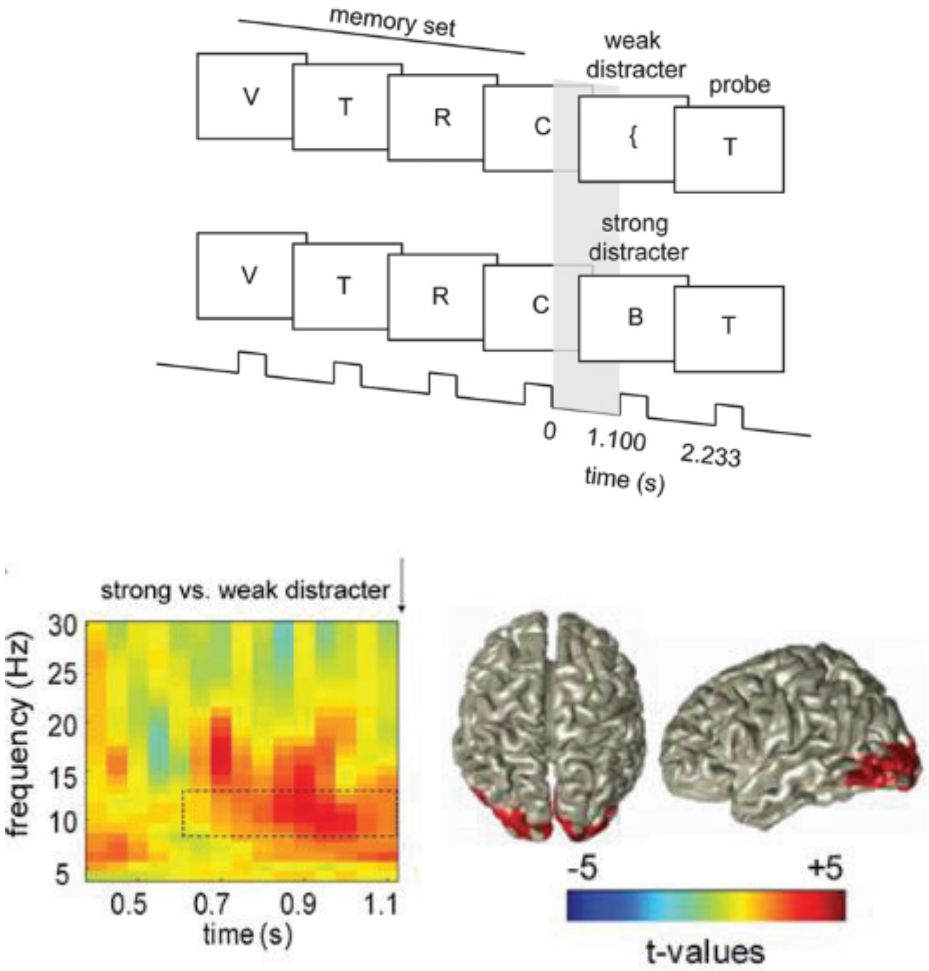

Figure 10*: Design and results of the memory task used in Bonnefond and Jensen, 2012.* ***Top:*** *Design of the task. 1.1s after a memory set of four consonants, a distractor was presented to the subjects. There were two types of distractors depending on the block trials. Half of the block contained trials with "weak" distractors (a symbol) and the other half contained trials with "strong" distractors (a consonant). After this, a probe was presented, and the subject had to press a button to indicate whether the probe was part of the memory set or not.* ***Bottom left:*** *Time-frequency representation of power when comparing strong and weak distracters. Results revealed higher alpha power in anticipation of strong distracters r than of weak distracters.* ***Bottom right:*** *Source analysis of the alpha activity for the same period comparing strong to weak distracters (8–12 Hz; 0.6–1.1 s; t values are masked corresponding to a p-value of 0.05). Results are significant in the left occipitotemporal cortices (red areas; Adapted from Bonnefond and Jensen, 2012).*

However, recent results and reviews have questioned the role of alpha increase as a mechanism for suppressing distractors processing in particular in attention tasks. Foster and Awh (2019) presented evidence that alpha decrease is important for signal enhancement but reported limited evidence for a role of alpha power in distractor suppression (Foster & Awh, 2019). Although studies have shown that distractor suppression is an important component of visual attention, the authors bring to their review the view that perception at a relevant location can also occur through signal enhancement, which directly improves processing at attended locations. To support their claim, they cite several studies demonstrating that the topography of alpha activity follows the attended location, even in the absence of a distractor. To complete, research has demonstrated that alpha-band activity followed the cued location when the target location was cued but not when the distractor location was cued (Noonan et al., 2016). This finding suggests that alpha-band activity plays a role in signal enhancement but offers no evidence for a role in distractor exclusion.

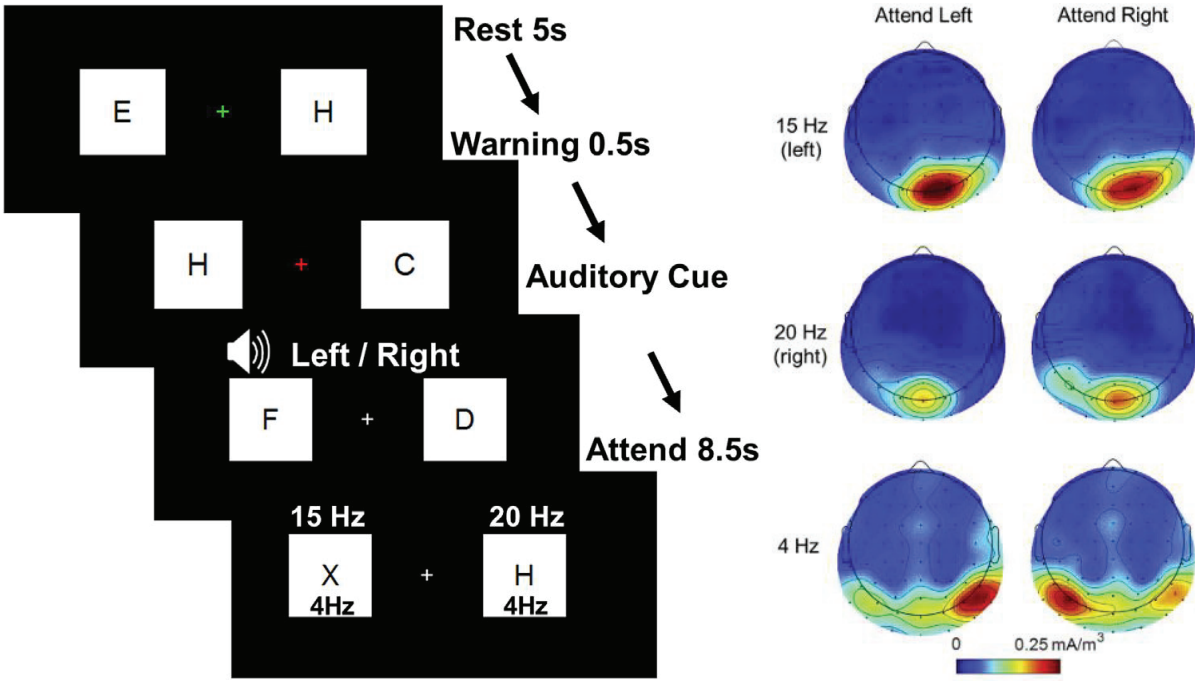

Figure 11*: Example of a steady-state visual evoked potentials (SSVEP) task.* ***Left****, presentation of the task. Black letter sequences changing at 4 Hz were superimposed on white flickering squares (15Hz or 20Hz). Each stimulus is presented at different frequency of flash.* ***Right*** *topoplot of the amplitude of the SSVEP (15Hz, 20Hz, 4Hz). Results showed no suppression of SSVEPs amplitude of the unattended stimuli but an enhancement in the attended side of stimuli (adapted from Antonov et al., 2020)*

Moreover, three studies used steady-state visual evoked potentials (SSVEPs), i.e., the activity generated by visual stimulations at a certain frequency, to test for the link between alpha oscillations and excitability (Antonov et al., 2020; Gundlach et al., 2020; Zhigalov &

Jensen, 2020; **Figure 11**). They all reported an absence of relation between alpha power, in particular the contralateral increase to the unattended side, and the amplitude of the SSVEPs within the same hemisphere. However, the localization of this alpha increase was parietal while SSVEPs were observed over occipital regions (Zhigalov & Jensen, 2020). This alpha increase could either reflect the gating of the information in higher-order regions as suggested by Zhigalov & Jensen (2020) or an inhibition process preventing attention shifts to the unattended side. This could be particularly important in these studies in which covert attention was maintained on the same side for several seconds. It is possible that the authors did not observe a link between occipital alpha and occipital SSVEP amplitude because the rhythmical stimulations might prevent the detection of alpha oscillations (see Samaha et al., 2020 for a short discussion on that issue).

In any case, the link between alpha increase and functional inhibition e.g., protecting perceptual, memory, or reasoning processes from distractors remains to be validated. In particular, the context of the experiment, e.g. the frequency of the distractor, the perceptual load, or the paradigm used to study the suppression of the distractor might play a role (Gutteling et al., 2021; Noonan et al., 2016; van Moorselaar & Slagter, 2020; Wöstmann et al., 2022).

2.1.3. Alpha phase and frequency influence perception and attentional modulation

As I mentioned above, alpha oscillations could be described as pulses of inhibition, therefore perception should also be influenced by the phase of alpha oscillations but also by their frequency as it impacts the duration of the window of excitability.

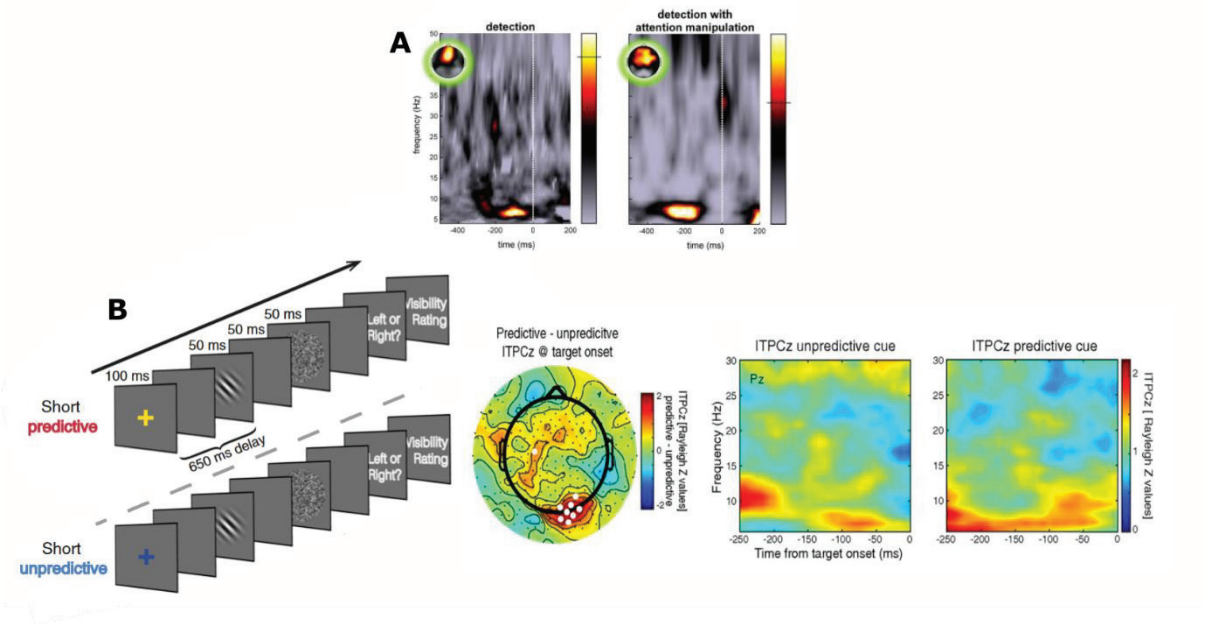

Figure 12: (A) *Two examples of results of correlation between phase and behavior. These results showed that the alpha phase before stimulus influence behavior.* ***Left****, the pre-stimulus alpha phase was strongly predictive if the subject perceives or not a peripherical flash.* ***Right****, the same task with a spatial cue. Results showed that the alpha phase was significatively linked with the detection of a flash light in the attend position (adapted from VanRullen et al., 2011).* ***(B) Left****: Task orientation discrimination design. The predictability of the stimulus onset was manipulated using a cue (650 and 1400ms post-cue).* ***(B) Right****: Topography and time frequency representation of the intertrial phase concentration. Results showed that in trials in which subject could predict the stimulus onset, the alpha-band phase concentration before the stimulus was higher than in trials in which they could not predict the timing (unpredictable trials). These results therefore revealed that alpha phase can be adjusted in anticipation of predictable stimuli to optimize their processing (adapted from Samaha et al., 2015).*

Many studies have demonstrated periodicities in perception and attention (for a review see VanRullen, 2016). Several studies have indeed shown that the phase of alpha oscillation before the stimulus influenced the likelihood of perceiving a near-threshold stimulus as well as the amplitude of early evoked potentials (Alexander et al., 2020; Busch et al., 2009; Busch & VanRullen, 2010; Dou et al., 2021; A. M. Harris et al., 2018; K. E. Mathewson et al., 2009; Samaha et al., 2017; VanRullen et al., 2011;**Figure 12A**). Moreover, a transcranial magnetic stimulation (TMS) study showed a relationship between the alpha phase and the likelihood of perceiving a (occipital) stimulation-induced phosphene in participants (Dugue et al., 2011). In addition, this phase influence depended on alpha power in line with the alpha inhibition hypothesis (Fakche et al., 2022)

Similarly to alpha power, some studies have reported evidence showing that the alpha phase could be under top-down control using tasks in which the timing of stimulus display

was predictable. The alpha phase was adjusted before the stimulus onset either to optimize (alignment of the excitable phase) or suppress (alignment of the inhibition phase) the processing of relevant or irrelevant information respectively (Bonnefond & Jensen, 2012a; Samaha & Postle, 2015; Solís-Vivanco et al., 2018, **Figure 12B**).

Moreover, it has been directly and indirectly shown that when the onset of two simple stimuli, presented successively at a given position, occurs within a cycle of alpha oscillations, they would be considered/integrated by the neural system as a single item (e.g., Samaha & Postle, 2015; Shen et al., 2019; see also Baumgarten et al., 2015 in the somatosensory domain). For instance, Samaha and Postle (2015) specifically showed that the alpha peak frequency of each participant was correlated with the likelihood of perceiving one or two visual flashes when two flashes were presented with a short delay between them .

Similarly, one study has shown that the frequency of alpha oscillations could also be under top-down control. Wutz et al. (2018) showed that the instruction of the task (i.e., the context) could influence the frequency of oscillations adjusted in anticipation of stimuli so that when two stimuli presented closely in time need to be integrated, the frequency of anticipatory oscillations would be slower than when the two stimuli need to be segregated to perform the task. The idea is that the two stimuli would have a higher likelihood to be processed within a cycle if the frequency was slower.

However, there is only sparse evidence for alpha phase/frequency adjustment in anticipation of relevant/irrelevant stimuli and one study did not find phase adjustment in anticipation of predictable stimuli in a cross-modal (visual/auditory) attention task. Some authors reported no evidence of phase alignment in anticipation of targets or distracting stimuli (van Diepen et al., 2015). These authors presented to subjects a cue indicating to identify targets in the visual or auditory domains presented simultaneously. If subjects had to attend to visual stimuli, they had to inhibit the processing of the simultaneous auditory stimulus to perform optimally. For visual stimuli, they had to respond according to the orientation of gratings and for stimuli according to tones. The fact that the authors did not find an anticipatory adjustment of the alpha phase might result from (1) the lack of learning period and (2) the low difficulty level of the task. In particular, given that the two types of stimuli do not share any common characteristics, the unattended stimulus could be poorly distracting. This is highlighted by the small difference in response time between the experiment where both stimuli are presented at the same time and the one where only one is presented.

2.1.4. Generators and laminar profile

The origin of alpha oscillations is not consensual in the literature.

Although in this thesis there will be no result on the laminar profile of alpha oscillations, it seems nevertheless important to address this point in more detail. It should be

noted that in our study number 2 (see chapter 2), we use a headcast to perform a high-resolution MEG which we hope will allow us to study alpha oscillations at the laminar level (for details see below section 3.2.2).

It is important to start with a quick remembering of the cortex composition. The cortex is composed of six layers with a characteristic distribution of neuronal subtypes and their intra-cortical and sub-cortical connections(Palomero-Gallagher & Zilles, 2019; Remmelzwaal et al., 2020 see **Figure 13**). The Molecular Layer is the first layer, and it comprises a few dispersed neurons. It mostly consists of pyramidal neuron apical dendrite extensions, horizontal pyramidal neurons, and axons, horizontal Cajal cells (Cajal-Retzius cells), and glial cells. Layer I is the main target of interhemispheric cortico-cortical Afferences. Layer II is the outer granular layer, which contains numerous small pyramidal and stellate neurons. Small and medium-sized pyramidal neurons, as well as non-pyramidal neurons with axons orientated vertically in the cortex, constitute Layer III, the outer pyramidal layer. Layer III is the principal source of cortico-cortical Efferences. These three first layers could be grouped under the name supragranular layers. Layer IV, the inner granular layer, is the primary target of Thalamo-Cortical Afferences originating from Type C thalamic neurons as well as intra-hemispheric cortico-cortical Afferences. Large pyramidal neurons are found in Layer V, the inner pyramidal layer. These neurons' axons exit the brain and attach to subcortical structures like the Basal Ganglia. Layer VI has a mix of big, tiny, and multiform pyramidal neurons. Efferent fibers are sent into the thalamus by Layer VI, forming a precise and particular link between the cortex and the thalamus. Both excitatory and inhibitory connections exist. Neurons provide excitatory fibers to thalamic neurons and collaterals to the reticular nucleus of the thalamus, which inhibits the same or nearby thalamic neurons. These two last layers are grouped under the name of infragranular layers. This layer also receives connection from the feedback pathway (Bonnefond et al., 2017; Markov et al., 2014)

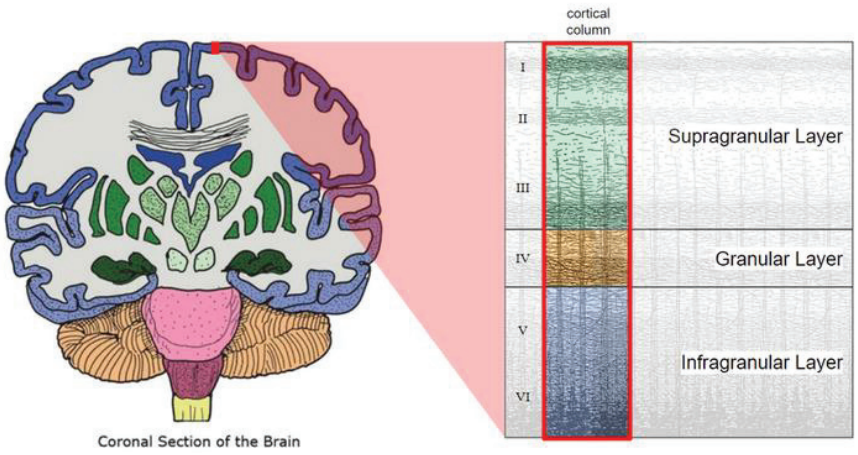

***Figure 13**: The cerebral cortical layers; the cortex is composed of six layers with a characteristic distribution of neuronal subtypes. Supragranular layer (I-III), granular layer (IV), and the infragranular layer (V-VI) in the neocortex. (Adapted from Remmelzwaal et al., 2020)*

First, some studies investigated the laminar profile of alpha oscillations in the visual cortex. In vivo, laminar recording in the visual cortex revealed alpha generators across all cortical layers except in the inferotemporal cortex in which alpha generators were found only in supragranular and infragranular layers (Bollimunta et al., 2008). Synchronization of alpha is often stronger in deeper layers than in superficial (Buffalo et al., 2011; but see Haegens et al., 2015). Alpha oscillations could involve somatostatin cells engaged via lateral connections or trans-laminar fast-spiking neurons engaged by layer 6 neurons (Bortone et al., 2014; Olsen et al., 2012) or layer 5 pyramidal cells (Buchanan et al., 2012) but further research is needed to evaluate their behavior during alpha oscillations. Layer 1 interneurons might also be involved as dendrites from layers 2/3A, 3B, and 5, in which alpha oscillations are observed, reach this layer (Angelucci & Bullier, 2003; Tamura et al., 2004).

But other studies worked on the possibility that alpha oscillations could be generated in other regions. The thalamus, in part, could play the role of generator of alpha oscillation (Hughes et al., 2011; Hughes & Crunelli, 2005; Lorincz et al., 2008, 2009). More recently, a study on cats has highlighted a strong coherence between the thalamus activity, in the lateral geniculate nucleus, and the alpha rhythm in the visual cortex (Lorincz et al., 2009). The activity rhythm of this relay could play a role in the temporal segmentation of inputs arriving in the visual cortex. Furthermore, it has been shown that lesion of the posterior thalamus, reduces alpha activity (Lukashevich & Sazonova, 1996). The pulvinar, another nucleus of the thalamus, is connected to layer 2/3 of a given visual area and layer 4 of the connected visual area below in the hierarchy and as such might be able to control the flow of information between visual regions (Saalmann & Kastner, 2011). Granger causality analyses in monkey data indeed showed that alpha oscillations in the pulvinar would drive alpha oscillations in V4 and temporo-occipital area (TEO) (Saalmann et al., 2012).

2.1.5. Alpha oscillation beyond early sensory region and top-down control of alpha

2.1.5.1. Alpha in high order area

We have seen in the sections above the role of alpha oscillations in the early sensory areas. We will now focus on its potential role in higher areas including in some networks.

We saw briefly in section 1.3.3 the role of the VAN (see also **Figure 14**). This network has been associated with the capture of attention by unattended, but relevant, stimuli (Corbetta et al., 2008; Corbetta & Shulman, 2002). According to the authors, in these both papers, avoiding the capture of attention by irrelevant stimuli required the inhibition of the VAN. We can therefore suggest that alpha oscillations can play an inhibitory role in the VAN, in certain tasks that require focus on a target to respond. An element that allows us to detail this theory is the paper of Solis-Vivanco et al. (2021). The authors showed that decreased distractor interference over participants was linked with increased alpha/beta power in the VAN.

Another network where alpha can play a role is the default mode network (DMN). DMN is engaged during internal concentration. During a task, this network's activity usually diminishes (Ossandon et al., 2011; Raichle, 2015). This network contains bilateral and symmetrical cortical areas, in the medial and lateral parietal, medial prefrontal, and medial and lateral temporal cortices (Raichle, 2015). Ossandon and colleagues (2011) used a task that consisted of a visual target search. Subjects, who have intracranial electrodes, had to find the letter “T” among thirty-five letter “L”. They randomly alternated between the easy condition (target in grey color and distractor in black) and the difficult condition (all the letters are grey). Over the DMN, they detected a significant decrease in gamma activity but also an increase in alpha/beta activity for a shorter period in the easy condition compared to the difficult. This finding suggests that, in the difficult condition, it was necessary to inhibit the DMN by alpha/beta activity for a longer period to succeed in the task.

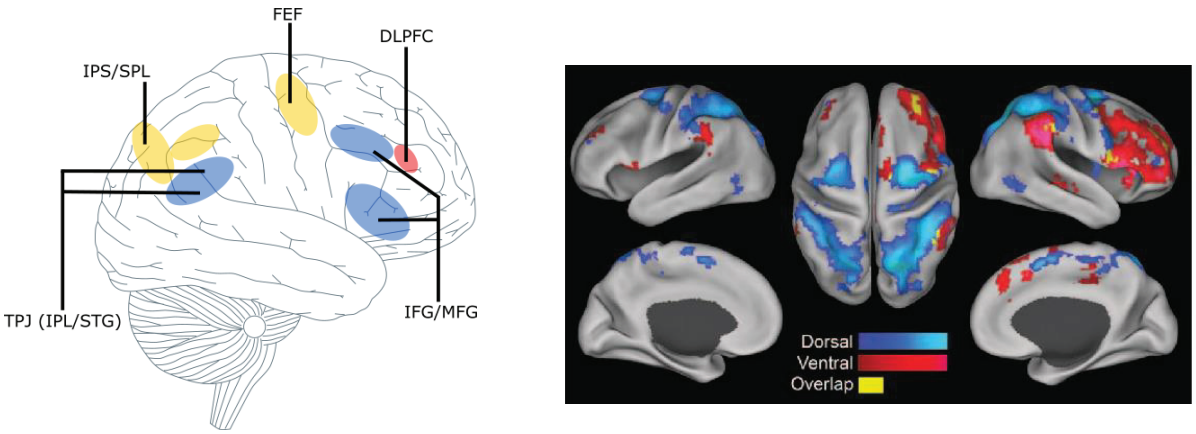

***Figure 14**: **Left**, Dorsal attention network (DAN, in yellow) and ventral attention network (VAN, in blue; only a part of the regions of the VAN are depicted here). FEF: frontal eye fields, IPS: inferior parietal sulcus, SPL: superior lobe, IFG: inferior frontal gyrus, IPL inferior parietal lobe, MFG: middle frontal gyrus, TPJ: temporoparietal junction. DLPFC: dorsolateral prefrontal cortex (adapted from Aboitiz et al., 2014). **Right**, fMRI results highlighting the VAN and the DAN (Adapted from Vossel et al. 2013)*

2.1.5.2. Top-down control of alpha

The process through which the mind adaptably influences bottom-up sensory processing (i.e., exogenous) is known as top-down processing (i.e., endogenous). It involves our expectations, attentional concentration, and other cognitive factors. Many studies have shown the top-down control of alpha oscillations. For example, in a study with monkeys, the authors found that electrostimulation of V4 induced alpha oscillation in V1 (van Kerkoerle et al., 2014). Another study has shown that top-down control of alpha oscillations could originate in brain regions of the dorsal attention network (DAN; see **Figure 14**) such as the frontal eye field (FEF) and the parietal cortex (Zhigalov & Jensen, 2020). A few covert attentional studies have revealed, using EEG, MEG, and TMS that FEF (as well as the right inferior gyrus) was involved in the top-down control of posterior alpha power modulation (Marshall, Bergmann, et al., 2015; Popov et al., 2017; Wang et al., 2016). Additionally, involvement of the dorsolateral prefrontal cortex (DLPFC) in controlling posterior alpha phase adjustment (see section 2.1.3) has been found in working memory and a bimodal attentional task (Bonnefond & Jensen, 2012a; Solís-Vivanco et al., 2018).

One of the brain structures that may therefore be involved in the top-down control of alpha is the DLPFC. This role has been highlighted by several teams in different tasks involving working memory or attentional task (Bonnefond & Jensen, 2013; Zanto et al., 2010).

The role of these different regions in different contexts and how they interact remain however unclear (see next section).

2.2. Open questions regarding alpha oscillations and axes of the thesis

My thesis consists of three chapters testing overlapping and distinct questions.

First, as discussed in section 2.1.2, there is still a debate regarding whether **alpha oscillations are involved in the disengagement of irrelevant areas** and/or in suppressing the processing of unattended information/distractors. **Testing this hypothesis was one of the main goals of this work and involved the three chapters**.

Moreover, most experiments studied alpha modulation in primary cortices (and parietal cortex) but few teams have attempted to determine whether these alpha oscillations are associated with inhibition of irrelevant information processing in brain regions higher up the sensory cortical hierarchy (see Snyder & Foxe, 2010 for an EEG study with limited spatial resolution). It thus remains to be clearly determined whether **these oscillations are also involved in the functional inhibition of higher-level regions**, especially since an opposite role of these oscillations, i.e., a facilitating role, has been demonstrated in monkeys at the level of the temporal cortex (Mo et al., 2011). Moreover, Solis-Vivanco et al. (2021) have shown that upper-band alpha/beta (10-20Hz) were associated with an inhibition of the ventral attention network (VAN), which encompasses the inferior and medial frontal gyri and the temporoparietal junction (see **Figure 14**), during a cross-modal attention task. This network has been associated with the capture of attention by unattended, but relevant, stimuli (Corbetta et al., 2008; Corbetta & Shulman, 2002). Corbetta et al. (2002, 2008) suggested that the inhibition of the VAN was crucial for preventing the capture of attention by irrelevant stimuli. In line with that idea, Solis-Vivanco et al. (2021) reported that higher alpha/beta power in the VAN was associated with lower distractor interference over subjects. Only this study has reported this alpha/beta increase over the VAN so far. Whether alpha increase related to functional inhibition can be found in higher-order regions including the VAN **will be addressed in the three chapters.**

Furthermore, as mentioned in section 2.1.3, there are also contradictory evidence regarding the existence of **alpha phase adjustment** in anticipation of a predictable stimulus. **This will be addressed in the first chapter of the thesis**.

As also discussed in section 2.1.2, modulations of alpha oscillations have mainly been observed during stimulus anticipation in attentional or memory tasks (Bonnefond & Jensen, 2012; Capilla et al., 2014; Haegens et al., 2012; Thut, 2006; but see e.g. Bauer et al., 2014;). **Thus, it remains to be tested whether alpha oscillations can play an inhibitory role during stimulus processing**. This could be particularly crucial in complex cognitive tasks (e.g., reasoning) requiring inhibition of visual processing to reason more abstractly. **This is the goal of the third chapter.**

Finally, as discussed in section 2.1.4, relatively few studies have identified **the brain regions that may control these sensory alpha oscillations**. As most experiments in the

oscillation literature have focused on attention, results have revealed the involvement of the dorsal attentional network namely the frontal eye field (FEF), cortex, parietal cortex or even the pulvinar (Marshall, O'Shea, et al., 2015; Marshall, Bergmann, et al., 2015; Popov et al., 2017; Saalmann et al., 2012). The evidence is scant, however. Furthermore, in tasks requiring cognitive control and inhibition, such as reasoning or Stroop tasks, the dorsolateral prefrontal cortex (DLPFC) plays a particularly important role. Thus, it remains to be determined whether and how this brain region is involved (in the same frequency band or via cross-frequency coupling) in the control of the power and the phase (see Solis-Vivanco et al., 2018) of sensory alpha oscillations. **This will be addressed in the three chapters.**

3. General outline of the thesis

To answer these questions, three MEG experiments have been conducted. Each will be described below and will constitute the chapters of this thesis

3.1. Experiments

The data for the word-color and reasoning tasks were acquired before the beginning of my thesis.

3.1.1. Word and color task

This experiment was an adaptation of the Stroop task involving a visual cue indicating, at each trial, whether the participants should process the color of the ink of the word ('color' condition) or the word itself ('word condition'). The ink and the color indicated by the word were incongruent. This experiment was designed to address points 1, 2, 3, and 5 about (1) whether visual alpha oscillations can emerge in high-level visual regions (here in particular the visual word form area, VWFA, which should be inhibited for subjects to be able to report the color of the 'ink'; see Polk et al. 2008), but also in the VAN (2) whether alpha inhibition phase can be adjusted in order to optimally suppress the processing of the word in the 'color' condition (the timing of the onset of the stimulus was predictable) and (3) whether these alpha oscillations are controlled by the DLPFC.

3.1.2. Faces and names task

This experiment is similar to the task presented above. We designed this task because the design of the previous task was not adapted for optimal distractor suppression. In this task, participants were asked at the beginning of each block to either attend the name or the face of a stimulus by combining a name on top of a face. More specifically they were asked to determine whether the name/face was more considered as female or male. The names and faces could be either congruent or incongruent. This experiment will answer questions 1, 2,

and 5 about whether visual alpha oscillations can emerge in high-level visual regions, (here in particular the VAN, the visual word form area, VWFA, which should be inhibited in the condition where subjects have to attend faces and the Fusiform Face Area, FFA, in the opposite condition) and whether these oscillations are controlled by the DLPFC. In addition, we aim at analyzing the laminar profile of alpha oscillations in this task (future direction; see section 2.1.4 and see below).

3.1.3. Reasoning task

This experiment we used was a reasoning task hypothesized to involve the inhibition of the visual cortex by the DLPFC in order to perform well as demonstrated by an fMRI experiment (Prado & Noveck, 2007). Specifically, subjects were given a rule and asked to respond whether the stimuli that appeared afterward confirmed this rule or not. For example, the rule could be "If there is a J, then there is not a square" and the stimulus a J in a square. In that example, participants must overcome the so-called "matching bias", the tendency to answer "correct" whenever the stimuli presented match the ones mentioned in the rule, to perform well. This experiment will address points 1, 2, 4, and 5 mentioned in section 2.2 as to whether visual alpha oscillations reflect functional inhibition during stimulus processing in a high-level cognitive task and whether the DLPFC exerts top-down control over these posterior oscillations.

3.2. Techniques

3.2.1. Behavior analysis

Behavioral data are informative regarding the processing performed by the brain. Analyses of hit rate and response time (RT) inform about the task difficulty and the processing time

3.2.2. High-resolution MEG (and MRI)

For analyzing brain oscillatory activity, different techniques are available. We used MEG for the three experiments to investigate the role of alpha oscillations (see section 1). We chose MEG because this technique combines a high spatial and temporal resolution which was necessary to answer the questions formulated above. Moreover, the advantage of measuring magnetic fields rather than electric fields, as in EEG-is that they pass through the skull and other tissues between the active neurons and the MEG detectors without distortion (unlike EEG, where the signal is more blurred or fuzzy).

In our second study (chapter 2), we used high-resolution MEG that is expected to allow us to detect the activity with excellent spatial precision, which can go up to the laminar scale. This precision is possible thanks to individual headcasts that drastically reduce head movements within the MEG and thus significantly improve its spatial resolution(Bonaiuto et

al., 2018; Meyer et al., 2017). Two factors reduce precision of results in MEG data. The co-registration between anatomical MRI and the MEG data and the movement of the head during the acquisition which can create ~5mm of uncertainty. In previous studies, the headcast reduced head movements by under 0.2 mm in the x and y dimensions, and under 1.5 mm in the z dimension, while co-registration error was under 1.5 mm in any dimension (Bonaiuto et al., 2018). In our study, we adapted this headcast to the supine position of the subject which already reduces the head movements, especially on the z-axis. These headcasts were designed by Denis Schwartz and Sébastien Daligault from the anatomical MRI of each subject using a 3D printer available at the Cermep imaging center of Lyon (**Figure 15**). I have been involved in the development of this headcast, including the improvement of the design and pilots to check the reproducibility of the repositioning of the headcast and the MEG coils. To obtain this headcast we first extracted an image of the skull from an MRI image of the subject. Based on it, we constructed a foam head-cast that fit with the participants' scalp and the MEG dewar (Bonaiuto et al., 2018; Meyer et al., 2017). First, scalp surfaces with coils positions were extracted from the MRI scan. Next, the surfaces obtained were modelized to print with the 3D printer. The 3D printed model was then placed inside a replica of the MEG dewar and the space between was filled with polyurethane foam to create the participant-specific headcast with a location for MEG fiducial coils placed during scanning.

***Figure 15**: Design of the headcast used for the study in the chapter 2*

3.2.3. MEG data analysis

3.2.3.1. Preprocessing

To obtain results with MEG there are some steps to follow. As we see above (section 1), the magnetic fields due to neural activity are extremely weak, thus measuring them is challenging both in terms of required sensitivity and also in the ability to suppress interference several orders of magnitude stronger than the signals of interest. Before analysis, MEG data often undergo several preprocessing steps. First is artifact detection and removal. The different types of artifacts are blinks, saccades, and muscles contraction during the period of interest. Muscles artifacts can result from neck or jaw contraction. The activity produced

by this contraction adds noise higher than recorded brain activity. For the blinks and saccades, in addition to the fact that produce a little muscles contraction around the eyes, all our tasks are visual so if the subject closed his eyes or did not look at the desired location, this did not allow him to perform the task properly. To detect all these artifacts, we started with automatic detection by computing the z-score followed by visual control. The z-score describes the position of a point s in terms of its distance from the mean when measured in standard deviation units. There is another important element to check, the head movement. Using the coils on the subject (for the first and last study) or in the headcast (for the second study) it is possible to follow head movement during the task and see the relative position to the MEG sensors. This step is important because when evaluating MEG data at both the sensors and sources levels, head motions may reduce statistical sensitivity. As a result, it is advised to include head motions in the offline MEG analysis (for further information see Stolk et al., 2013).

3.2.3.2. Time frequency and sensor analysis

We saw above that oscillations can be described by three features, frequency, power, and phase (see section 1 and **Figure 4A**). The best way to characterize their temporal dynamics is the time-frequency analysis. This analysis measures the changes in power and phase of neural oscillations across time at different frequencies. This allows us to see the dynamic of these changes. The time-frequency representation (TFR) allows us to see the results of this analysis in one graph with the time on the x-axis, frequency on the y-axis, and the power on the color scale. This type of analysis can be calculated for each MEG sensor to see what they record individually. Thus, we can define if activity comes from left occipital regions, for example, but it is difficult to be more precise. Moreover, Planar gradients of the MEG field distribution were computed for the sensor-level studies (Bastiaansen & Knösche, 2000). In order to approximate the signal obtained by MEG systems with planar gradiometers, we employed the closest neighbor approach to determine the horizontal and vertical components of the estimated planar gradients. The biggest signal of the planar gradient is often situated above the source; therefore, this format makes it easier to analyze sensor-level data. To enhance precision, it is necessary to turn to another type of analysis, the source analysis.

3.2.3.3. Source analysis

The goal of the source analysis is to estimate the source producing the activity recorded by sensors. There are several techniques and parameters for estimating sources. In this paragraph, we will first see the general functioning of the forward and inverse model. Then we will discuss the methods that we have used during this thesis.

Before it is necessary to align the anatomical MRI of the subject and the sensor of the MEG. For this step, we used fiducials placed on the subject during the MRI session and those placed in the headcast during the MEG session. It is commonly referred to as co-registration.

The forward model (also called a gain or lead field matrix) allows to calculate an estimate of the field measured by the MEG sensors for a given current distribution. To do this, one of the methods is to build so-called "realistic" models of the different tissues of the head. These models are built for each subject individually from their anatomical MRI. -Image processing methods, call segmentation, are then used to extract the different brain structures. We calculate the leadfield, i.e., for each point of the constructed mesh we simulate a source and look at the sensors to see the results that will be recorded if this was the case during our experiments.

The next step is to compute the inverse model. It consists of estimating the distribution of the current sources having produced the magnetic fields measured at the surface of the scalp, each source is represented by a current dipole. There are several techniques to solve the inverse problem, but we will develop here only the beamformer method. Among other methods we can mention minimal norm estimation (MNE; Pascual-Marqui et al., 1994), low-resolution brain electromagnetic tomography (Loreta; M. Hämäläinen & Ilmoniemi, 1994) or dSPM (dynamic statistical parametric mapping; Dale et al., 2000). The MNE is a distributed inverse solution that discretizes the source space into locations on the cortical surface or in the brain volume using many equivalent current dipoles. It estimates the amplitude of all modeled source locations simultaneously and recovers a source distribution with minimum overall energy that produces data consistent with the measurement.

The beamformer is a spatial filtering method. It is an approach consisting of calculating at each point of the space a filter which applied to the data extracts the contribution of the source placed in this point and cancels the contribution of the other sources. We used two types of methods during this thesis: Dynamical Imaging of Coherent Sources (DICS) and the Linearly Constrained Minimum Variance (LCMV). The first one is based on estimation calculated in the frequency domain (Gross et al., 2001). The second one is on the time domain (Van Veen et al., 1997).

3.2.3.4. Statistics

For the statistic part of our MEG analyses, we have used the nonparametric cluster-based permutation analysis (Maris & Oostenveld, 2007). To summarize, the first step is to calculate paired t-tests for each data sample between two conditions over subjects, which are then thresholded at $P < 0.05$. The second step is to select significant samples to group into connected sets (clusters) based on temporal, spatial, and spectral adjacency. Then we keep the sum within each cluster, and the procedure is repeated 1000 times on randomly shuffled

data in the condition assignment within each individual. From this distribution, the cluster probability of each is computed. Clusters are labeled as significant under a P-value (e.g., $P \leq 0.05$).

Chapter 1: Functional inhibition of the ventral attention and default mode networks during an attentional task

Alpha-Beta oscillations implement the inhibition of the ventral attention and default mode networks during an attention task

Ferez M., Luther L., Jensen O., Bonnefond M.

(submitted)

Abstract

Selective attention is a crucial mechanism that allows us to focus on relevant information or, conversely, to ignore irrelevant information. Recently, several studies have provided results questioning the link between alpha oscillations and functional inhibition. In this MEG study with 20 participants, we used a modified Stroop task to determine (1) whether alpha oscillations are associated to functional inhibition over high-order visual regions as well as the ventral attention network (VAN), (2) whether alpha phase is adjusted in anticipation of relevant and irrelevant stimuli. We did not find a significant increase of pre-stimulus alpha power and phase in the attend-color condition compared to the attend-word condition, in line with the absence of Stroop effect at the behavioral level. However, we found higher alpha/beta power (10-20 Hz), compared to control conditions, in the VAN in anticipation and during the processing of stimuli in all conditions. We also found higher alpha/beta in several nodes of the default mode network (DMN). The alpha-beta power in several node of the VAN and DMN was associated with faster reaction times indicating that the inhibition of these networks might help to perform the task. In addition, we found stronger theta (4 Hz) power in anticipation and during stimulus processing over the cognitive control network. Furthermore, this theta power was associated with faster reaction times possibly indicating that good performances in the task involved a high level of cognitive control.

Introduction

Selective attention is a crucial mechanism that allows us to focus on relevant information and, conversely, to ignore irrelevant information. For instance, it has been shown that ignoring elements of a stimulus in a working memory task would allow to remember more efficiently (Zanto & Gazzaley, 2009). Understanding this mechanism seems therefore crucial.

Over the past few years, many research groups suggested that alpha oscillations (~10Hz) would be involved in such a mechanism as an increase of alpha amplitude would be associated with a decrease of the excitability and vice versa (for a review see Foxe & Snyder, 2011; Jensen et al., 2012; Klimesch et al., 2007). In visual attention tasks, it was shown, using magnetoencephalography (MEG) and electroencephalography (EEG), that alpha amplitude decreased over posterior regions contralateral to the attended stimulus (Capilla et al., 2014; Dombrowe & Hilgetag, 2014; Gould et al., 2011; Ikkai et al., 2016; Kelly et al., 2009; Rihs et al., 2009; Rihs et al., 2007; Thut, 2006; Worden et al., 2000). Similar results were found over somatosensory areas in somatosensory attention paradigms (Haegens et al., 2012; Haegens, Händel, et al., 2011; Trenner et al., 2008) . An increase of alpha amplitude was further observed over posterior regions ipsilateral to the attended side, in particular when a distracter was presented on the unattended side, (Green et al., 2017; Gutteling et al., 2021; Haegens et al., 2012; Ikkai et al., 2016; Kelly et al., 2006; Rihs et al., 2009; Sauseng et al., 2009; Siegel et al., 2008; Wildegger et al., 2017). In working memory tasks, an increase of alpha

power was also observed in the non-engaged stream (Bonnefond & Jensen, 2012; Jokisch & Jensen, 2007; Park et al., 2014; Payne et al., 2013). This alpha increase would allow to protect perceptual and working memory processes from distractors. In addition, an increase of high-alpha/low beta amplitude has been observed in the ventral attention network (VAN), interpreted as reflecting inhibition of this network (see Corbetta & Shulman, 2002), during a goal-driven task (Solís-Vivanco et al., 2021).

Recently, several studies have provided results questioning the link between alpha oscillations and functional inhibition (Antonov et al., 2020; Foster & Awh, 2019; Gundlach et al., 2020; Zhigalov & Jensen, 2020). These studies tested the link between excitability, as indexed by steady-state visual evoked potentials (SSVEPs) and alpha oscillation using EEG or MEG. They reported no link between the non-attended SSVEPs and the ipsilateral alpha increase in amplitude, space, or latency. In particular, one of this study showed that the target/distractor' SSVEPs was localized in the early occipital cortex whereas the alpha modulation originated in the occipito-parietal cortex (Zhigalov & Jensen, 2020). They hypothesized that the parietal increase could implement a gating rather than a gain control mechanism. However, it is possible that rhythmical visual stimulation could alter the detection of alpha modulation in the early cortex (see Samaha et al., 2020 for a discussion) Altogether, these studies showed that the link between alpha oscillations and functional inhibition remains to be clarified. Furthermore, alpha modulation has been mostly reported in early visual regions; whether a similar mechanism could be observed over higher order visual regions remains to be investigated (but see Capilla et al., 2014; Snyder & Foxe, 2010).

In addition to the top-down modulation of alpha amplitude, different studies have shown that alpha phase could be adjusted in anticipation of relevant or irrelevant stimuli when the timing of stimulus presentation was predictable (Bonnefond & Jensen, 2012; Samaha & Postle, 2015; Solís-Vivanco et al., 2018). This adjustment appears to optimize behavioral performances by improving the processing of relevant stimuli and suppressing the processing of irrelevant stimuli. One study, however, did not find phase adjustment in anticipation of predictable stimuli (van Diepen et al., 2015). Finally, it is still unclear which brain regions are involved in the control of posterior alpha. A few covert attentional studies have revealed, using EEG, MEG and TMS that frontal eye field (FEF) (as well as the right inferior gyrus) was involved in the top-down control of posterior alpha power modulation (Marshall, Bergmann, et al., 2015; Popov et al., 2017; Wang et al., 2016). Additionally, an involvement of the left frontal gyrus in controlling posterior alpha phase adjustment has been reported in a working memory and a bimodal attentional tasks (Bonnefond & Jensen, 2012; Solís-Vivanco et al., 2018). The role of these different regions in different cognitive tasks or in controlling alpha amplitude versus phase remains to be further explored.

The goal of the experiment presented in this paper was to determine (1) whether alpha oscillations are associated to functional inhibition over high-order visual regions as well

as the VAN (see Solís-Vivanco et al., 2021) and (2) whether alpha phase is adjusted in anticipation of relevant and irrelevant stimuli and (3) which brain regions are involved in controlling visual alpha amplitude and phase.

To investigate these questions, we used MEG and designed a cue-based modified Stroop task inspired by the Stroop task (Stroop, 1935). In the Stroop task, participants are asked to report the color of the ink of a word indicating a different color. In the current study, a cue indicated, in each trial, to the participants whether they should report the color of the ink (attend-color condition), or the color indicated by the word (attend-word condition). In an fMRI study that used a Stroop task, the authors reported an increase of the BOLD signal in the 'color area' and a decrease in visual word form area while participants were reporting the color of the ink (VWFA; Polk et al., 2008). As a negative correlation between alpha oscillation and BOLD signal has been shown in several EEG-fMRI tasks (e.g. Laufs et al., 2006; Scheeringa et al., 2011), we hypothesized that alpha oscillations should increase in the VWFA and possibly decrease in the color area in the attend-color condition. Moreover, as in our task design participants could predict stimuli onset, we hypothesized that the alpha phase would be adjusted in anticipation of the stimuli but with a different adjusted phase in the VWFA and the color area in the attend-color condition. More precisely, we expect that, at the moment of the processing of the stimulus, the phase adjusted in VWFA would be associated with inhibition, to optimally suppress the processing the word, and the phase adjusted in the color area would be associated with excitation, to optimally process the color of the ink. We predicted that alpha amplitude and phase modulations would be correlated with performance.

We did not find a slower reaction times in the color than in the attend-word condition. This absence of effect might result from the presentation duration or the training of participants. We found no significant modulation of alpha power and phase in anticipation of the stimuli in the attend-color compared to the attend-word condition. We however found higher alpha/beta power in the VAN in anticipation and during processing of stimuli in both conditions. We also found alpha/beta in several nodes of the default mode network (DMN) indicating a possible inhibition of this network in anticipation and during stimulus processing. The alpha-beta power in some nodes of the VAN and DMN was associated with faster reaction times indicating that the inhibition of these two networks might help to perform the task. In addition, we found strong theta power in anticipation and during stimulus processing over the right dorsolateral prefrontal cortex, the ACC, and the ventromedial prefrontal cortex, i.e., regions associated with cognitive control. High theta power was associated with faster reaction times, possibly indicating that good performances in the task involved a high level of cognitive control.

Methods

Participants

The study was carried out at the Donders Institute for Brain, Cognition and Behaviour. Twenty healthy native Dutch-speaking volunteers (age: 23 ± 2.95 years; 15 females) participated in the experiment after providing written informed consent according to the Declaration of Helsinki and the local ethics board. They were recruited from Radboud University's research participation scheme. All subjects had normal or corrected-to-normal vision and were right-handed according to the Edinburg Handedness Inventory (Oldfield, 1971).

Stimulus material and procedure

The cue-based modified Stroop task (see ***Figure 16***) was designed using MATLAB (MathWorks) and Psychtoolbox (psychtoolbox.org). The background of the screen was black during the entire experiment. Following an intertrial period of 1500 to 2000ms during which blinks were allowed, a trial started with a white dot presented during 1200ms (baseline period) followed by a cue during 100ms. The onset of the cue corresponding to the time 0 in our analyses. Three different cues, representing abstract geometrical shapes, were presented (see ***Figure 16***). One indicated to the participant to attend the word (attend-word condition) while another one indicated to attend the ink's color (attend-color condition). These two cues were presented in 80% of trials. The third cue indicated that the participants would just have to determine whether a stimulus was presented in the trial (detect condition; 20% of the trials). The association between a given cue and a given condition was randomized across participants. After a delay of 1200ms (i.e., constant across trials), during which participants were asked to fixate the central white dot, visual stimuli were presented centrally for 100ms. We used three colors, red, blue, and yellow. Each word designating a color was associated with incongruent colors of the ink. The word blue ('BLAUW' in Dutch) was written in red or yellow, the word red ('ROOD' in Dutch) was written in blue or yellow and the word yellow ('GEEL' in Dutch) was written in blue or red. Colored words were presented in 80% of the trials while no stimuli were presented in 20% of the remaining trials (525 trials in total). The participants also performed a similar task in fMRI another day (see procedure; data not analyzed here) with the aim of comparing Blood Oxygen Level Dependent (BOLD) signal and time-frequency power variations. Trials without stimuli were used in order to get a better BOLD signal estimate of the anticipatory activity in the fMRI data. They were also used in the present experiment in order to keep the design similar between recording methods. Participant were asked to respond as fast and accurate as possible by pressing one of the three buttons of a response pad. Each button was associated with a color and the association was randomized across participants. In the attend-color and attend-word conditions, participants were asked to press any button when no stimulus was presented. In the detect

condition, the first and second buttons were associated with the 'stimulus present' and 'stimulus absent' responses respectively. Reaction time (RT) and response accuracy (RA) were recorded along the experiment. Trials of each condition were randomly presented.

In addition, two localizer tasks were performed. In the word localizer task, participants were presented with words, pseudo-words or checkerboards for 80ms with an intertrial interval of 800ms. We used 120 highly imaginable nouns (3-7 letters and 1-3 syllables in length). Pseudo-words were derived from them so that the frequency distribution of consonants was similar between words and pseudo-words. Checkerboards were rectangles and extended from 2° to 6° away from fixation with approximately the same vertical size as letter strings. The different categories of stimuli were presented in different blocks (6 per condition) of 20 trials. The task of participants was to detect deviants (words and pseudo-words with lower-case letters and checkerboards with missing black squares; 5% of trials). In the color localizer task, participants were presented with colored or grayscale paintings (215 trials in each condition). Stimuli were presented in center of the screen and measured 10*6cm at a distance of 80cm. The task of the participants was to detect drawings of a child among known paintings (5% of trials). However, these tasks were performed at the end of the recording session, participants moved more than during the main task and were more tense generating many muscular artifacts. An issue with the code of the triggers further impacted the analyses. The remaining number of trials did not allow us to localize the areas specialized in color and word processing in each participant and to perform region of interest analyses at the source level.

Data acquisition

Neuromagnetic activity was recorded at a sampling rate of 1200Hz, using a 275 first-order axial gradiometers whole-head MEG system (VSF/CTF Systems, Port Coquitlam, Canada) housed in a magnetically shielded room. To measure the subject's head position relative to the MEG during the experiment, three marker coils were placed respectively at the nasion and the left and right ear canals. During the experiment, horizontal and vertical eye movements were recorded using vertical and horizontal EOG electrodes. Subjects were in the supine position during the recording.

An anatomical T1 MRI of the participants was acquired with a 3T Siemens Sonata system (Erlangen, Germany) with a voxel size of $1mm^3$. For the co-registration of the MRI and the MEG data, tablets of Vitamin E were used and placed at the position of the coils.

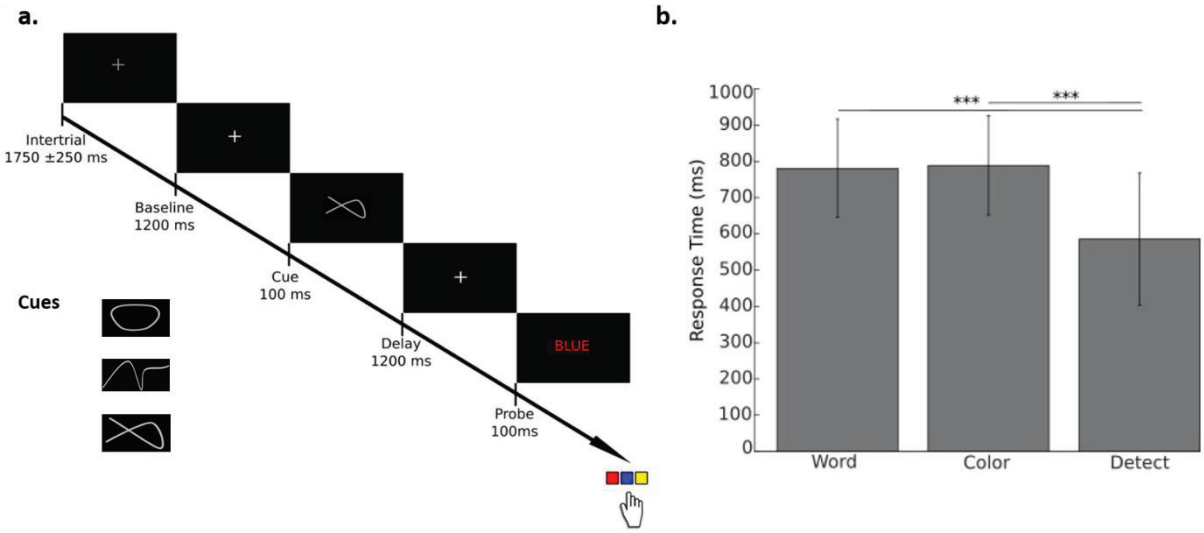

Figure 16 Task design and behavior results. *(**a**) Following a 1200ms baseline, a cue (the three types of cue used are presented below the task design) instructed the participants to either attend the color of the ink (attend-color condition; 40% of the trials), the color designated by the word (attend-word condition; 40% of the trials) or to determine whether a stimulus was presented (detect condition; 20% of the trials). Participants were asked to respond as accurately and fast as possible following the presentation of the stimuli. A stimulus was presented in 80% of the trials in each condition. (**b**) behavioral results. Mean of response times (RT) of all subjects for trials with correct answers and conditions with a stimulus presented on the screen. Error bars represent standard error of the mean. No significative difference between word and attend-color conditions was observed. Significant differences between the mean RT in word/color condition and detect condition were observed (*** = p<0.001).*

Procedure

The experiment was conducted over three consecutive days for each participant. During the first day, inclusion criteria were confirmed, general information about the study and informed consent letters were provided, and detailed instructions about the experiment were presented. Participants then performed a practice session composed of 150 trials inside the MEG room (60 trials for the two main conditions and 30 for the detect condition). This training session was necessary for the participants to get familiar with the cue-stimulus delay. This familiarity allowed us to test whether alpha phase was adjusted in anticipation of stimuli (see Bonnefond & Jensen, 2012; Samaha et al., 2015; Solís-Vivanco et al., 2018). During the second day, the MEG experiment or an fMRI experiment with a similar task was conducted (fMRI analyses performed separately). During the third day, the fMRI or the MEG experiment was performed depending on the neuroimaging technique used during the second session. During the fMRI session, the MRI of each subject was obtained. Participants were asked to wear no make-up during recordings and to wash their hair and change their clothes between the fMRI and the MEG session when the fMRI session occurred first. We did not observe

different noise levels in the MEG recordings (using fieldtrip data quality check procedure) between participants who performed the fMRI first and those who performed the MEG first.

Data analysis

Reaction times (RTs) were obtained from the subjects' response pad responses. RTs shorter than 250ms or longer than the mean + 2std were excluded.

The MEG analyses were performed using the Fieldtrip software package (Oostenveld et al., 2011). MEG data were epoched 1000ms before the onset of the cue until 600ms after stimulus onset. An automatic rejection, based on a z-score algorithm across sensors exceeding a threshold given by the data variance within each participant, of eye blink or saccades, SQUID jumps, or muscles artifacts was run. Additional visual inspection was applied to the remaining trials before including them in further analyses. Only epochs without artifacts and with correct answer were considered. 60% of the trials were kept in average.

For the sensor-level analyses, Planar gradients of the MEG field distribution were calculated (Bastiaansen & Knösche, 2000). For this purpose, we used a nearest neighbor method where the horizontal and vertical components of the estimated planar gradients were derived, therefore approximating the signal measured by MEG systems with planar gradiometers. This representation facilitates the interpretation of the sensor-level data, because the largest signal of the planar gradient is typically located above the source.
Time-frequency representations (TFRs) were obtained using a fast Fourier transformation approach with a 3 cycles long adaptive sliding time window ($\Delta T = 3/f$; e.g., ΔT = 300 msec for the 10Hz frequency). A hanning taper (ΔT long) was multiplied by the data before the Fourier transformation. For the planar gradient, the TFRs of power were estimated for the horizontal and vertical components and then summed. The power for the individual trials was averaged over conditions and log- transformed.

In order to determine the amplitude of the alpha activity phase-locked prior to stimulus onset, TFR of the power of averaged epochs (i.e., the event related fields; ERF) were calculated as well.

Source localization for the main task was performed using a frequency domain beamforming approach based on an adaptative filtering technique (Dynamic Imaging of Coherent Sources, DICS; Gross et al., 2001). We obtained cross-spectral density matrices by applying a multitaper FFT approach (ΔT = 300 msec; one orthogonal Slepian taper resulting in 4 Hz smoothing) on data measured from the axial sensors. A realistically shaped single-shell description of the brain was constructed, based on the individual anatomical MRIs and head shapes (Nolte, 2003). The brain volume of each participant was divided into a grid with a 1-

cm resolution and normalized to the template MNI brain (International Consortium for Brain Mapping, Montreal Neurological Institute, Canada) using SPM8 (www.fil. ion.ucl.ac.uk/spm). The lead field and the cross-spectral density were used to calculate a spatial filter for each grid point (Gross et al., 2001), and the spatial distribution of power was estimated for each condition in each participant. A common filter was used for both conditions, i.e., it was based on the cross-spectral density matrices of the combined conditions. The regularization parameter was set at 5%. As in the sensor-level analyses, the estimated power was averaged over trials and log transformed. The contrast between conditions was performed and averaged across participants. The source estimates were plotted on a standard MNI brain found in SPM8.

Statistics

Regarding the behavior, accuracy and response time (RT) were analyzed using t-tests. The significance of power differences observed between conditions at both sensor and source levels were assessed using a cluster based nonparametric randomization test (Maris & Oostenveld, 2007). This test controls for the Type I error rate in situations involving multiple comparisons over sensors, frequencies, and times by clustering neighboring sensors, time points, and frequency points that show the same effect.

By randomly permuting the data across the two conditions and recalculating the test statistic 1000 times, we obtained a reference distribution to evaluate the statistics significance of a given effect (Monte Carlo estimation). Sensors or voxels for which the t value of the difference between conditions exceeded an a priori threshold ($p < .05$) were selected and subsequently clustered on the basis of spatial adjacency, and the maximum sum of the t values within a cluster was used at the cluster-level statistic.

Results

Similar performances in the attend-color and in the attend-word condition

We did not observe any differences between the attend-word and attend-color conditions in terms of accuracy (respectively: 92.4±5.1; 91.5±4.9), but we did observe a significant difference between these conditions and the detect condition (97.3±3.6; tstat(19)=-5.91,p=1.08e-5; tstat(19)=-5.94,p=1.01e-5).

Analysis of RTs, for trials with correct answers, revealed no difference between the attend-word and the attend-color conditions (see ***Figure 16***; respectively 781 ± 135.7ms vs 788.9 ± 137.1 ms). We observed a significant difference between word or attend-color condition and detect condition (585.9 ± 181.9 ms; tstat(19)= 7.95, p=1.83e-7 and tstat(19) =7.27, p=6.70e-7).

To summarize, subject responded faster and with higher accuracy when they just had to detect whether a stimulus was presented.

Whether it results from training or from the stimulus duration presentation, we could not find a Stroop effect (i.e., a slower RT in the attend-color condition).

We further analyzed the number of interference errors, i.e., reporting the color of the word and of the ink in the attend-color and attend-word condition. We observed a higher number of interference error compared to the other error participants could make (i.e. reporting a color that was not presented in either dimension) in both conditions ($F(1,19) = 30.73$, $p = 2.39*10^{-5}$) while the response times to both types of errors were not different.

No difference in anticipatory alpha power and phase in attend-color vs attend-word condition

We then quantified the alpha power from the MEG data for the attend-color condition and the attend-word condition. The TFR of power did reveal several time-windows with increased alpha power in the attend-color condition over the left temporal cortex. These increases of alpha power occurred every ~600ms (possibly following a delta rhythm) with a burst occurring just after the onset of the stimulus. None of these effects did however survive multiple comparisons correction ($p < 0.01$ before correction).

Similarly, in the averaged epochs (testing for the alpha phase alignment), we found bursts of strong alpha power in the attend-color condition but as for the analysis above, these effects did not survive multiple comparisons correction. In both conditions, higher alpha power of the average epochs was however observed over temporal regions compared to baseline ($p < 0.05$) indicating a general alpha phase adjustment effect.

Alpha/Beta increase in the ventral attention and the default mode networks in anticipation of relevant stimuli

In both conditions, we observed a power increase in the 5-7Hz and 10-20 Hz range over middle and right scalp regions before and during stimulus processing ([attend-color+ attend-word]; **Figure 17a**). The cluster-based randomization test controlling for multiple comparisons over time (baseline vs. anticipatory period), frequency (4-30 Hz), and sensors revealed that this difference was significant from 700ms before stimuli onset (cluster-level statistic [CS] = 80535, $p = 9.9*10^{-4}$; one cluster only was found as the two frequency bands were connected on a few data points). The effect reported also survived an FDR correction at sensor level. Also, as in Solis-Vivanco et al. (2021), we explored the association between averaged power values of both conditions and the number of total interference errors along

the task. We found that stronger power (baseline corrected) during the anticipatory period was inversely related with interference errors but this effect did not reach significance (attend-color condition: r=-0.3; p=0.14; attend-word condition: r=-0.2; p = 0.2) which was expected given the low number of participants (Schönbrodt & Perugini, 2013). The statistical test (baseline vs anticipatory period) also highlighted a significant decrease in the 10-25 Hz range over the left hemisphere (CS =-8301, $p = 9.9*10^{-4}$) and in the 8-12Hz over the occipito-temporal cortex (CS =-108, p=0.04). We interpreted this decrease as reflecting motor and stimulus processing anticipation respectively (see Solis-Vivanco et al., 2021 for a discussion and further analyses on a similar effect).

The power increase of 10-20 Hz was further explored at source level (15 Hz; CS = 4842, $p = 9.9*10^{-4}$; the regions reported here also survived an FDR correction at source level**; Figure 17b**). More precisely, we labelled the top significant areas using the AAL atlas by Tzourio-Mazoyer et al. (2002), and found the right inferior frontal gyrus (IFG; MNI [42 32 12]), the right medial frontal gyrus (MFG, MNI [42 20 50]), the right temporo-parietal junction (TPJ, MNI [58 -52 24])), the right middle temporal cortex [-64 – 4 – 14]. All these regions have been found to be part of the ventral attention network (VAN) or connected to it (Alves et al., 2019).

We further found the bilateral medial superior prefrontal cortices (mPFC; MNI[-16 40 20] and [22 40 24]), the right posterior cingulate cortex/ cuneus (PPC; MNI [6 -42 10]; the right angular cortex (MNI[42 -60 24]) and the right temporal pole (MNI[66 10 -20]). All these regions have been found to be part of the default mode network (DMN; Alves et al., 2019; Buckner & DiNicola, 2019). The power over these regions was stronger in anticipation of the word onset and during stimulus processing.

We could not independently localize the effect observed in the 5-7Hz as it merged with the upper band effect due to frequency smoothing associated with the source localization (but see below). We however observed the bilateral anterior cingulate cortex (ACC: MNI[-10 20 28] and [12 34 30]), the right middle frontal node (MNI[34 48 22]) in addition of the other sources. Some of these regions have been found to be part of the 'cognitive control network' (CNN; Cole et al., 2012; Cole & Schneider, 2007).

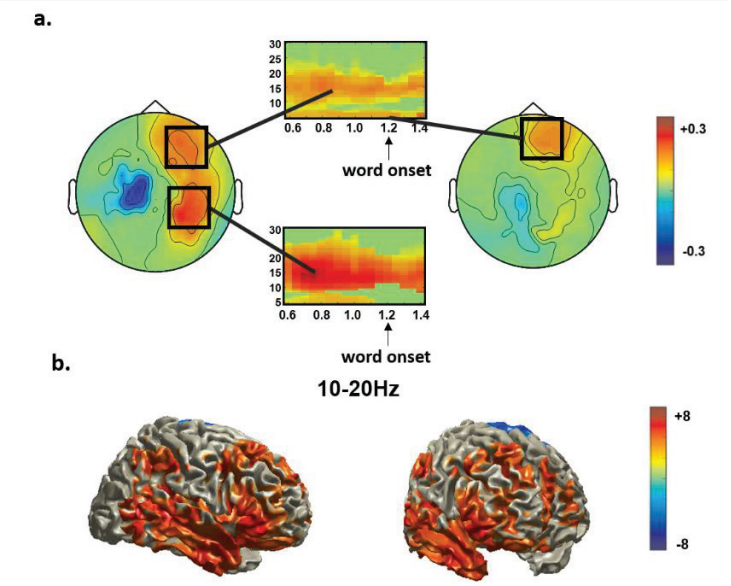

***Figure 17**: **High alpha/beta power over the VAN and the DMN in anticipation and during the processing of relevant stimuli.** (a) Results from cluster-based permutation tests in each condition. Time-frequency representations (TFR) of power from 0.6 to 1.4 s after the cue (word onset at 1.2s compared to baseline (pre-cue period). 5-7Hz and 10-20Hz power was stronger than during baseline over a right fronto-temporal cluster in anticipation and during stimulus processing. 10-25Hz power was lower than during baseline over a left central cluster (b) Source localization of the right 10-20Hz increase (and decrease) compared to baseline. The regions observed are part of the VAN and DMN.*

We further analyzed the contrast between conditions. While we did not find differences between word and attend-color conditions, we found stronger 10-20Hz over right temporal and frontal sensors as well as left sensors in both attend-color (CS = 16509, p = $9.9*10^{-4}$ and CS = 87, p = 0.049) and attend-word (CS = 38599, p = = $9.99*10^{-4}$ and CS = 183, p = 0.03) conditions compared to the detect condition (Figure 18a and b). We also observed an increase over the frontal sensors in the 4-7Hz band, but this effect did not survive multiple comparison (but see **Figure 18a** and **b**, time window [1.2 1.4s]).

In the attend-color condition, this 10-20Hz effect (CS = 2722, p =0.008, **Figure 18c**) was localized over the right medial and superior frontal cortex ([MNI[8 60 -2]), the IFG (MNI [54 24 22]), the mid-frontal gyrus (MNI[34 18 44]), the TPJ (MNI [48 -48 20]), the right PCC (MNI[10 -34 16]), the ACC (MNI[-6 34 26] and [12 40 10]). As mentioned above, these regions are part of the VAN and DMN. We also found the caudate nuclei (MNI [-6 10 6] and [6 12 -10]), left SMA (MNI [49 59 62]) and left precentral gyrus (MNI [-46 6 32]). These regions might be associated with stronger motor anticipation in the detect condition (i.e., with a decrease of the beta power in this condition resulting in the stronger beta power for the contrast word/color condition vs detect condition observed in **Figure 18**).

In the attend-word condition, this 10-20Hz effect (CS = 1821, p =0.006; **Figure 18d**) was localized over the IFG (MNI [56 28 12]), the middle frontal gyrus (MNI[26 24 38]), the TPJ, MNI [50 -50 20])), the junction between the middle and posterior cingulate cortex (MNI[-2 -34 30] and [4 -34 30]), the ACC (MNI[-6 34 26] and [8 40 26]) and the right superior medial frontal cortex (MNI [6 60 10]). As in the color condition, we also found the caudate nuclei (MNI [-6 6 -10] and [4 12 -10]), the left SMA (MNI [-6 -12 50]) and left precentral gyrus (MNI [-48 2 36]).

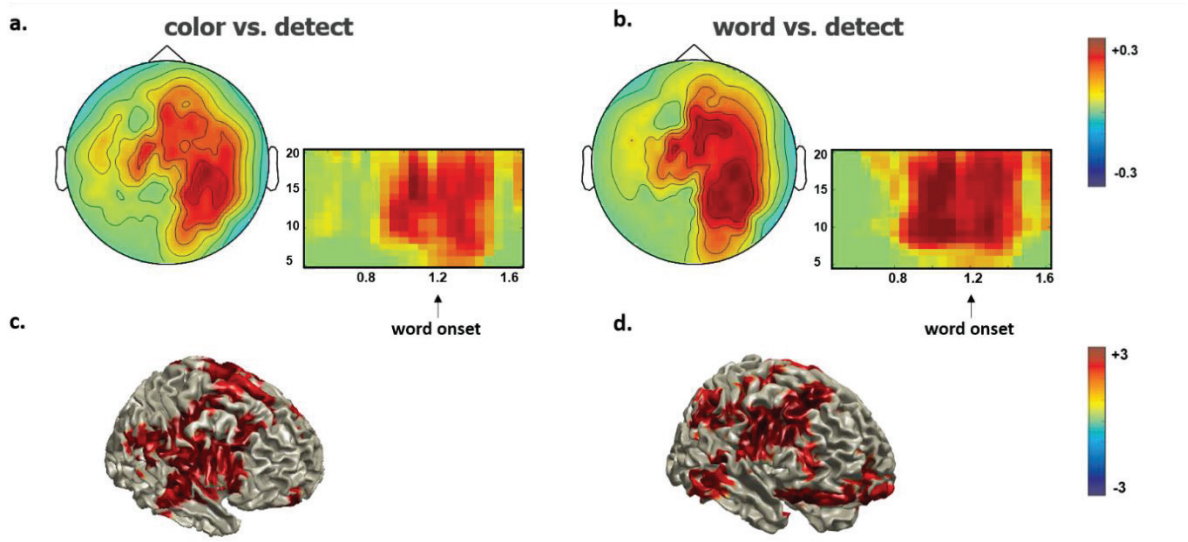

***Figure 18**: **Alpha/Beta increase over the DMN and the VAN in the attend-color and attend-word compared to the detect condition. (a)** Results from cluster-based permutation tests for the contrast attend-color vs. attend-detect condition. Time-frequency representations (TFR) of power from 0.6s to 1.6s after the cue to 0.4s (word onset at 1.2s) **(b)** Similar contrast in the attend-word condition **(c)** Source localization of the 10-20Hz increase (red areas) in the attend-color condition. The networks observed are part of the VAN and DMN networks **(d)** Source localization of the 10-20Hz increase (red areas) in the attend-word condition.*

Stronger theta power over the cognitive control networks and alpha/beta over the ventral attention and the default mode networks in fast than in slow reaction time trials.

We then tested whether the effects reported above were related to performances. We therefore performed a median split of the trials with fast and slow reaction times in all the conditions.

We observed a stronger alpha decrease in fast trials (7-11Hz; **Figure19a**; CS = -12151; p = 0.01) over occipital sensors in anticipation of the stimulus (1 to 1.2s post cue) in the attend-color condition (this effect was just below the significance level in the attend-word

condition). This cluster extended after stimulus onset in higher frequency band (up to 15Hz). Furthermore, we observed stronger 9-15Hz in the attend-color condition and in the attend-word condition at right temporal and frontal cluster and higher frontal theta power in fast than in slow trials from 0.8 to 1.4s post-cue (CS = 15893, p = 0.002 in the attend-color condition CS = 11593, p = 0.02 in the attend-word condition; **Figure19b**). No significant differences were observed between fast and slow RT in the detect condition.

In the attend-color condition, the source localization of the 9-15Hz (**Figure19c left**) increase revealed the involvement of the right IFG (MNI[56 36 8]), the right precuneus-superior parietal cortex (MNI[14 -42 64]), the bilateral medial frontal cortex (MNI[-8 58 4] and [18 58 -0]) and the right temporal lobe (MNI[64 10 -22]). Still in the attend-color condition, the 7-11Hz decrease was observed over the bilateral calcarine (MNI [-0 -104 -0]). In the attend-word condition, the source localization of the 9-13Hz (**Figure19d left**) effect revealed the involvement of the right IFG (MNI [54 14 12]), the right TPJ (MNI[52 -40 22]), the right superior orbitofrontal cortex (MNI[18 32 -20]), the right inferior temporal cortex (MNI[58 -2 -34]) and the right temporal lobe (MNI[68 10 -18]).

In the attend-color condition, the 4-7Hz (**Figure19c right**) effect could be clearly localized over the right middle frontal gyrus (MNI [44 20 38]), the right inferior frontal gyrus (MNI[42 36 -2]) and the bilateral ACC (MNI -2 44 4] and [12 38 8]). In the attend-word condition (**Figure19d right**), this effect was localized over the right middle frontal gyrus (MNI [36 32 32]), the ACC ([-0 32 24]) and the right median orbitofrontal (([16 62 -8]). As mentioned above, these regions have been involved in cognitive control.

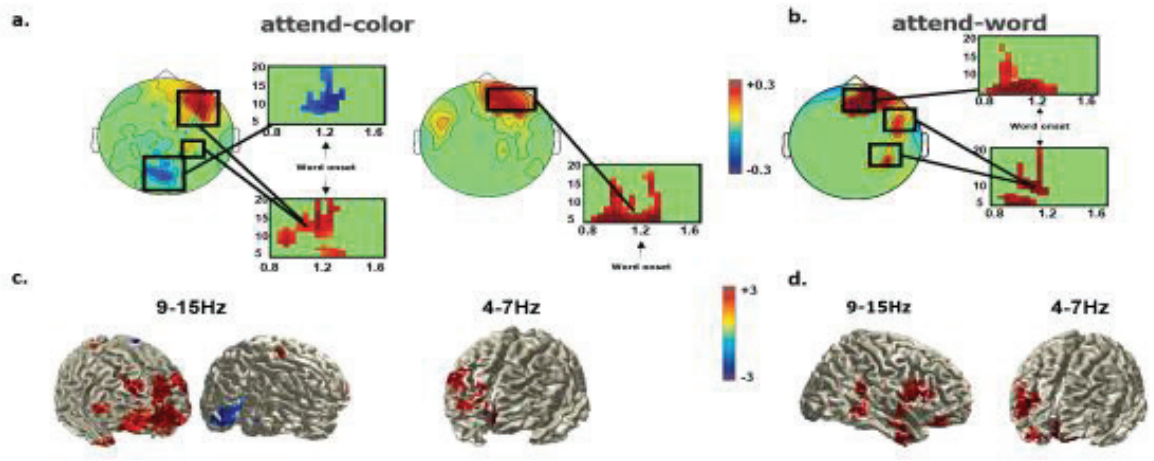

***Figure 19**: **Faster RT are associated with stronger alpha/beta over the DMN and part of the VAN and theta over the DLPFC and ACC (a)** Results from cluster-based permutation tests for the contrast fast vs. slow reaction trials (median split) in the attend-color condition. Time-frequency representations (TFR) of power from 0.8s to 1.6s after the cue (word onset at >1.2s). 7-11Hz decrease was stronger over occipital regions in fast trials in anticipation of stimulus while 9-15Hz and 4-7Hz power were stronger in the right temporo-frontal regions and in the frontal region respectively for the period around stimulus presentation (0.8 to 1.4s) **(b)** Same contrast in the attend-word condition. Like in attend-color condition, fast trials were associated with stronger 9-15Hz power in the right temporal and frontal cluster and higher frontal 4-7Hz power for the 0.8 to 1.4s around stimulus presentation. **(c)** Source localization of the right 9-15Hz increase in the 0.8-1.2s window and of the 4-7Hz increase in the 0.8-1.4s window in the attend-color condition. Red areas indicate significant increases and blue areas significant decrease. The networks observed are part of the DMN, VAN and of the cognitive control network **(d)** Source localization results in the attend-word condition. Red areas indicate significant increases. The networks observed are similar to the ones observed in the attend-color condition.*

Discussion

In this study, we had two main objectives. The first objective was to determine whether alpha oscillations are associated to functional inhibition over high-order visual regions as well as over the VAN (see Solís-Vivanco et al., 2021).The second objective was to determine whether alpha phase is adjusted in anticipation of relevant and irrelevant stimuli and finally which brain regions are involved in controlling visual alpha amplitude and phase.

Behaviors results did not show the expected effect, i.e., response time slower in the attend-color than the attend-word condition as reading is automatic and difficult to overcome (Augustinova & Ferrand, 2014) and, as a consequence, word are expected to be particularly distracting when participants have to report the color of the ink (Stroop, 1935).These results

could be explained by the presentation duration of the stimulus or the training of the participants.

As alpha power has been associated with functional inhibition (Klimesch et al., 2007), we expected stronger prestimulus alpha power, and possibly alpha phase adjustment (see e.g. Solis-Vivanco et al., 2018), in the VWFA in the attend-color than in the attend-word condition. Our time frequency analysis at the sensor level did not however reveal a significant effect after correction for multiple comparison. One explanation could be that some participants had a dominant VWFA over the right hemisphere which could have blurred the group-level analyses. Indeed, a right-lateralization of the language network has been shown in ~7.5% of the right-handed individuals and would be correlated with the lateralization of the VWFA (Gerrits et al., 2019; Knecht et al., 2000). Some studies have even revealed more variability for the lateralization of the VWFA than of the language network (see Carlos et al., 2019). We could not perform the region of interest analyses in the current task to test this hypothesis (see method section). An increased number of participants might further be necessary to reveal such effect. Another explanation could be the absence of the main expected behavioral effect in our task, i.e., a longer RT for the attend-color than the attend-word condition. Indeed, there is currently a hot debate in the literature regarding the link between alpha oscillations and functional inhibition, more precisely the filtering of distracting information (Antonov et al., 2020; Foster & Awh, 2019; Zhigalov & Jensen, 2020). However, many factors impact our general ability to suppress distractors and possibly the presence of high alpha power over sensory regions. One factor is the difficulty of the relevant task, more precisely the perceptual load. According to Lavie (2005), participants would particularly need to efficiently filter out distractors when the perceptual load is high. Gutteling et al. (2021) tested this hypothesis by varying the noise level of faces to manipulate the perceptual load of the target stimuli and the salience of the distractors. They found a stronger ipsilateral alpha power (i.e., contralateral to the distractor) in the high load condition than in the low load condition. It is therefore possible that the perceptual load, e.g., due to training, was too low in the current task to induce a necessity for distractor filtering and hence an increase of alpha oscillations over e.g., the VWFA in the attend-color condition. In addition, behavioral experiments revealed that a stable position of distractors over a block favored their filtering (Noonan et al., 2018; van Moorselaar & Slagter, 2020). The change of attention in each trial might have further impacted the filtering of the distracting information (e.g., the word in the attend-color condition) and therefore the alpha increase.

We further expected a pre-stimulus decrease of alpha power over the VWFA in the attend-word condition and over the 'color area' in the attend-color condition. This difference might have been hindered by a lack of spatial precision. Again, region of interest analyses might have helped to reveal this effect. We however observed a stronger alpha decrease over the occipito temporal regions in the attend-color condition in fast trials (below the significance level in the attend-word condition). We hypothesize that this decrease reflected

higher excitability level in visual regions involved in the relevant processing (e.g., the 'color area') allowing better processing of the stimuli and therefore a faster response.

We found an increase of pre-stimulus alpha/beta power in the VAN in the attend-word and attend-color condition compared to baseline and to the detect condition. This network has been associated with the capture of attention by unattended, but relevant, stimuli (Corbetta et al., 2008; Corbetta & Shulman, 2002). Corbetta et al. (2002, 2008) suggested that the inhibition of the VAN was crucial for preventing the capture of attention by irrelevant stimuli. In line with that idea, Solis-Vivanco et al. (2021) reported that higher alpha/beta power in the VAN was associated with a lower distractor interference over subjects. We observed a similar trend, i.e. a negative relation between alpha/beta in the VAN and interference errors (reporting the color of the word and of the ink in the attend-color and attend-word condition respectively) but the number of participants in our study might be too low to get a significant effect (Schönbrodt & Perugini, 2013). Here, we however reported a stronger alpha/beta power over the inferior frontal gyrus, part of the VAN, in fast reaction time than in slow reaction time trials possibly indicating a link with optimal performance.

Our results also showed an increase of alpha/beta power in the medial prefrontal cortex, right posterior cingulate cortex, angular cortex, and temporal pole in anticipation and during stimulus processing. These regions belong to the default mode network (DMN) which are activated during internal focus. The activity of this network commonly decreases during task (Ossandon et al., 2011; Raichle, 2015). Ossadon and collaborators (2011) observed a decrease of gamma activity during their task, but also an increase of alpha/beta activity over the DMN. We therefore suggest that the alpha/beta increase we observed over these regions would be associated with the inhibition of the DMN. We also found a higher increase of alpha/beta power in several of these regions when we compared fast RT with slow RT trials in both attend-color and attend-word conditions. These results indicate that a stronger inhibition of the default mode network might be associated with better performances.

Finally, we found an increase of theta power over the ACC, the ventromedial prefrontal cortex, and the right dorsolateral prefrontal cortex (DLPFC) before and during stimulus processing compared to the pre-cue period in both the attend-color and attend-word conditions. In addition, a stronger theta over these regions, together with a larger posterior alpha decrease, was associated with faster reaction times. It has been shown that ACC and DLPFC play a key role in cognitive control (Matsumoto & Tanaka, 2004). More specifically, some studies revealed a correlation between theta power over midfrontal and dorsolateral regions and conflict effects (e.g. Cohen & Donner, 2013). A recent study revealed that the anticipation of conflict was associated with increased frontal theta and posterior alpha decrease and that these two measures were associated with faster conflict resolution (Kaiser et al., 2022). In the current study, the word and the ink's color were incongruent in all trials maintaining a response's conflict during the entire experiment. A strong theta power

over the ACC and the DLPFC, as well as a lower posterior alpha decrease, might therefore be necessary to perform well in the current task.

This theta effect together with the absence of alpha increase over specific sensory regions indicate that the conflict occurred more at a decision-making level than at a perceptual level.

To conclude, we showed that good performance in an cued modified Stroop task with incongruent information relied upon an inhibition of the VAN and DMN, reflected by an alpha/beta increase, and an involvement, revealed by a theta increase, of the ACC and DLPFC.

This chapter revealed the inhibition of the VAN and DMN, reflected by an alpha/beta increase, in a cue-based modified Stroop task with incongruent stimuli. However, we did not observe an increase of alpha power over sensory regions. This result might have resulted from the difficulty level of the task as demonstrated by the lack of Stroop effect. In addition, the feature attended varied across trials which could have an additional impact on the ability to filter the distracting information (e.g., the word in the attend-color condition) and thus on the need for alpha increase. We therefore developed a new task based on a face-name Stroop-like effect. The participants were not trained the day before to insure a high-level difficulty in this task. We further used a block rather than a cue-based design to optimize distractor filtering.

Chapter 2: Functional inhibition over high-order visual regions

Functional inhibition of high-order visual regions by alpha oscillations

Ferez M., Clausner T., Lukacs J., Gbadoe M., Daligault S., Schwartz D. and Bonnefond M.

(submitted)

Abstract

Selective attention is a crucial mechanism that allows us to focus on relevant information or, conversely, to ignore irrelevant information. Recently, the link between functional inhibition and alpha oscillation has been questioned by several studies. In this MEG study, we used a face-name Stroop-like task to test (1) whether alpha oscillations are associated with functional inhibition over high-order visual regions as well as in the ventral attention network (VAN) and (2) which areas are involved in the top-down control of alpha activity in visual regions. We found a faster response time in attend-name compared to the attend-face condition and a congruency effect in both conditions but higher in the attend-face condition. We observed stronger alpha power over the VWFA in the attend-face compared to the attend-name condition. This alpha increase over VWFA was further associated with faster reaction time in the attend-face condition. We did not observe an increase of alpha power over FFA in the attend-name condition. Our results further showed an increase of alpha power over the left parietal and frontal cortex. During the prestimulus period, we observed an increase of delta oscillation activity over the left occipitotemporal and parietal cortices. We also found an increase of beta oscillation in the VAN before the stimuli onset. Altogether these results indicate that the inhibitory role of alpha/beta oscillations operates beyond early sensory regions in particular in challenging tasks.

Introduction

Focusing on relevant information and ignoring irrelevant information is an important mechanism in our daily lives, enabled by selective attention. Last decades, many studies investigated the role of alpha oscillations (~10Hz) in this mechanism.

Magnetoencephalography (MEG) and electroencephalography (EEG) studies, using a visual attention paradigm, reported a decrease of alpha amplitude over posterior regions contralateral to the attended stimulus (Capilla et al., 2014; Dombrowe & Hilgetag, 2014; Gould et al., 2011b; Ikkai et al., 2016; Kelly et al., 2009; T. Rihs et al., 2009; T. Rihs et al., 2007; Thut, 2006; Worden et al., 2000). Furthermore, some studies revealed an increase of alpha power over posterior regions ipsilateral to the attended side. This was particularly true when a distracter was presented on the unattended side (Green et al., 2017; Gutteling et al., 2021; Ikkai et al., 2016; Kelly et al., 2006; Rihs et al., 2009; Siegel et al., 2008; Wildegger et al., 2017). This increase of alpha amplitude in the non-engaged stream was also observed in working memory tasks and could be interpreted as allowing to protect of working memory from distractors (Bonnefond & Jensen, 2012; Jokisch & Jensen, 2007; Park et al., 2014; Payne et al., 2013). Moreover, several teams obtained comparable results over the somatosensory area during somatosensory attention tasks (Haegens, Händel, et al., 2011; Haegens et al., 2012; Trenner et al., 2008). Finally, alpha/beta increase has also been observed in the ventral

attention network during a goal-driven task (Ferez et al., submitted; Solís-Vivanco et al., 2021).

In recent years, the link between alpha oscillation and functional inhibition has been challenged by several teams (Antonov et al., 2020; Foster & Awh, 2019; Gundlach et al., 2020; Zhigalov & Jensen, 2020). With the help of EEG or MEG associated with tasks using steady-state visual evoked potentials (SSVEPs), i.e., presentation of visual stimulation at a certain frequency, these teams investigated the relation between excitability, as indexed by the amplitude of the SSVEPs, and alpha oscillations. Theirs results did not reveal a link between ipsilateral alpha increase in amplitude, space, or latency and attended and non-attended SSVEPs. Zhigalov and Jensen (2020) showed that the target/distractor's SSVEPs were localized in the early occipital cortex whereas the alpha modulation originated in the occipito-parietal cortex. They postulated that the parietal increase could result from a gating of the flow of information in the brain rather than a direct gain (excitability level) control mechanism. However, as was discussed in other papers, the use of flickers, as stimuli, could alter the detection of alpha modulation in the early visual cortex (Samaha et al., 2020). Altogether, these results indicate that it is important to further investigate the role of alpha oscillations in functional inhibition. Moreover, the modulations of alpha activity have been studied mainly in primary visual areas, it remains to be determined whether alpha modulations can be observed in higher-order visual areas (but see Foxe & Snyder, 2011).

The brain regions involved in the control of posterior alpha are still not clearly known. The top-down control of posterior alpha power has been studied in covert attention tasks using EEG, MEG, and transcranial magnetic stimulation (TMS) (Marshall, O'Shea, et al., 2015; Popov et al., 2017; Wang et al., 2016). These three papers showed that the frontal eye field (FEF) was involved in controlling posterior alpha. Other frontal areas, such as the dorsolateral prefrontal cortex (DLPFC) could be involved in controlling alpha activity in non-spatial tasks such as working memory or reasoning tasks (Bonnefond & Jensen, 2012; Solís-Vivanco et al., 2018). The role of these different regions in different cognitive tasks or in controlling alpha amplitude or phase remains to be further explored.

In this paper, the goal was to determine (1) whether alpha oscillations are associated with functional inhibition over high-order visual regions as well as in the ventral attention network (VAN; see Solís-Vivanco et al., 2021) and (2) which areas are involved in the top-down control of alpha activity in visual regions.

We investigated these questions using MEG and an object-based attention task. We used faces with first names written on top of them. At the beginning of each block, participants were instructed to attend to faces or first names and to report whether they were female or male faces/names. In a previous study, we did not report a clear alpha modulation over the visual word form area (VWFA) in anticipation of color words in the condition in which

participants were expected to report the color of the ink (Ferez et al., submitted). This study had some limitations. First, we only used incongruent trials, i.e., ink color and color word were systematically different. This prevented us from analyzing congruency effects on behavior and alpha modulation. In the current study, we included both congruent and incongruent trials. Second, the instructions regarding the element to attend changed with each trial depending on the cue. This might prevent the implementation of an efficient distractor suppression (van Moorselaar & Slagter, 2020; Wöstmann et al., 2022). For the current study, we used a block design. Third, anatomically, the area highly specialized in processing words (VWFA) and the area specialized in processing color (although not specifically) are close to each other, which might have blurred out the detection of specific modulations. In our new study, the two areas highly specialized in the process of the stimuli, the VWFA for the first name and the fusiform face area (FFA) for the faces, are more clearly defined anatomically by different lateralization. VWFA is predominantly lateralized in the left hemisphere (Cohen et al., 2002), whereas FFA is localized in both hemispheres, but typically shows a right-hemispheric dominance in adults (Hildesheim et al., 2020). We hypothesized that, when the participant had to attend to the first names, anticipatory alpha power would be higher in FFA and lower in VWFA. The reverse was expected in trials in which they had to attend to the faces. We further predicted that performance would depend on these alpha power modulations. We further hypothesized that the dorsolateral prefrontal cortex (DLPFC) would be involved in controlling these posterior modulations (Bonnefond et al., 2012; Solis-Vivanco et al., 2018; Sperling et al., 2001). Finally, we expected that alpha/beta power would be modulated over the VAN (Ferez et al., submitted; Solís-Vivanco et al., 2021) and that higher alpha/beta power would be associated with better resistance to distractors. We found that subjects responded faster in the attend-name condition, and we saw a congruency effect in both conditions (attend-face and attend-name) with slower response time in incongruent trials. We also found alpha power increase over the VWFA in the attend-face compared to the attend-name condition. This increase over VWFA in the alpha band was further associated with faster reaction time in the attend-face condition. However, we did not find an increase of alpha power in FFA in the attend-name condition. Our results showed an increase of alpha power over the parietal cortex. Moreover, we showed that anticipatory beta power increased in the VAN in attend-face condition.

Methods

Participants

The study was carried out at the Neuroimaging center of Lyon (CERMEP). Forty healthy native French-speaking volunteers (age: 26.4 ± 3.19 years; 24 females) participated in the experiment after providing written informed consent according to the Declaration of Helsinki and the local ethics board. All subjects had a normal or corrected-to-normal vision and were right-handed according to the Edinburg Handiness Inventory (Oldfield, 1971).

Stimulus material and procedure

This task with faces and names was designed using Python (3.7) and Psychopy (psychopy.org). The task was composed of 7 blocks. At the beginning of each block of 200 trials (1400 trials in total), subjects were instructed to either attend to faces or names. The trial started with a period of 1900ms during which a white cross was presented in the center of the screen indicating that blinks were allowed. The white cross then switched to grey followed by a baseline period of 700 to 1100ms. Then, while the fixation cross remained on the screen, the stimulus was presented in the center until the subject pressed a button. The minimum presentation time was 400ms, even if the participants had pressed the button before, while the maximum time was 1500ms. The sequence of baseline followed by the stimulus was repeated five times before the subject could blink again. Participants were asked to respond as fast and accurate as possible by pressing one of the two buttons of a response pad. Each button was associated with a gender and the association was randomized across participants. Reaction time (RT) and response accuracy (RA) were recorded throughout the experiment. The background of the screen was grey during the entire experiment.

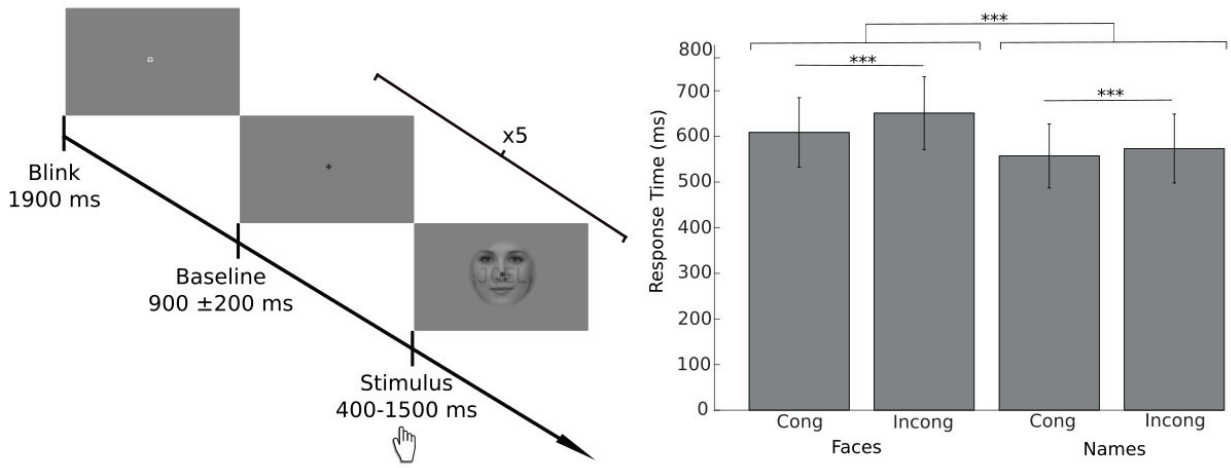

Figure 20 Task design, and behavior results**. **Left**: Trial started with a period of 1900ms during which blinks were allowed. This period was followed by a baseline period of 700 to 1100ms with a switch of the cross' color from white to grey. The stimulus (the first name on top of a face) was presented until the subject pressed a button (minimum/maximum presentation time: 400/1500ms). The baseline and stimulus sequence were repeated five times. Participants were asked to respond as fast and accurate as possible by pressing one of the two buttons of a response pad. **Right**: Behavioral results. Mean of response times (RT) over subjects for each condition, for trials with correct. Error bars represent standard error. A significant difference between Names and Faces conditions, and between congruent (Cong) and incongruent (Incong) conditions (= p<0.001).*

Stimuli were 4° large with a distance of 66cm between the eyes of the participants and the screen. They were grey faces of women (60 faces) or men (60 faces) with the first name of women (60 names) or men (60 names) written in the middle in grey letters. Faces were created by averaging ten random faces for each gender from a face database (VGGFace2). First names were composed with 4 letters only, which can be frequently heard in everyday life. After each session, subjects completed a questionnaire about the familiarity of the names presented during the task. Presentation of face and name could be congruent (e.g., the face of women with a name associated with the female gender) or incongruent (e.g., the face of women with a name associated with the male gender).

In addition, two localizer tasks were performed. For both, participants had to fix the grey cross in the center of the screen and pressed the button when they detected that the color of the cross was darker. This small change of color occurred between 250 and 350ms after the trial onset and in only 10% of the trials appears. In the face localizer task, a blink period of 1900ms was followed by a baseline period from 700ms to 1100ms. Then, we presented faces or scrambled faces (ratio 50:50) for a duration of 1000ms. The sequence of baseline followed by the stimulus was repeated five times (160 trials in total). For the name localizer task, the sequence is the same as the face localizer task except for the type of stimuli. We presented names or pseudo-names, i.e., the letters of the names presented before were randomly mixed (ratio 50:50; 160 trials in total).

Data acquisition

MRI acquisition

Minimum two weeks before the MEG session, each participant underwent an MRI scanning protocol, acquired with a 3T Siemens Sonata system (Erlangen, Germany), for two reasons. First, the scalp image of participants was used to create their individual headcast (see below). Second, the MRI scans were used for the MEG source localization. T1-weighted sagittal anatomical images were acquired using a magnetization-prepared rapid gradient-echo (MPRAGE) pulse sequence. Spatial resolution was set to 1mm isotropic, with repetition time (TR) of 2100ms, echo time (TE) of 3.33ms, inversion time (TI) of 900ms, and grappa factor of 3. For the co-registration of the MRI and the MEG data allowing accurate source localization, tablets of Vitamin E, with the shape of the coils of the MEG, were used and placed respectively at the nasion and the left and right ear canals, and their location was later used to place the MEG coils on the head-cast during the MEG recording.

Head-cast construction

We extracted an image of the skull from the MRI images of the subjects. Based on this representation, we constructed a foam head-cast that fit with the participant's scalp and the MEG dewar (Bonaiuto et al., 2018; Meyer et al., 2017). First, scalp surfaces with coils positions

were extracted from the MRI scan using the brainstorm toolbox (https://neuroimage.usc.edu/brainstorm/). The surfaces obtained were modelized to select head orientation in the MEG dewar (minimizing the distance of the head from the sensors while allowing the subjects to see the screen that was located in front of them during the task) with Rhinoceros 3D (https://www.rhino3d.com) to obtain a file which was printed with the 3D printer Raise 3D N2 Plus (https://www.raise3d.com). The 3D printed model was then placed inside a replica of the MEG dewar and the space between was filled with polyurethane foam (Flex Foam-it! III; https://www.smooth-on.com) to create the participant-specific head-cast into which the fiducial coils were placed during scanning.

MEG acquisition

The neuromagnetic activity was recorded at 1200Hz, using a 275 first-order axial gradiometers whole-head MEG system (VSF/CTF Systems, Port Coquitlam, Canada) contained in a magnetically shielded room. During the entire session, 3 marker coils were placed in the head-cast, respectively at the nasion and the left and right ear canals to measure the subject's head position relative to the MEG. Participants were in the supine position during the recording. We recorded eye position at 1000Hz with the eye tracker Eyelink 1000 Plus (SR Research) which was calibrated before starting the task.

Data analysis

Reaction times (RTs) were obtained from the subjects' button box responses. RTs shorter than 300ms or longer than means + 2std were excluded.

The whole analysis was performed using MATLAB with the Fieldtrip software package (Oostenveld et al., 2010). MEG data were epoched 0.7s before the onset of the visual stimulus until the time of the subject's response or until 1s after the stimulus onset if the response time exceeded this time. After that, based on a z-score algorithm across sensors exceeding a threshold given by the data variance within each participant, an automatic rejection of SQUID jumps, or muscles artifacts was run. Using eye tracker data, we rejected periods with eye blinks, saccades, and bad fixation of the central cross during stimulus presentation. All the epochs were visually inspected. Only epochs without artifacts and with correct answers were kept (76.4%). One subject was removed from the analysis due to a low number of trials without artifacts.

Planar gradients of the MEG field distribution were calculated for the sensor-level analyses (Bastiaansen & Knösche, 2000) using the nearest neighbor method. This method allows approximating the signal measured by the MEG system with planar gradiometers by deriving the horizontal and vertical components of the estimated planar gradients. This representation facilitates the interpretation of the sensor-level data as the largest signal of the planar gradient is typically located above the source. Time-frequency analyses were

performed in the 3-40Hz band with a step of 1Hz. The power spectrum was calculated using the multi-taper convolution method with a hanning taper for each frequency over a sliding adaptative time window of 3 cycles (ΔT=3/frequency; e.g. ΔT = 300ms for 10 Hz). The power for the individual trials was averaged over conditions and log transformed.

Source analysis was performed using a frequency domain beamforming approach based on an adaptative filtering technique (Dynamic Imaging of Coherent Sources, DICS; Gross et al., 2001). We obtained cross-spectral density matrices by applying a multitaper FFT approach (ΔT = 300 msec; one orthogonal Slepian taper resulting in 3 Hz smoothing) on data measured from the axial sensors. A realistically shaped single-shell description of the brain was constructed, based on the individual anatomical MRIs and head shapes (Nolte, 2003). The brain volume of each participant was divided into a grid with a 1-cm resolution and normalized to the template MNI brain (International Consortium for Brain Mapping, Montreal Neurological Institute, Canada) using SPM8 (www.fil.ion.ucl.ac.uk/spm). The lead field and the cross-spectral density were used to calculate a spatial filter for each grid point (Gross et al., 2001), and the spatial distribution of power was estimated for each condition in each participant. A common filter was used for both conditions, i.e., it was based on the cross-spectral density matrices of the combined conditions. The regularization parameter was set at 5%. As in the sensor-level analyses, the estimated power was averaged over trials and log-transformed. The contrast between conditions was performed and averaged across participants. All source data were estimated within the alpha range. The source estimates were plotted on a standard MNI brain found in SPM8.

As the time windows of the different effects were relatively short, we used a linearly constrained minimum variance (LCMV) scalar beamformer spatial filter algorithm to generate maps of source activity on a 1-cm grid, and lambda of 5% (Van Veen, van Drongelen, Yuchtman, & Suzuki, 1997). The beamformer source reconstruction calculates a set of weights that maps the sensor data to time series at the source locations, allowing to reconstruct the signal at source level. We performed time–frequency analyses on these reconstructed time series and subsequently averaged the power in the alpha band (8-14Hz) or in the beta band (14–30 Hz) over the two windows of interest.

Statistics

Behavioral accuracy, and response time (RT) were analyzed using repeated-measures ANOVA (RM-ANOVA) with factors condition (attend-face and attend-name) congruency (congruent and incongruent), and type of stimulus (female/male). A Greenhouse– Geisser correction was used in case of violation of sphericity assumption and the Tukey-Kramer test was used for post hoc comparisons with alpha =0.05.

Power differences at both sensor and source levels between conditions were assessed using a cluster-based nonparametric randomization test (Maris & Oostenveld, 2007). By

randomly permuting the data across the two conditions and recalculating the test statistic 1000 times, we obtained a reference maximum sum distribution ($p < .05$) to evaluate the statistical significance of a given effect (Monte Carlo estimation).

Results

Response time analysis showed that participants were faster for the attend-name condition compared to the attend-face condition (**Figure 20**; respectively 565.2±157.4 ms;629.1±138.6ms $F(1,39)=354.07$, $p<0.001$). Subjects were also faster for the congruent trials in both the attend-name and attend-face conditions ($F(1,39)=161.9$ $P<0.001$). This analysis further showed a significant interaction between congruency and conditions ($F(1,39)=68$ $P<0.001$). Post-hoc analyses revealed that the difference between congruent and incongruent was higher in the attend-face than in the attend-name condition (respectively Tukey post hoc(0.05) p= 1.06e-10;p=4.27e-7).

Analysis of the accuracy showed that subjects performed better in the attend-face condition compared to the attend-name condition (respectively: 94.7%, 91,5% $F(1,39)=41.5$, $p<0.001$). Accuracy was also lower in the incongruent compared to congruent trials ($F(1,39)=145.3$ $p<0.001$). However, it is important to note that accuracy, as it is classically understood, did not exactly apply here. Indeed, the subjects were asked to answer if they considered the faces as more feminine or masculine which implies a subjective part. For the attend-name condition, the results can be altered by the level of familiarity. These results will not be analyzed further.

To summarize, in both conditions, subjects answered faster and with higher accuracy in congruent trials than in incongruent trials.

Anticipatory left occipito-parietal alpha power increase and beta power increase over the VAN in the attend-face condition

After artifact rejection, in the attend-faces conditions we kept, on average, 265 congruent trials (with a minimum of 198 and a maximum of 302) and 253 incongruent trials (with a minimum of 169 and a maximum of 308). For the attend-names condition, we kept, on average, 275 congruent trials (with a minimum of 189 and a maximum of 323) and 268 incongruent trials (with a minimum of 176 and a maximum of 315).

The cluster-based analysis, over time from 600ms to the stimulus onset, sensors, and over frequencies from 3 to 30Hz, of the contrast between attend-face and attend-name conditions revealed a stronger delta (3Hz) and alpha/beta power in the 600ms pre-stimulus period (although not sustained; see **figure 21**) over left occipito-parietal and temporal sensors (8-14Hz or temporal with short time windows up to 22Hz and up to 30Hz for parietal in the late window; see below) and stronger beta power over left-parietal, right parieto-frontal (8-

30Hz) left temporo-frontal (14-30Hz) sensors in the 200ms pre-stimulus period (cluster-level statistic [CS] = 5633, p = 0.038; **Figure 21 top**). Source-level (DICS) analysis in the 600ms period in the 8-14Hz revealed left occipito-parietal and temporal regions ([CS] = $1.25e^3$, p = 0.008;], **Figure 21 bottom**). More precisely, this analysis revealed the left occipitotemporal cortex (LOT; MNI[-47 -63 -11]), the left inferior parietal cortex (MNI[-53 -38 54]), the left occipito-parietal cortex (MNI[-28 -77 42]), the left medial frontal cortex (MNI[-32 27 32]), the bilateral precuneus/cingulate posterior cortex (MNI[-7 -49 26] and [14 -51 26]). We suggest that the LOT possibly included the, functionally defined, visual word form area (VWFA).

We further found involvement of the left pre and postcentral cortex (MNI[-51 -9 57]), and the left supplemental motor area (MNI[-14 3 64]). These regions are likely associated with a stronger motor preparation in the attend-name condition (associated with faster RT).

Using LCMV (**Figure 22**), to better localize the short event in the beta band prior to stimulus presentation, we found peaks in the right medial frontal gyrus (MNI[36 28 40]), the right inferior frontal gyrus (MNI[42 34 2])and the right medial temporal cortex ([40 -50 14]). These regions might belong to the VAN.

We also observe a bilateral inferior frontal lobe (MNI[-30 -70 44] [26 -68 54]), the bilateral precuneus/cingulate posterior (MNI[-6 -50 16] [2 -50 16]) and the bilateral superior frontal cortex (MNI[-6 32 42] [20 28 34]). Some of these regions might belong to the default mode network.

The left supplementary motor area (MNI[-8 18 46]) and left paracentral lobule (MNI[-8 -42 78]). The modulation over these regions might reflect the earlier motor preparation in the attend-name condition.

Analyses in the gamma band (50-70 Hz) for the same period (400ms before the onset of stimulus) did not show any significant result.

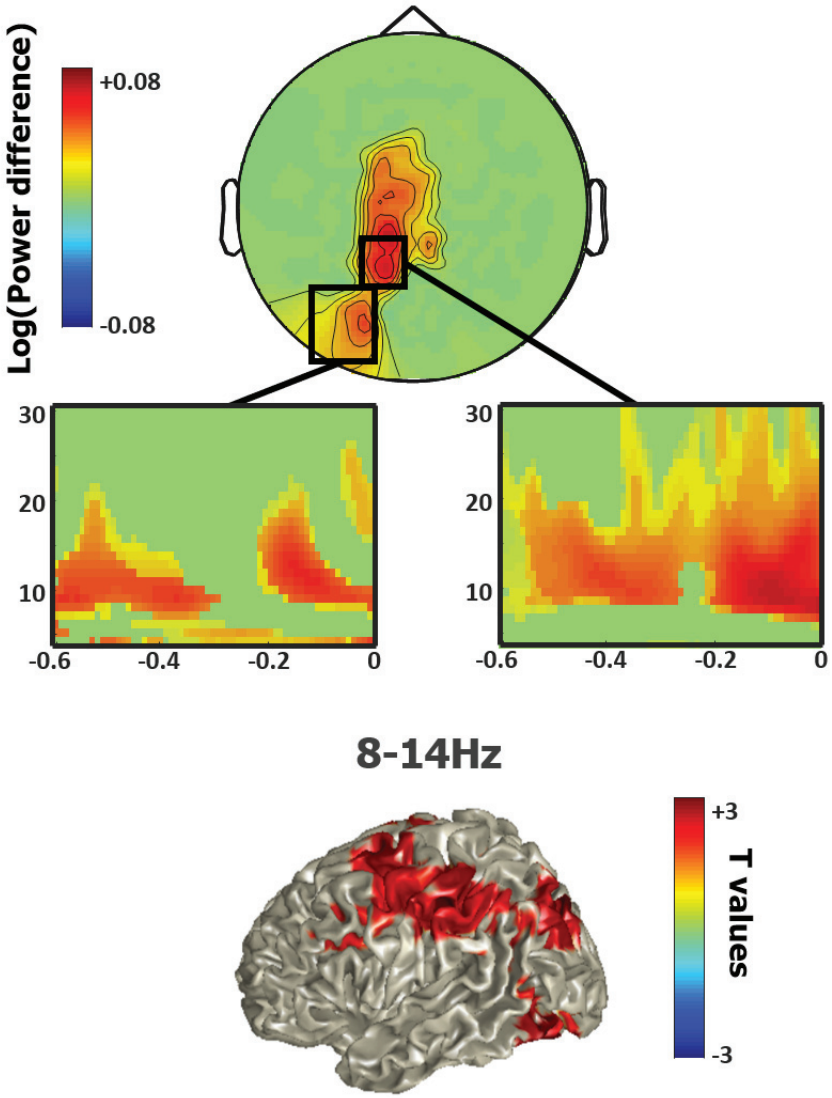

Figure 21: Higher delta and alpha/beta power over the left occipitotemporal and parietal cortices in the attend-face condition compared to the attend-name condition in anticipation of stimuli. Top*: Result of the cluster-based permutation test for the 600ms period before stimulus onset in the 3-30 Hz frequency band comparing attend-face and attend-name (threshold p <0.05; p=0.038). Time-frequency representations (TFR) of power during the 600 ms before the onset of the stimulus.* ***Bottom****: Source (DICS) representation of the 8-14 Hz increase for the contrast between attend-face and attend-name condition for the 400ms before stimulus onset period. Red areas indicate a significant increase (p <0.05).*

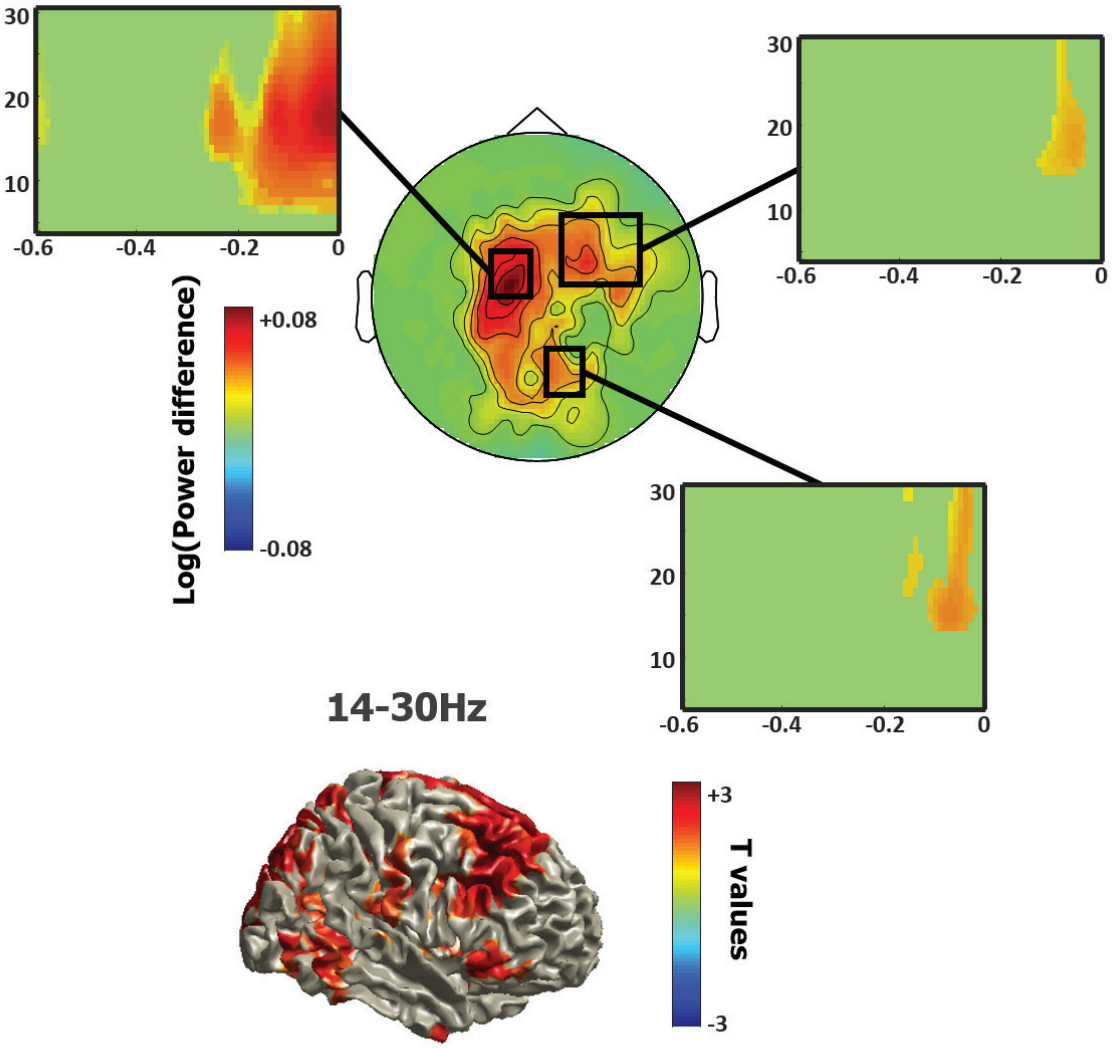

***Figure 22**: **Higher beta power over the VAN in the attend-face condition**. **Top**: Result of the cluster-based permutation test for the 600ms period before stimulus onset in the 3-30 Hz frequency band over the Van during attend-face. Time-frequency representations (TFR) of power during the 600ms before the onset of the stimulus. **Bottom**: Source (LCMV) representation of the 14-30 Hz increase for the contrast between attend-face and attend-name condition for the 200ms before stimulus onset period. Red areas indicate a significant increase (p <0.05).*

Alpha power enhanced in anticipation of stimuli for face's condition in occipitotemporal cortex regions for trial with short RT

The number of the remaining trials after artifact rejection, in the attend-faces conditions we kept, on average, 130 fast congruent trials and as many slow trials (with a minimum of 94 and a maximum of 151) and 124 fast incongruent trials and as many slow trials

(with a minimum of 83 and a maximum of 153). For the attend-names condition, we kept, on average, 153 fast congruent trials and as many slow trials (with a minimum of 91 and a maximum of 161) and 131 fast incongruent trials and as many slow trials (with a minimum of 84 and a maximum of 154).

We also explored the influence of anticipatory alpha power over behavioral performances. Specifically, we hypothesized that left temporal (VWFA) alpha increase would be associated with faster RT in particular in the incongruent condition in which the name is interfering with the decision regarding the gender of the face. Limiting this interference would require particularly strong inhibition of the VWFA. We, therefore, classified trials in each condition (separating congruent and incongruent trials) as fast or slow (in terms of a median split of RT within conditions in each participant). In the attend-face incongruent condition, we observed an alpha increase over left parietal, occipitotemporal and frontal sensors in fast compared to slow trials (**Figure 23 A**). The cluster-based permutation test computed over time from 600ms to 0ms before the stimulus, sensors and over frequencies from3Hz to 30 Hz showed a significant difference in the 8-14Hz band in the 600 to 400ms period and the 100ms to 0ms period before the stimulus onset. It also revealed a frontal theta component (5-7Hz) in the 500 to 0ms period before stimulus onset ((overall cluster-level statistic [CS] = 31703^3, p = 0.01; **Figure 23 B**).

We also observed beta power increase (from 18 Hz up to 30Hz) over the left and middle frontal sensors in the 600ms to 400ms pre-stimulus window but we did not further analyze further this effect in the present form of the manuscript. We only observe stronger left alpha-beta power over motor areas in fast trials in all other conditions.

The source-level analysis (LCMV) of alpha modulation (8-14Hz; **Figure 23 C**) in the 100ms-0ms time window revealed a left network ([CS] = 5780, p = 0.009) including a left occipitotemporal regions (MNI coordinates [-56 -60 -6] LOT), the left superior parietal lobe (MNI[-20 -78 44]) and the left inferior frontal gyrus (MNI coordinates [-46 40 4]). The source-level analysis of the 5-7Hz effect revealed an frontal network (([CS] = 3174, p = 0.01; **Figure 23 D**) including a bilateral anterior cingulate cortex (ACC: MNI[-0 46 6] and [6 44 6]]), a right middle/superior frontal node (MNI[28 44 16]), a bilateral superior frontal cortex (MNI[-20 32 52] [24 28 52]). These regions belong to the cognitive control network.

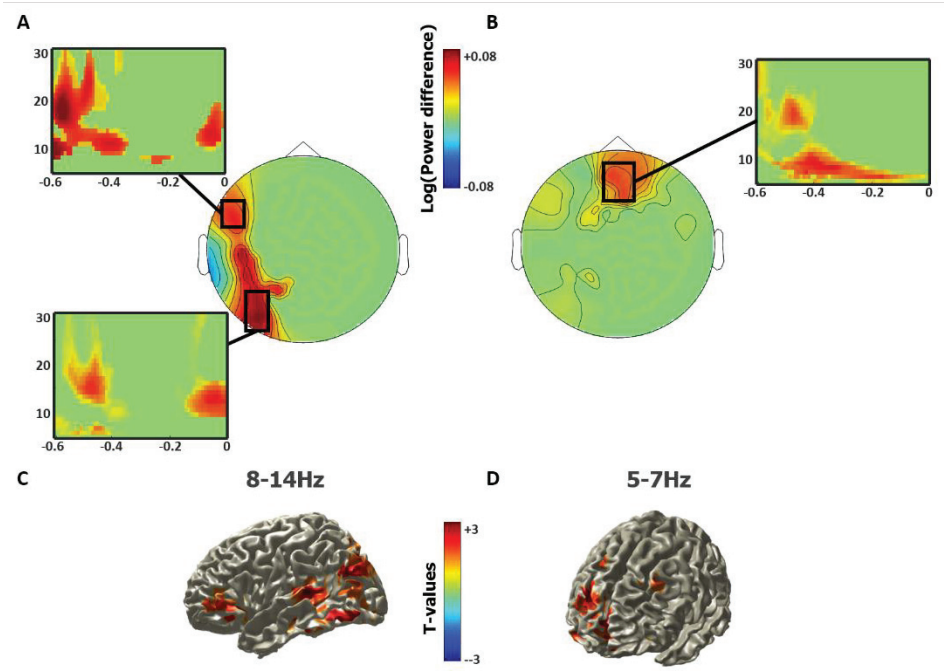

Figure 23: Stronger alpha power over the left occipitotemporal cortex in fast versus slow trials in incongruent condition of the attend-face condition*. **A & B**: Result of the cluster-based permutation test for the 600ms period before the stimulus onset in the 3-30 Hz frequency band (threshold p <0.05). **C**: Source (LCMV) representation of the 8-13 Hz increase. **D**: Source (LCMV) representation of the 5-7 Hz increase. Red areas indicate a significant increase (p <0.05).*

Discussion

In this study, our goal was to determine (1) whether alpha oscillations are associated with functional inhibition over high-order visual regions as well as in the ventral attention network and (2) which areas are involved in the top-down control of alpha activity in visual regions.

Our results revealed a stronger alpha power over the left occipitotemporal cortex (LOT), which we interpreted as being the posterior part of the visual word form area (VWFA), in the attend-face compared to the attend-name condition. In addition, this occipito-temporal alpha was stronger in fast RTs in the attend-face condition. As faster RTs were associated with stronger alpha power, we interpret the alpha difference between attend-face and attend-name as resulting from an increase in the former rather than a decrease in the latter condition. However, this did not exclude the possibility that alpha decreased over the LOT/VWFA in the attend-name condition (Levy et al., 2013). Moreover, we expected a lower alpha power over FFA in the attend-face condition (possibly reflecting a higher alpha power in the attend-name condition) but the lower amplitude observed over bilateral temporal sensors did not survive multiple comparison corrections. Together, these results indicate that alpha oscillations over the LOT/VWFA could prevent the processing of the distracting name during face processing. Given the names were written on top of the face, spatial attention

could not be used to implement this process. We however did not find an increase of alpha amplitude over the FFA in the attend name condition, even in trials with fast reaction times.

There is currently a hot debate in the literature regarding the role of alpha oscillations in inhibition (Foster & Awh, 2019). For instance, some studies did not report an anticipatory alpha increase when the position of the distractor was predictable (Moorselaar & Slagter, 2019; Noonan et al., 2016). Other studies did not report a link between alpha increase and distractor processing (e.g. Antonov et al., 2020; Zhigalov & Jensen, 2020). However, as reported in Zhigalov and Jensen (2020), the source of the alpha increase observed was the parietal cortex and was possibly associated with a gating mechanism of the flow of information rather than a gain mechanism in the early sensory cortex. It remains to be clearly understood in which context an alpha increase can be observed over sensory areas, i.e., associated with preventing the processing of distractors (Bonnefond and Jensen, in prep.).

One parameter influencing the presence of high alpha power seems to be the difficulty of the task, more precisely the perceptual load. Lavie (2005) formulated the perceptual load hypothesis according to which our capacity to process stimuli is limited, and observers need therefore to efficiently filter out distractors when the perceptual load is high. This hypothesis was specifically tested by Gutteling et al. (2021). They varied the noise level of faces to manipulate the perceptual load of the target stimuli and the salience of the distractors. They found a stronger ipsilateral alpha power (i.e., contralateral to the distractor) in the high load condition than in the low load condition. Interestingly and in line with this idea, overall reaction times were slower in the attend-face condition than in the attend-name condition. The attend-face condition might be associated with a higher perceptual load, and therefore a stronger need for inhibition. This could explain the alpha increase observed over LOT/VWFA in the attend-face condition while no alpha increase over FFA was observed in the attend-name condition. The stronger salience of the name (in the middle of the screen) could also explain these results. Gutteling and collaborators further reported an effect of the salience of the distractor in the high load condition. Given their spatial position, the names could be considered stronger distractors than the faces in our current task. However, an effect of congruence (a longer RT when faces and names were incongruent) was found in both conditions, indicating that the faces were distracting in the attend-name condition as well.

Another parameter that could influence the presence of alpha increase over sensory regions is the frequency of a distractor at a given spatial position. It was indeed shown that the presence of distractors influences overall alpha power independently of distractor strength (Haegens et al., 2012; van Diepen & Mazaheri, 2017). Furthermore, it was also shown that the inhibition of the processing of the predictable distractor was only effective in a block design (i.e. when the position was similar across trials) and not in a flexible design in which the position of the distractor was indicated in each trial (Noonan et al., 2016). In general, if distractors are always at the same position during a task, they stop capturing attention over

time (Vatterott & Vecera, 2012). This aspect is in line with the predictive processing models in which statistical regularities of the environment are used to limit the processing of the less informative stimuli (Friston, 2005; Friston, 2019; Rao & Ballard, 1999). We here used a block design with the same instruction and the same position of target and distractors. This type of design, based on a stable position/feature of distractors, could allow implementing more easily the inhibition needed to suppress the processing of the distractor. This could further explain our result showing an increase of alpha power over the LOT/VWFA in the attend-face condition.

The coordinates reported for the LOT/VWFA in the fMRI literature are quite distributed (Dehaene & Cohen, 2011) and appear quite posterior in the current study. The localizer task will further help to determine whether a similar region is more activated for words than pseudo-words. The localizer task for faces will allow disentangling the sources more specifically associated with face processing (Burra et al., 2017). Furthermore, one of the sources we reported was close to the supramarginal gyrus, a region also implicated in the reading function (Juphard et al., 2011; Poldrack et al., 1999) and which might need to be inhibited in addition to the LOT/VWFA.

We further observed an increase of alpha power over the parietal cortex. As mentioned above, Zhighalov and Jensen also reported an (ipsilateral) increase over the parietal cortex. They suggested that this parietal increase would serve to gate the feed-forward information from the early visual regions. However, they used a spatial attention task while we used an object-based attention task. This parietal alpha increase may implement inhibition over the VWFA as such region has been involved in inhibitory control e.g. during Stroop tasks (Okayasu et al., 2022).

Similarly, we found an increase over the left dorsolateral prefrontal cortex which has also been involved in such inhibitory control. It remains to be determined whether this prefrontal and parietal alpha increase play a role in controlling VWFA alpha increase using connectivity tools.

In addition to the alpha power increase, the connectivity between VWFA and V1, and between VWFA and higher-order regions may play a role in implementing the suppression of the processing of the distractors. In particular, an anti-phase relationship or a decrease of the connectivity in the alpha-band could be implemented (Bonnefond et al., 2017). It has been shown that the strength of feedback connectivity, for low-frequency oscillations, between FFA and V1 predicted the upcoming percept but also the strength of post-stimulus neural activity (Rassi et al., 2019). In line with this result, we can also hypothesize increased connectivity in the alpha band between FFA and V1 in the pre-stimulus period in the attend-face condition and, between VWFA and V1 in the attend-name condition. In addition, the

coupling of alpha and gamma oscillations band could be altered in VWFA in the attend-faces condition (see Pascucci et al., 2018; Bonnefond et al., 2017).

The fast reaction times in the incongruent trials of the attend-face condition were further associated with pre-stimulus strong theta over the ACC/DLPFC, i.e. brain regions associated with cognitive control (Matsumoto & Tanaka, 2004). Such result is in line with the result of our previous experiment using a modified Stroop task. Similarly, we interpret these results as indicating that strong theta power over the ACC and the DLPFC, might help to resolve response conflict in the current task.

We also observed a prestimulus increase of beta power in the VAN in the attend-face condition. This network has been shown to be involved when attention is captured by unattended, but relevant, stimuli (Corbetta et al., 2008; Corbetta & Shulman, 2002). According to Corbetta et al. (2002, 2008), inhibiting the VAN is essential for preventing the capture of attention by unattended stimuli. It remains to be determined whether beta power in the VAN is associated with performance (Ferez et al., submitted). The next step will therefore consist in determining whether beta power is further correlated with the interference error (e.g., indicating the gender of the names in the attend-face condition) ratio, as observed in the study of Solís-Vivanco and collaborators (2021). The analysis of the modulation of alpha and beta power during stimulus processing, in particular the analysis of the congruence effect, might provide further insights into the role of these frequencies in the LOT/VWFA and VAN during this task.

We also observed an increase of delta oscillation activity over the left occipitotemporal sensors (source localization remains to be performed) during the prestimulus period. Lakatos et al. (2018) have shown that delta-band oscillations in the primary visual cortex could entrain to the rhythm of the stream, increasing response gain for events that are relevant to the task. These authors suggested that a crucial component of selective attention to rhythmic auditory or visual input streams is the entrainment of cortical delta oscillations. In addition, another study in epileptic patients implanted in the auditory cortex performing an intersensory audiovisual task revealed a phase-amplitude coupling between delta phase and alpha power (Gomez-Ramirez et al., 2011). The authors also showed an increase in alpha power in the auditory cortex at the arrival of the auditory stimulus when the subject had to pay attention to the visual stimulus. Together, these results suggest that alpha oscillatory activity may be mediated by training its amplitude at frequencies without the delta band. It will be interesting to continue our investigation to clarify the link between alpha and delta oscillations in our task as alpha power increase seems to occur every ~300ms.

In addition, we used headcasts in the current task. We hope to be able to explore source localization more precisely, possibly down to the laminar level (Bonaiuto et al., 2018; Meyer et al., 2017). Based on the paper of Bonaiuto and collaborators (2020), our analysis

will further use the link vectors between the pial and white matter surfaces to approximate the orientation of cortical columns and increase precision (Bonaiuto et al., 2020). This type of analysis will provide information regarding the laminar profile of alpha oscillations in our task. Our hypothesis is we will find a predominance of alpha in the infragranular layer in the LOT/VWFA.

This second chapter showed that prestimulus alpha power increased over the VWFA in attend-face compared to the attend-name condition. This study also showed an increase of beta power in the VAN in prestimulus period in face condition. This result indicates that the inhibitory role of alpha/beta oscillations might operate beyond sensory regions. Subsequently, we aimed at determining whether a similar mechanism is at play during high-level cognitive processes, such as a reasoning task. To test this hypothesis, we, therefore, used a reasoning task involving the inhibition of the visual cortex to perform well.

Chapter 3: functional inhibition over the visual cortex during reasoning

New evidence for a role of alpha oscillations in functional inhibition

Ferez M, Bayle D., Noveck I, Van der Henst J.-B., Bertrand O., Mattout J., Bonnefond M.

(In prep.)

Abstract

To protect high-level cognitive process, it was shown that the suppression of the processing of irrelevant information is an essential mechanism. Alpha activity (~10Hz) might be involved in such a mechanism. In this MEG study we used a reasoning task to determine the involvement of alpha oscillations in inhibitory processes associated with higher order cognitive processes. Our results showed, after the stimulus presentation, an increase of alpha power in occipitotemporal regions. This increase possibly allows the disengagement of visual areas in order to allow abstract reasoning. We also observed an increase of alpha power in the ventral attention network (VAN). The inhibition of this network is thought to be crucial for preventing the capture of attention by irrelevant stimuli. In our case, it could help the subject to resolve our task and answer correctly. Altogether, our results, provide evidence in favor of the implementation of functional inhibition by alpha oscillations during a reasoning task.

Introduction

Recent studies have shown that the suppression of the processing of irrelevant information is an essential mechanism to protect high-level cognitive processes such as working memory (e.g. Zanto & Gazzaley, 2009) or to allow the efficient selection of the relevant information e.g., in the Stroop task (Polk et al., 2008). Therefore, it appears crucial to understand which neural mechanism underlies functional inhibition in the brain and how this activity is top-down controlled.

The results of numerous magnetoencephalography (MEG) and electroencephalography (EEG) studies suggest that alpha activity (~10Hz) might be involved in such a mechanism (for a review, see Foxe & Snyder, 2011; Jensen et al., 2012; Klimesch et al., 2007).

For instance, in visual and somatosensory attentional paradigms, a decrease of alpha activity has been observed in the (engaged) visual/somatosensory area contralateral to the attended side (Capilla et al., 2014; Dombrowe & Hilgetag, 2014; Gould et al., 2011; Grent-’t-Jong et al., 2011; Haegens, Handel, et al., 2011; Ikkai et al., 2016; Jongen et al., 2006; Kelly et al., 2009; T. A. Rihs et al., 2007, 2009; Sauseng et al., 2005; Thut et al., 2006; Trenner et al., 2008; Voytek et al., 2017; Wildegger et al., 2017; Worden et al., 2000; Wyart & Tallon-Baudry, 2008; Yamagishi et al., 2005, 2008). Interestingly, an increase of alpha activity in the (non-engaged) ipsilateral side has been reported especially when a distracter was presented in the unattended side (Green et al., 2017; Gutteling et al., 2021; Haegens et al., 2012; Ikkai et al., 2016; Kelly et al., 2006; T. A. Rihs et al., 2009; Sauseng, Klimesch, Heise, et al., 2009; Siegel et al., 2008; Wildegger et al., 2017) . More generally, an increase of alpha power has been observed in the non-engaged stream in working memory task (Bonnefond & Jensen, 2012; Jokisch & Jensen, 2007; Park et al., 2014; Payne et al., 2013) or in the ventral attention

network during goal-driven tasks (Solís-Vivanco et al., 2021). The interpretation is that the increase of the posterior alpha activity during the retention period is necessary for protecting working memory from external events. Even more convincing regarding the inhibition hypothesis is the negative correlation found, using EEG-fMRI combined, between alpha activity and the signal BOLD (e.g. Laufs et al., 2006; Scheeringa et al., 2011).

However, the role of alpha oscillations in functional inhibition has been challenged recently, in particular in attention tasks (Antonov et al., 2020; Foster & Awh, 2019; Gundlach et al., 2020; Zhigalov & Jensen, 2020). These studies used steady-state visual evoked potentials (SSVEPs), i.e., activity generated by visual stimulations at a certain frequency, to test for the link between alpha oscillations and excitability using EEG or MEG. The authors showed that the observed ipsilateral alpha increase was not related, in amplitude, space and latency, to the attended and non-attended SSVEPs. Specifically, Zhigalov and Jensen (2020) showed that the alpha modulation originated in the occipito-parietal cortex (see also Capilla et al., 2014) while the target/distractor response originated in the early occipital cortex. These authors suggest that the parietal increase could result from a gating rather than a gain control mechanism. Alternatively, it could implement spatial attention, more specifically it could prevent unwanted shift of attention. As discussed in other papers (e.g. Samaha et al., 2020), the detection of alpha modulation in the early cortex could have been altered by the response to the flickers. In any case, the link between alpha oscillations and functional inhibition remains an open question.

Moreover, if these studies seem to highlight those alpha oscillations are engaged in several processes, their involvement in inhibitory processes associated with higher order cognitive processes such as reasoning remains to be demonstrated.

Finally, how posterior alpha activity is controlled is still not clear. Transcranial magnetic stimulation studies showed that perturbation of the activity of the right frontal eye field (FEF) during the delay period of a visuo-spatial attentional task impaired both the identification of target visual stimuli and the posterior alpha desynchronization. However, this experiment did not provide insights regarding how FEF control posterior alpha activity (Marshall, O'Shea, et al., 2015). More recently, an MEG study has also highlighted the role of FEF in the top-down control of the alpha activity in early sensory area (Popov et al., 2017). However, while FEF seems involved in spatial attention (Bisley, 2011), other frontal areas, such as the dorsolateral prefrontal cortex (DLPFC) could be involved in controlling alpha activity in non-spatial task such as working memory or reasoning tasks (Bonnefond & Jensen, 2012, 2013; Solis-Vivanco et al., 2018; Zanto et al., 2010).

In order to further explore the functional role of alpha activity in high level cognitive processes, we used MEG and adapted a reasoning task used in Prado and Noveck (Prado & Noveck, 2007). In this fMRI study, the authors showed that overcoming a perceptual bias in a perceptual reasoning task involved the functional inhibition of the visual cortex by the DLPFC. More specifically, they observed that the increase of the BOLD signal with task difficulty was

associated with a decrease of the BOLD signal over visual cortex. We hypothesized and found that the decrease of the BOLD activity they observed in the visual cortex is reflected by an increase in alpha power and that this activity is controlled by the DLPFC which involvement is revealed by an increase of gamma activity.

Methods

Participants

The study was carried out at the Neuroimaging center of Lyon (CERMEP). Twenty-one healthy native French-speaking volunteers (age: 25 ± 1.78 years; 11 females) participated in the experiment after providing written informed consent according to the Declaration of Helsinki and the local ethics board. All subjects had normal or corrected-to-normal vision and were right-handed according to the Edinburg Handedness Inventory (Oldfield, 1971).

Stimulus material and procedure

The reasoning task was designed using Presentation 10.2 software (Neurobehavioral Systems, http://www.neurobs.com/). A trial was composed of a conditional statement followed by a pictorial target item. The conditional rule described a letter and shape relation (e.g., ‘‘If there is a J then there is a square’’) and the target item was based on a letter-in-shape combination (e.g., a J-in-a square). The study used a within subject 2*2 factorial design with the factors (i) Mismatch Level (0-mismatch, **0M**, and 1-mismatch, **1M**, between the conditional rule and the target item) and (ii) Kind of rule (AA, affirmative throughout and AN, with a negation in the consequent, 120 trials per condition; see **Figure 24A**). To avoid predictability, 120 fillers were included using other kind of mismatching levels (2-mismatch) and of rules.

Each trial started with the presentation of a central dot in the screen during 1s (**Figure 24B**). The two parts of the conditional rule then appeared one line at a time, after 1s and 2s, respectively, at which point the central dot reappeared for 1s. This was immediately followed by the target item, which remained on screen until the subject judged whether the target verified the rule or not and press a button. Participants performed the experiment in eight blocks of 75 randomized trials.

Data acquisition

Neuromagnetic activity was recorded at a sampling rate of 600Hz, using a 275 first-order axial gradiometers whole-head MEG system (VSF/CTF Systems, Port Coquitlam, Canada) housed in a magnetically shielded room. Three marker coils were placed respectively at the nasion and the left and right ear canals to measure the subject’s head position relative to the MEG during the experiment. During the experiment, horizontal and vertical eye movements were recorded using vertical and horizontal EOG electrodes.

After the MEG acquisition, an anatomical T1 MRI of the participants was acquired with a 1.5T Siemens Sonata system (Erlangen, Germany) with a voxel size of $1mm^3$. For the co-registration of the MRI and the MEG data, tablets of Vitamin E were used and placed at the position of the coils. One participant was unable to perform the MRI.

Data analysis

Reaction times (RTs) were obtained from the subjects' button box responses. RTs shorter than 300ms or longer than the mean + 2std were excluded.

The MEG analyses were performed using the Fieldtrip software package (Oostenveld et al., 2011). MEG data were epoched 0. before the onset of the visual stimulus until the time of the subject's response or until 1s after the stimulus onset if the response time exceeded this time. Based on a z-score algorithm across sensors exceeding a threshold given by the data variance within each participant, an automatic rejection of eye blink or saccades, SQUID jumps, or muscles artifacts was run. Additional visual inspection was applied to the remaining trials before including them in further analyses. Only epochs without artifact and with correct answer were considered.

For the sensor-level analyses, planar gradients of the MEG field distribution were calculated using a nearest neighbor method where the horizontal and vertical components of the estimated planar gradients were derived, thus approximating the signal measured by MEG systems with planar gradiometers (Bastiaansen & Knösche, 2000). This representation facilitates the interpretation of the sensor-level data, because the largest signal of the planar gradient is typically located above the source. Time–frequency representations (TFRs) were obtained using a fast Fourier transformation approach with a 3 cycles long adaptive sliding time window ($\Delta T = 3/f$; e.g., ΔT = 300 msec for the 10Hz frequency). A hanning taper (ΔT long) was multiplied by the data before the Fourier transformation. The TFRs of power were estimated for the horizontal and vertical components and then summed for the planar gradient. The power for the individual trials was log transformed after averaged over conditions and log transformed.

Source localization of the power effects observed at the sensor level was performed using a frequency domain beamforming approach based on an adaptative filtering technique (Dynamic Imaging of Coherent Sources, DICS; Gross et al., 2001). We obtained cross-spectral density matrices by applying a multitaper FFT approach on data measured from the axial sensors. A realistically shaped single-shell description of the brain was constructed, based on the individual anatomical MRIs and head shapes (Nolte, 2003). The brain volume of each participant was divided into a grid with a 1-cm resolution and normalized to the template MNI brain (International Consortium for Brain Mapping, Montreal Neurological Institute, Canada) using SPM8 (www.fil. Ion.ucl.ac.uk/spm). The lead field and the cross-spectral density were used to calculate a spatial filter for each grid point (Gross et al., 2001), and the spatial distribution of power was estimated for each condition in each participant. A common filter

was used for both conditions, i.e., it was based on the cross-spectral density matrices of the combined conditions. The regularization parameter was set at 5%. As in the sensor-level analyses, the estimated power was averaged over trials and log transformed. The contrast between conditions was performed and averaged across participants. All source data were estimated within the alpha and the gamma range according to sensor-level results (see results section). The source estimates were plotted on a standard MNI brain found in SPM8.

The Note that for source analysis, 20 subjects were included in the source reconstruction, as for one subject the MRI was missing.

As the time windows of the different effects were relatively short, we confirmed our DICS results using a linearly constrained minimum variance (LCMV) scalar beamformer spatial filter algorithm to generate maps of source activity on a 1-cm grid, and lambda of 5% (Van Veen, van Drongelen, Yuchtman, & Suzuki, 1997). The beamformer source reconstruction calculates a set of weights that maps the sensor data to time series at the source locations, allowing to reconstruct the signal at source level. We performed time–frequency analyses on these reconstructed time series and subsequently averaged the power in the alpha band (7–11 Hz) over the two windows of interest.

Statistics

Regarding the behavior, accuracy, and response time (RT) were analyzed using repeated-measures ANOVA (RM-ANOVA) with factors mismatching level (0-mismatch and 1-mismatch) and type of rule (AA and AN). A Greenhouse– Geisser correction was used in case of violation of sphericity assumption and a Bonferroni test was used for post hoc comparisons.

The significance of power differences observed between conditions at both sensor and source levels were assessed using a cluster based nonparametric randomization test (Maris & Oostenveld, 2007). This test controls for the Type I error rate in situations involving multiple comparisons over sensors, frequencies, and times by clustering neighboring sensors, time points, and frequency points that show the same effect. We analyzed frequencies from 3 to 40 Hz (using 1-Hz increments; 3 cycles time-windows) from the stimulus onset to 1s after stimulus onset.

By randomly permuting the data across the two conditions and recalculating the test statistic 1000 times, we obtained a reference distribution to evaluate the statistics significance of a given effect (Monte Carlo estimation). Sensors or voxels for which the t value of the difference between conditions exceeded an a priori threshold ($p < .05$) was selected and subsequently clustered on the basis of spatial adjacency, and the sum of the t values within a cluster was used as cluster-level statistic. The cluster with the maximum sum was used as test statistic.

Results

In a short interview realized after the recordings, we asked the participants whether they implemented a specific strategy. They simply reported that rules that included negations required more effort to be understood.

Behavior

Overall performances for each condition are shown in **Figure 24.A**, ANOVAs were carried out on accuracy and response times (correct trials only; **Figure 24.C**). A main effect of 'mismatch level' was only found for response times (response times, p=1,06e-10, F=147,96; accuracy, *p* =0.63, F= 0,23). Responses were faster in the 0-mismatch condition than in the 1-mismatch condition. A main effect of 'type of rule' was also found in response times but also in a lesser way in accuracy (response times p= 1,46e-6 F=45,47; accuracy p=0,48 F=0,51). Responses were faster and more accurate for the AA rule than for AN rule condition. These results could be explained by the difficulty to answer with a negative form instruction.

A

Rule	Target item	Correct Response	Mismatching Level	Number Of trials	Accuracy (%)	Median (±std) Reaction times (ms)
If J then square (AA)	J	Yes	0	120	94.1	641.6 (±301.4)
If J then not square (AN)	J	No	0	120	93.3	900 (±499.3)
If J then square (AA)	J	No	1	120	94.1	898.3 (±431.6)
If J then not square (AN)	J	Yes	1	120	92.5	1008.3 (±504.1)

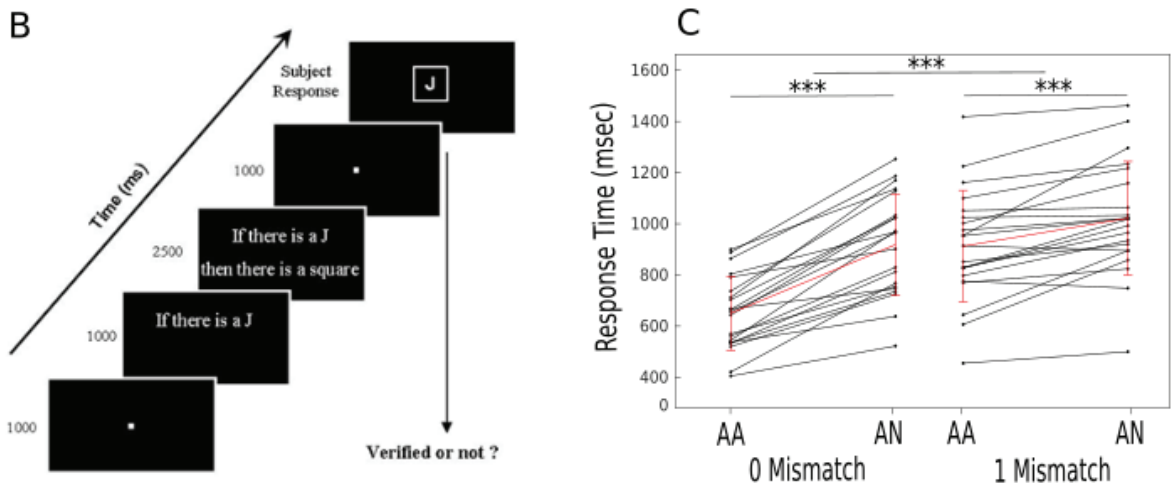

***Figure 24**: **Stimuli, task design and behavior results. A. Overall conditions**. Mismatch Level (0-mismatch, **0M**, and 1-mismatch, **1M**, between the conditional rule and the target item) and rule type (AA, affirmative throughout and AN, with a negation in the consequent). Accuracy and median of RT for each condition. **B. Timing of one trial.** Each trial started with the presentation of a visual fixation mark (a central dot) in the center of the screen for 1000ms. The two parts of the conditional rule then appeared one line at a time, with the first part (e.g., "If there is a J") appearing at 1000ms and the second part ("then there is a square") at 1500ms. The rule then disappeared, and the central dot reappeared for 1000ms. This was immediately followed by the target item, which remained on the screen until subjects pressed a button. **C. Behavior results**. RTs were shorter for 0 Mismatch than for 1 Mismatch and in AA than AN condition. Red lines represent the median RT and the red bar the standard deviation. *** p<0,001.*

MEG analyses

Alpha amplitude increases with 'mismatch level'

We first focused on the difference of power between the 1M and 0M conditions.

We observed a stronger power in the 7-11Hz band in the 1M condition (see **Figure 25.A**). A cluster-based randomization test controlling for multiple comparisons over time, frequency, and sensors revealed one cluster (cluster-level statistic [CS] = 7.21e+4 $p < 0.05$) encompassing different time windows over the occipital and left temporal and frontal channels (0.2-0.45ms),

the right parietal channels and the right central channels (peaking later; 0.25-0.5ms; **Figure 25.B**).

To illustrate this effect, **Figure 25.C** represents the time course of the power for the frequency band 7-11 Hz. It shows that the, classically observed, stimulus induced decrease of alpha power is less important in the 1M condition and exhibit different time courses for three groups of channels.

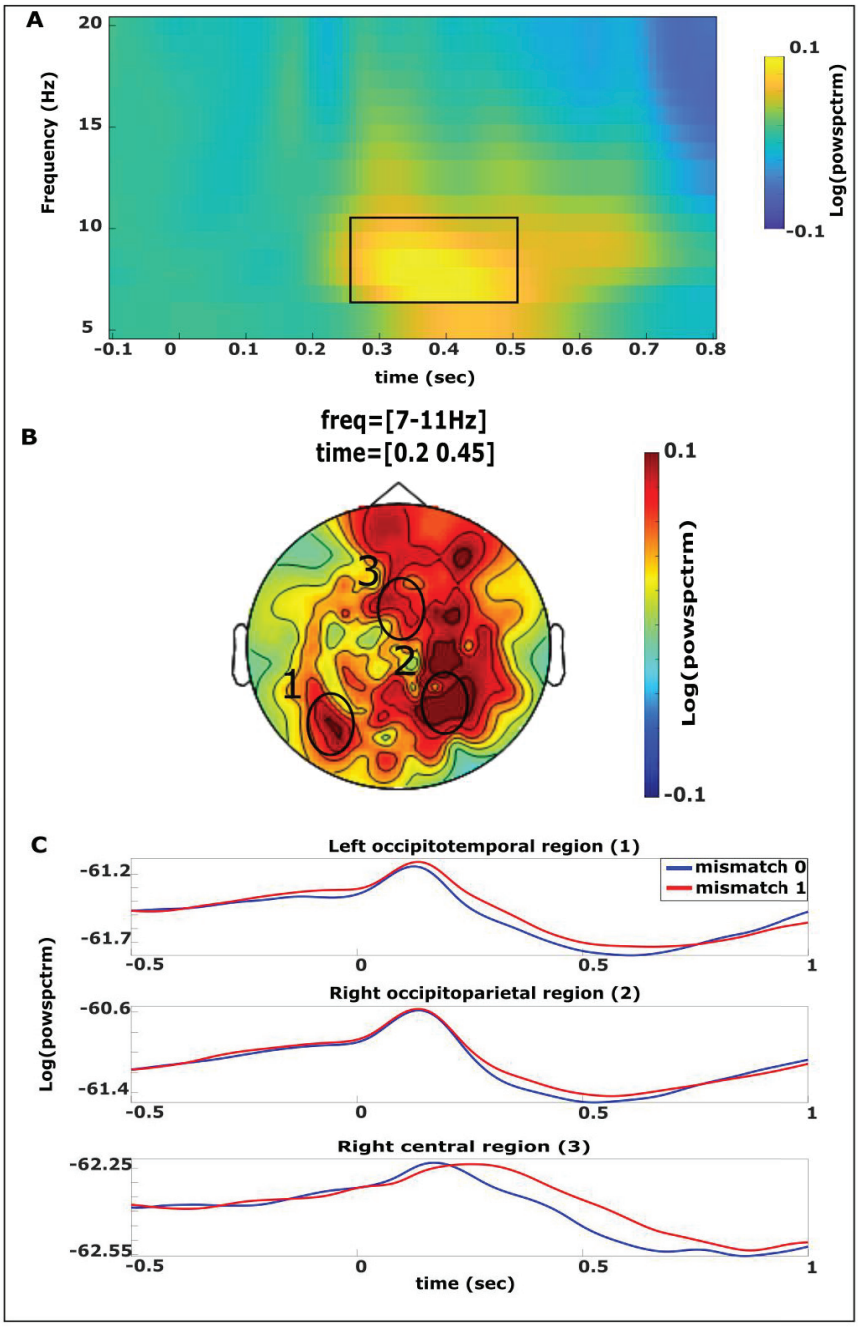

Figure 25: ***Alpha power is stronger in the 1-Mismatch condition over the left occipito-temporal, the right occipito-parietal and temporal and the central sensors.***

A. *Time-frequency representation of the contrast 1-mismatch (1M) vs 0-mismatch (0M) averaged over all sensors. The alpha power is stronger in the 1M condition than in the 0M condition. 0 corresponds to the stimulus onset.*

B. *Topography of the alpha power modulations (7–11 Hz; for the period 0.2–0.45s). The cluster randomization analysis revealed a significant cluster in left occipitotemporal (**1**) sensors first, then in right occipitoparietal and temporal (**2**) and right center (**3**) sensors ($p < 0.05$)*

C. *Time course of the alpha power in the 1M (red) and 0M (blue) conditions on different sensors averaged over the 7-11Hz frequency band.*

The LCMV performed in the window in which all effects were observed ([0.2 0.45s], cluster statistics CS = 4074 p = $9.9*10^{-4}$) revealed alpha increase peaks over the bilateral cuneus (MNI[42 21 47]) and the left inferior temporal cortex (MNI[-56 -60 -10]). These regions are associated with visual processing (**Figure 26**).

It also showed the bilateral pallidum (MNI[-24 -2 2] [30 2 2], the bilateral superior frontal cortex (MNI[-30 34 34] [26 38 36]), the left medial frontal cortex -28 22 42], the left inferior frontal opercular [-42 16 10], the bilateral inferior parietal cortices (MNI[-50 -52 40] [44 -54 50]), the bilateral superior parietal cortex (MNI[-26 -58 50] [38 -56 64]) and the left and right cerebellum (MNI[-22 -68 -36] [36 -78 -28))These regions could belong or be connected to the cognitive control network.

We also observed the bilateral precuneus (MNI[2 -50 40] [12 -48 40]) and the right medial/posterior cingulate cortex (MNI[12 -38 28]). These regions might be part of the default mode network, but further investigations are required as we did not observe the frontal part of such network.

Finally, these results revealed the right medial frontal cortex [38 10 38], the right inferior frontal gyrus (MNI[52 8 6]), the right insula (MNI([38 4 8]), the right medial temporal cortex (MNI[56 -8 -20]), the right superior temporal cortex (MNI[44 -44 12]). These regions might be part of the ventral attention network.

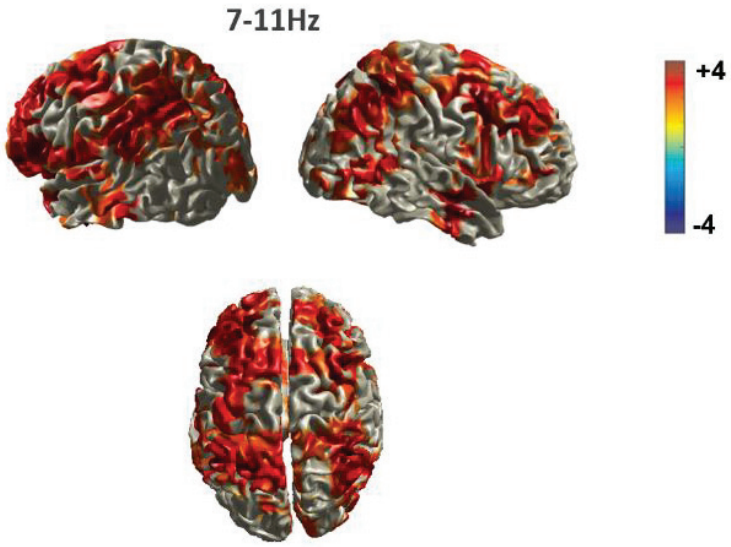

***Figure 26**: Source (LCMV) representation of the 7-11 Hz activity. Alpha power is stronger in the 1-Mismatch condition over the left cuneus, the right lingual gyrus and cuneus, the left occipito-temporal, cortex, the bilateral cognitive control network, the VAN and the bilateral precuneus. Red areas indicate a significant increase (p <0.05).*

Alpha power is correlated with RT

We did not observe stronger alpha power for fast than for slow trials (median split) in the 1M condition. However, we observed a negative correlation between alpha and behavior for the difference between 1M and 0M specifically on left occipitotemporal sensors for frequency 7-11 Hz. (r=-0,55; p=0.01; **Figure 27**). Over participants, higher posterior alpha in 1M condition was associated with faster RT.

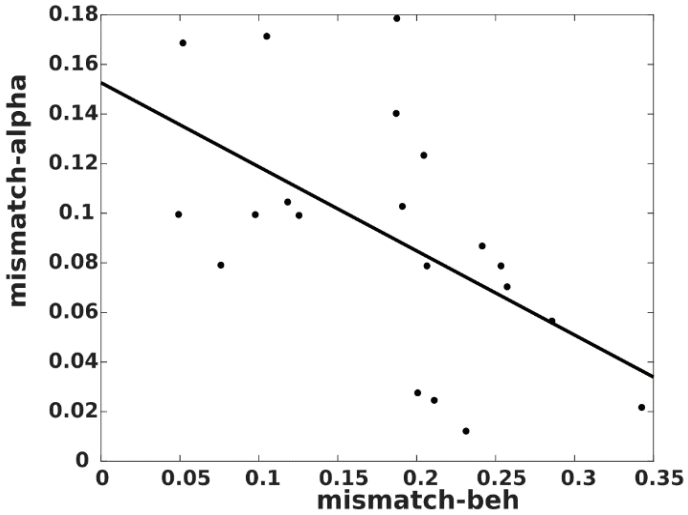

Figure 27*: Correlation between the alpha power (averaged over occipitotemporal sensors and frequency band 7-11 Hz) and reaction times for the difference between 1M and 0M. (r=-0,55; p=0.01)*

No alpha difference between sub-conditions

We then quantified the alpha power from the MEG data for the sub-condition (i.e., 0MAA, 0MAN, 1MAA and 1MAN. The TFR of power did reveal time-windows, from 400ms to 600ms after the stimulus appears, with increased alpha power in the 0MAN compared to 0MAA condition over the right central cortex but these effects did not survive multiple comparisons correction ($p < 0.05$ before correction).

Similarly, we found bursts of strong alpha power in the 1MAN compared to 1MAA condition for the period from 400ms to 800ms after the stimulus appears over the right central cortex, but as for the analysis above, these effects did not survive multiple comparisons correction.

No increase of gamma power over frontal regions

Our analysis of the gamma did not show significant results in the period after the stimulus appears on the screen contrary to that we expected.

Discussion

The goal of the present study was to determine the role of alpha oscillations in a reasoning task involving functional inhibition of the visual area.

We manipulated the matching level between the target items and the items mentioned in the rules in order to create a perceptual bias, i.e., the tendency to reject mismatching items even if they verify the rule. First, behavior results showed a clear mismatching effect with longer response times in the one mismatching (1M) condition compared to the 0 mismatching (0M). Moreover, we showed that responses were faster and more accurate for the conditions with affirmative instruction rule (AA) than for the conditions with negative instruction rule (AN). These results indicate that rules with negation increases the decision time. These results confirmed previous findings reporting an increase of response times with rules complexity (Prado & Noveck, 2006, 2007).

The time frequency analyses revealed higher alpha power in the 1M than in the 0M condition, first over posterior sensors and over parieto-temporo-fontal sensors (later peak). Source level analysis indicated the involvement of the left occipito-temporal cortex, the left inferior cortex and of a bilateral fronto-parietal cortex in the early window. We interpret the alpha increase over the bilateral cuneus as reflecting the disengagement from visual processing to allow abstract reasoning. In line with this interpretation, this region showed a decrease of BOLD signal, when the DLPFC BOLD increased, in the fMRI task using a similar paradigm of Prado et al. (2007).In addition, the stronger alpha power over the left temporal cortex might indicate further suppression of the processing of the letter as the left temporal cortex has been associated with processing letters (e.g. James et al., 2005). The occipital alpha increase might have been necessary in both the 1M condition and 0M condition in the trials with rules involving one negation (AN). Indeed, participants might have to overcome the bias to consider these matching items as validating the rule. Region of interest analyses over the occipital cortex in the four conditions will allow to test for this hypothesis. A new study involving additional rules such as rules including a negation in the first part of the rule might further help to highlight this effect (see Prado et al. 2007).

We did not find stronger alpha power in fast than in slow reaction times trials in the 1M condition. However, we used a median split which was maybe not sensitive enough to reveal such effect. We will perform more fine-grained analyses to determine whether there is a link between alpha power and behavior at subject level. We however observed a correlation between the alpha power and RT differences between 1M and 0M conditions across participants. This correlation was specific to the left occipito-temporal cluster. This indicates that an efficient inhibition of the occipital and left temporal cortex in the 1M condition might help to perform the task optimally and might depend on participants 'general ability. Such correlation will be performed at source level to further determine the specificity of the effect.

We further observed higher alpha power in regions belonging to the ventral attention network (VAN) and in the precuneus and posterior cingulate cortex which belong to the default mode network (DMN) in the 1M compared to 0M condition. The VAN has been associated with the capture of attention by unattended, but relevant, stimuli (Corbetta et al., 2008; Corbetta & Shulman, 2002). Corbetta et al. (2002, 2008) suggested that the inhibition of the VAN was crucial for preventing the capture of attention by irrelevant stimuli. In line with that idea, Solis-Vivanco et al. (2021) reported that higher alpha/beta power in the VAN was associated with a lower distractor interference over subjects. The inhibition of this network in our task help subject to overcome to the perceptual bias. Similarly, the DMN has been associated with focus on internal thoughts and is generally found to be inhibited during tasks (Ossandon et al., 2011; Raichle, 2015) in line with the alpha increase observed here). However, we did not observe the frontal part of the DMN. This might be due to technical reasons (low SNR or participants' position in the MEG) or the precuneus we observed might not be part of the DMN per se. Further investigations (e.g., more precise source localization) will allow to tackle this issue. The frequency band found over the VAN (and DMN) in the current task was lower than the frequency band reported in Solis_Vivanco et al. (2021) and Ferez et al. (submitted; 10-20Hz). More generally, the alpha frequency observed in the current task was relatively slow. It remains to be investigated whether the frequency depends on the specificity of the task performed or whether the mechanism behind is fundamentally different. A correlation between performance and alpha frequency over participants could provide further insights.

We did not find an increase of gamma oscillation over the DLPFC, dACC and inferior/superior parietal cortex but rather an increase in the 7-11Hz band (see Prado et al. 2007). More fine-grained analyses at the source level will help to determine the peak frequency observed over these regions which might be associated with theta band rather than alpha band. Preliminary results seem to indicate that this is the case (cf supplementary figure). Connectivity analyses between the nodes of these different networks and the occipital and left temporal cortex will allow to determine whether these regions are involved in controlling the posterior alpha oscillations.

Moreover, it will be necessary to refine the source localization by considering the head movements of the subjects. Indeed, in this task, the subjects were in a sitting position and asked for breaks outside the scanner between one to four times per session, which means that the head position could vary significantly during a session. In a future analysis, we will use e.g., an average position and reject trials with a head position above 2 standard deviations from the mean.

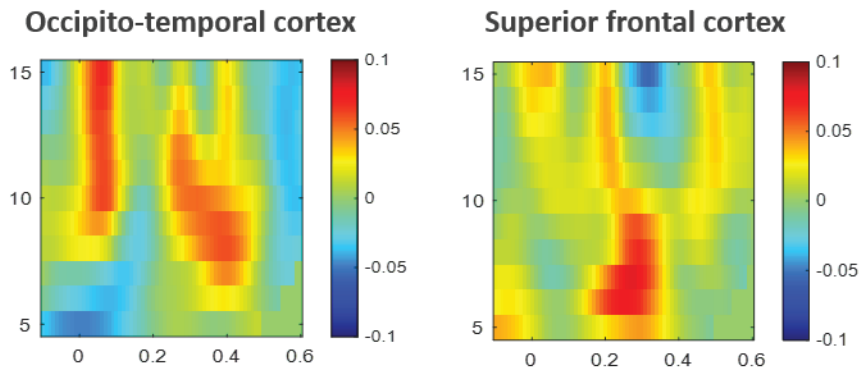

Supplementary figure: Time frequency over regions of interests indicate that the frequency band modulated in the bilateral superior frontal cortex is lower (rather in the theta band) than in the in the occipito-temporal cortex.

General Discussion

Summary of results

In this thesis, we have provided new insights into the role of the alpha oscillations in functional inhibition. Our results were not restricted to alpha oscillations as we also reported effects in the delta(<4Hz), theta (4-7Hz) and beta (15-30Hz) band.

In our first MEG study, a cue-based modified Stroop task, with always incongruency between color word and ink, we presented to subjects a cue in each trial indicating whether they had to attend the ink of the word or the color word itself. Stimuli were words indicating a color and were written using an incongruent ink color. In the attend-color condition, participants had to ignore the word to report the color of the ink. If alpha oscillations are linked to functional inhibition, we expected higher alpha power over the visual word form (VWFA) in this condition. This effect did not survive the correction for multiple comparisons. We however observed higher alpha/beta (10-20Hz) power in the ventral attention network (VAN), a network associated with the capture of attention by relevant but unattended stimuli, in anticipation and during the processing of stimuli in both the attend-color and attend-word conditions (see below for a detailed discussion of this effect). Higher alpha/beta power in this network was associated with faster reaction times in all conditions. We also found high alpha/beta power in the medial prefrontal cortex, the posterior cingulate cortex and the temporal pole indicating a possible inhibition of the default mode network (DMN) in anticipation and during stimulus processing (for a review see Raichle, 2015). In addition, we found that stronger theta power over the right dorsolateral prefrontal cortex, the ACC, and the ventromedial prefrontal cortex, e.g., regions associated with cognitive control, was associated with faster reaction times. This result indicates that good performances in the task might involve a high level of cognitive control (Cohen & Donner, 2013). The absence of alpha increase might be due to the low difficulty of the task and the irregularity of the distractor's position or feature (see below).

We therefore designed another task. We used faces with names written on the top and participants were asked to determine the gender of the faces or of the names in different blocks. We expected that participants would be required to suppress the processing of the unattended stimuli to perform the task optimally (e.g., names in the attend-face condition). We observed prestimulus alpha power increase in the left occipito-temporal cortex including left occipitotemporal cortex LOT/VWFA (but see discussion of the face-name paper, chapter 2) in the attend-face compared to the attend-name condition. This increase over LOT/VWFA in the alpha band was further associated with faster reaction times in the incongruent trials of this condition. We interpreted this alpha increase as reflecting the functional inhibition of the LOT/VWFA to prevent the processing of the name, i.e., the distractor in the attend-face condition. We further observed higher alpha power over the parietal and left frontal regions. We hypothesize that these regions are involved in the top-down control of alpha oscillations over LOT/VWFA. Connectivity analyses will allow to test this hypothesis (see below). Altogether these results indicate that the inhibitory role of alpha oscillations operates beyond early sensory regions. During the prestimulus period, we also observed an increase of delta

oscillation activity over the left occipitotemporal and parietal cortices. Finally, in the attend-face condition, we observed a pre-stimulus increase of beta power, in the VAN.

Finally, we aimed at determining whether alpha oscillations would be involved in inhibitory processes during a high-level cognitive process. In the task we used, participants were presented with a conditional rule that described the relation between a letter and a shape, e.g., if there is a J then there is a square, followed by the stimuli representing or not this relation. To perform well in this task, it has been shown that participants need to overcome a perceptual bias, the matching bias, i.e., he tendency to answer "correct" whenever the stimuli presented match the ones mentioned in the rule, in order to perform well. We showed that alpha oscillations over the occipital and left temporal cortex, a frontoparietal network and the VAN might be involved in implementing this process.

I discuss below how these different results resonate with the hypotheses and questions formulated in the introduction.

Alpha oscillations are involved in the disengagement of irrelevant areas

One goal of this thesis was to investigate the role of alpha oscillations in the disengagement of irrelevant areas, more precisely in the suppression of the processing of irrelevant or unattended information

Altogether, our results showed that two factors might influence the modulation of alpha oscillations over sensory regions, namely the difficulty of the task through e.g., the perceptual load or other factors and the regularity of the distractor's position or feature.

Regarding the first parameter, Lavie (2005) formulated the perceptual load hypothesis according to which our capacity to process stimuli is limited, and observers need therefore to efficiently filter out distractors when the perceptual load is high. In our first study (the task based on Stroop stimuli, chapter 1), we did not observe the expected behavioral effect i.e., response time faster in the attend-word than the attend-color condition as reading is automatic and difficult to overcome (Augustinova & Ferrand, 2014) and, as a consequence, word are expected to be particularly distracting when participants have to report the color of the ink (Stroop, 1935). It is therefore possible that the task was not demanding at the perceptual level and did not require distractor filtering and hence an increase of alpha oscillations over e.g., the VWFA in the attend-color condition. It is also possible that a few subjects exhibited a right dominance of the VWFA (for more details see discussion of the word-color study, chapter 1), an issue that might have been overcome in the face-name task (chapter 2) given the number of participants. However, an alternative or complementary hypothesis would be that the conflict occurred at the decision rather than at the perceptual level in this task (see below).

In our second study (face-name task) we found slower reaction times in the attend-face compared to the attend-name conditions. This indicates that the difficulty was higher in the attend-face condition. This larger difficulty could either result from a higher perceptual load, a stronger distractor interference, or both. The overall slower reaction times, in particular in the congruent condition, in the attend-face condition compared to attend-name, could be interpreted in favor of the first effect while the stronger reaction times difference between congruent and incongruent trials in the attend-face condition could be interpreted in favor of the second effect. The salience of the names as distractors might result from automatic reading (Augustinova & Ferrand, 2014) and from their position on the screen. The combination of the two factors, perceptual load, and distractor strength could be necessary to involve functional inhibition and therefore high alpha oscillations.

Interestingly, Gutteling et al. (2021) manipulated independently the perceptual load and the salience of the distractors in a spatial attention task. They found both a stronger ipsilateral alpha power (i.e., contralateral to the distractor) in the high load than in the low load condition and stronger alpha power for the more salient distractors but only in the high perceptual load condition. In our experiment, the attend-face condition might correspond to the second condition (high load and high distractor salience) and resulted in higher alpha oscillations in the LOT/ VWFA to perform the task.

Regarding the second parameter, it was shown that if distractors are always at the same position during a task, they stop capturing attention over time (Moorselaar & Slagter, 2019; Vatterott & Vecera, 2012). In our word-color task, we used a trial design, the object ignored varied across trials (cue-based task) while in the face-name task, the ignored object remains similar within a block. The block design could therefore allow to implement more easily the inhibition needed to suppress the processing of the distractor. This could further explain our result showing an increase of alpha power over the LOT/VWFA in the attend-face condition in the block design and not in the trial design. The impact of the design on the removal of distractors seems to be an important element to consider when designing the task, as well as other aspects. Indeed, several researchers have tried to design a guideline of rules to follow in order to help study the suppression of distractors (Wöstmann et al., 2022). In this paper they explained that if there is no difference in performance between highly-distracting and less-distracting trial it was possible that the intended distractor was effectively suppressed or that participants realized through experience that the distraction is unrelated to the task at hand, which did not necessarily suggest that the distraction is not distracting. This could explain our results in the word-color task due to the intensive training of the subject the day before they performed the task.

Our second task have combined high perceptual load, high distractor salience and stability of the feature/element ignored, therefore future studies manipulating these factors independently might allow to better characterize the role of each factor and of their combination in modulating anticipatory alpha oscillations.

An important limitation of these studies is the lack of functional specificity of the different target areas such as the 'color area' (e.g. V4), the FFA (and other face-related regions) and the VWFA (e.g. Vidal et al., 2010). For instance, it has been shown that, in the fusiform gyrus, there are distinct but also overlapping patterns of responses to faces and words (Harris et al., 2016). Another study showed that reading acquisition recruit brain parts involved in the object and face recognition (Dehaene & Cohen, 2011). This lack of specificity might have hindered some effects, e.g., alpha increase over regions processing faces in the attend-name condition of the face-name task.

Alpha oscillations play an inhibitory role during stimulus processing

Another question we asked in the introduction was whether alpha oscillations could implement function inhibition during stimulus processing, in particular during a high-level cognitive task.

In the reasoning task (chapter 3), we showed that alpha oscillations over occipital and left temporal, the frontoparietal network and the VAN were possibly involved in overcoming a perceptual bias.

In a similar fMRI task, Prado et al. (2007) found (using a psychophysiological interaction analysis) that mismatching level was associated with the inhibition of the occipital cortex by the DLPFC while in the current study, we observed high alpha oscillations over the same regions as these authors observed (bilateral cuneus) as well as the left temporal cortex, possibly involved in processing the letter (James et al., 2005). These results could indicate that alpha oscillations over occipital cortex could implement the inhibition of the visual cortex to overcome a perceptual bias in an abstract reasoning task. The trials analyzed involved one mismatch between the shape mentioned in the rule and the target stimuli. The letter was therefore particularly irrelevant in this condition and performing well might have further required letter processing suppression and therefore high alpha oscillations over the left temporal cortex., In addition, participants might have to overcome the matching bias in the 0-mismatch condition with a negation in the rule as the matching items could bias them into validating the rule by default. Region of interest analyses over the occipital cortex in the four sub-conditions will allow to test for this hypothesis. A new experiment including more rules will further help to refine the role of alpha oscillations in this reasoning process.

Although further analyses and experiments are necessary, these results indicate that alpha oscillations might play a key role to focus on internal processes while ignoring external distraction.

Alpha/beta oscillation are involved in the functional inhibition of regions outside the sensory networks

Another goal of our work was to determine whether alpha oscillations are involved in the functional inhibition of high-level brain regions. In our three studies, we observed higher alpha and/or beta oscillation in the VAN. This network has been associated with the capture of attention by unattended, but relevant, stimuli (Corbetta et al., 2008; Corbetta & Shulman, 2002). Corbetta and Shulman suggested that the inhibition of the VAN was crucial for preventing the capture of attention by irrelevant stimuli.

In our reasoning task, we showed an increase of alpha oscillation over the VAN in the 1-mimatch compared to the 0-mismatch condition. In the word-color task, we also found an increase of alpha/beta power over the VAN in the attend-word and the attend-color condition compared to baseline or detect condition in the prestimulus and stimulus processing periods. This increase was associated with faster reaction times. Moreover, in our face-name task we also showed an increase of beta oscillation power over the VAN in prestimulus period in the attend-face condition. Solís-Vivanco et al. (2021) reported that alpha/beta power over the VAN was associated with a lower distractor interference over participants in line with a functional inhibition role. Our results are therefore in line with this idea. The inhibition of the VAN, to prevent distraction, in anticipation of stimuli or during stimulus processing might be implemented by high alpha/beta oscillations.

In the word-color task (chapter 1) and reasoning tasks (chapter 3), we further observed an increase of alpha/beta power over regions that belong to the default mode network (DMN). It was shown that the DMN is implicated in mind wandering (Fox et al., 2015) and that the activity of this network commonly decreases during task (for a review see Raichle, 2015) allowing to be more focused on the task. We therefore suggest that the alpha/beta increase we observed would be associated with the inhibition of the DMN. This result is further in line with the intracranial results reported in Ossandon et al. (2011). In the easy condition compared to the difficult, authors found a significant decrease in gamma activity in the DMN, but they also showed an increase in alpha/beta activity for a shorter period. According to this study, in the difficult condition, it was necessary to inhibit the DMN by alpha/beta activity for a longer period to succeed in the task. This inhibition possibly allowed the participants to be more focused on the task.

Interestingly, the frequencies observed in the tree tasks over the VAN were different with alpha, alpha/beta or only beta without alpha (10-20Hz in the word-color task, 14-30Hz in the face-name task, and 7-11Hz for the reasoning task). As mentioned above, a goal-driven task was demonstrated to involve alpha/beta oscillations over the VAN (12-20Hz; Solís-Vivanco et al., 2021). But only Beta seems more surprising.

Indeed, beta activity is essentially studied in motor function (Pfurtscheller & Lopes da Silva, 1999). In line with this literature, we also found decreased beta power over the motor

network in two of our studies (word-color task and face-name task) in anticipation of response. However, new study suggested a role of inhibition in the motor action of the beta activity (Schaum et al., 2021). This inhibitory role could explain our results of the beta activity in the VAN to inhibit it but also the results where we have alpha/beta. Moreover, this rhythm could also be implicated in cognitive functions.

For instance, it has been suggested that, during attentional tasks, communications among task-relevant areas as the fronto-parieto-temporal attentional network would be set-up through phase synchronization in the beta band (Gross et al., 2004)., Furthermore, it was demonstrated that a variety of factors that influence the regulation of cognitive control are reflected in beta oscillations during a trial-and-error task in which monkeys had to choose which of four targets would be rewarded (Stoll et al., 2016). Authors showed that greater top-down communication between the visual and frontal areas, was associated with increased connectivity in the beta band. This last element leads us to question the role of beta oscillations in our different tasks, especially in the top-down control of alpha oscillations, which should be further investigated.

It has more recently been shown, in trial-by-trial analysis, that the sensorimotor beta activity is dominated by transient, high amplitude bursting events (little et al 2019). Moreover, authors explained that the probability of burst occurrence decreases before, and peaks after the movement, thus giving the appearance of slow beta amplitude modulation after averaging these bursts over multiple trials. We will apply similar analysis to our data to determine whether beta activity observed over the VAN and DMN is also associated with bursts. Such results would further associate these bursts with functional inhibition.

Further analyses at the source level will allow to confirm this discrepancy. The difference might result from the task specificities, i.e., attention vs reasoning process or from fundamentally different mechanisms. Answering this question will require further investigations.

No alpha phase adjustment in anticipation of stimulus

In anticipation of the stimulus, there is only sparse evidence of alpha phase adjustment. Some studies report a phase adjustment (Bonnefond & Jensen, 2013; Solis-Vivanco et al., 2018), while others do not (van Diepen et al., 2015). It therefore seemed important to investigate this question. That is why, in the word-color task (chapter 1), one of our goals was to test whether alpha phase could be adjusted in anticipation of the predictable stimulus to optimize the suppression of the distracting feature (e.g., the word in the color-condition). Our data did not show a significantly higher phase concentration over the left temporal sensors (i.e., over VWFA) in the attend-color condition. This absence of effect provides evidence against the idea that alpha phase can be adjust in anticipation of predictable stimuli, through top-down control, in order to optimize target processing or

distractor suppression. However, this absence of difference might also result from (1) a strong alpha phase adjustment in the attend-word condition (with opposite phase) as well in order to optimize the processing of the word (2) the right dominance of the VWFA in a few participants or (3) the absence of inhibition requirement in this task, in line with the absence of alpha power increase.

We however observed a phase adjustment over temporal sensors in both conditions. We will further explore this result at source level.

Further analyses needed to determine which brain regions may control these sensory alpha oscillations

In the three tasks, one of the objectives was to understand which higher order regions control these alpha oscillations. A few covert attentional studies have revealed, using EEG, MEG and TMS, that frontal eye field (FEF) and parietal cortex (as well as the right inferior gyrus) were involved in the top-down control of posterior alpha power modulation (Marshall, Bergmann et al., 2015; Popov et al., 2017; Wang et al., 2016). Other studies have additionally shown an involvement of the left frontal gyrus in controlling posterior alpha phase adjustment, in a working memory and a bimodal attentional tasks (Bonnefond & Jensen, 2012; Solís-Vivanco et al., 2018).

In all our tasks, we noted the presence of alpha/theta oscillations in frontal regions, and more precisely, in the regions associated with cognitive control. For the first study, it was in anticipation of the stimuli over the (right dorsolateral prefrontal cortex, the ACC, and the ventromedial prefrontal cortex. Moreover, this activity was associated with faster reaction. For our second study, before the stimuli, we observed an increase of alpha/theta activity in frontal regions in the attend-face incongruent for the faster trials. Finally, in our third study, we noted a peak of theta activity over the DLPFC, dACC and inferior/superior parietal cortex. These regions might be involved in controlling the posterior alpha oscillations. Indeed, it was shown that a link exists between the theta activity in frontal regions and alpha in posterior regions (Mazaheri et al., 2009, 2010). Mazaheri and collaborators (2009) showed in a Go-noGo task, that an error resulted in an increased frontal theta activity slightly earlier than a decreased posterior alpha activity. They hypothesized that serve to reflect a top-down modulation by which oscillatory alpha activity in visual areas is suppressed. In the second study, authors found also this anticorrelated activity between midfrontal theta activity and posterior alpha activity in a cross-modal attention task (Mazaheri et al., 2010). Depending on the type of task, theta activity could increase or decrease the posterior alpha activity. We will use connectivity tools such as amplitude-amplitude correlation, cross frequency coupling or granger causality analysis to test the hypothesis that this frontal theta activity controls the alpha activity in posterior regions.

Theta oscillations over the DLPFC and ACC is involved in detecting and resolving conflict

In addition, in the word-color task and also in incongruent trials face-name task, we found that stronger theta power over the right dorsolateral prefrontal cortex, the ACC, and the ventromedial prefrontal cortex, e.g., regions associated with cognitive control, were associated with faster reaction times. These results possibly indicating that good performances in the task involved a high level of cognitive control. These results are in line with a large literature showing the important role of ACC and DLPFC in cognitive control (Matsumoto & Tanaka, 2004) and the role of theta oscillations over midfrontal and dorsolateral regions to resolve conflict (Cohen & Donner, 2013). More recently, Kaiser and collaborators revealed that faster conflict resolution was linked with the anticipation of this conflict and with the increase of frontal theta power and posterior alpha power decrease (Kaiser et al., 2022).

The 7-11Hz increase over these regions in the reasoning task might further be associated with the involvement of cognitive control in this task. Refined source level and connectivity might provide insights regarding this point.

Delta oscillations over the left occipito-temporal and parietal cortices

In the face-name task, we also found a higher delta oscillations activity during the prestimulus period over the left occipito-temporal and parietal cortices. A study showed that the primary visual cortex's delta-band oscillations entrain to the rhythm of the stream, increasing response gain for task-relevant events and speeding up reaction times (Lakatos et al., 2008). The authors suggested that the entrainment of cortical delta oscillations is a key mechanism of selective attention to rhythmic auditory or visual input streams. Because of the design of our task, i.e., the five stimuli that follow each other, a kind of rhythmicity can also be distinguished in our study which could explain the delta activity recorded.

Moreover, another study with a similar selective attention intersensory audiovisual task involving epileptic patient implanted in the auditory cortex, showed a coupling between delta phase and alpha power (Gomez-Ramirez et al., 2011). The author also demonstrated that when the participant had to focus on the visual stimulus to hear the auditory stimulus, the alpha power in the auditory cortex increased. They concluded that these delta-entrained oscillations adjust the alpha-band power according to their phase. It will be interesting to continue our analysis to refine the relationship between alpha and delta oscillation in our task. Notably because our data showed that alpha appeared as burst at the occipital region which could be related to the delta rhythm.

Source localization in MEG, statistics, and inverse inference

Our experiments had some limitations such as the use of MEG for precisely localizing sources or the use of cluster-based statistical analyses. For instance, we found widespread networks in all three of our studies which might impact interpretations regarding e.g., the involvement of the DMN. It might result from an actual involvement of widespread networks but also from the lack of precision of the MEG or the statistical tools used. Indeed, cluster analyses present some limitations as they favor big clusters and might as such create spurious effects. However, most of the effects reported here also survived a more conservative FDR correction.

We observed increase alpha over subcortical regions (e.g., basal ganglia) in the different studies. Although surprising, this is in line with many studies showing that, unlike what was previously thought, subcortical regions can be detected with MEG (Pizzo et al., 2021). It has been shown that alpha oscillations play a role in the pulvinar level, especially in the regulation of attention (for a review see Froesel et al., 2021). Moreover, it was shown that alpha oscillations in the pulvinar would drive alpha oscillations in V4 and TEO (Saalmann et al., 2012) It will therefore be very interesting, especially in our face-name task using head-cast to reduce head movements, to analyze the alpha oscillations in the subcortical regions.

We plan to use the head localization measures recorded online during the task to further improve source localization (use of the mean head position, rejection of trials with important head movements etc.…). In particular, participants moved more during the reasoning task than during other tasks as they were in a sitting position.

In addition, this thesis relies on inverse inference. Indeed, we considered the regions observed to belong e.g., to the VAN, the DMN and the word specific areas and, as a consequence, the alpha increase over these regions to reflect (the suppression of) specific processes they have been associated to. This is a limitation of many neuroimaging studies. Region of interest analyses based on localizer task might provide additional evidence in favor of these interpretations.

To go further

First, it will be important to finalize and refine our analyses in the face-name and reasoning tasks. For instance, we used localizer tasks in the face-name condition which will allow to better define face specific regions and how the regions are modulated during the task. As mentioned above, we will perform connectivity analyzes to determine which brain regions control the posterior alpha oscillations we observed. In addition, we will perform connectivity between several regions of interest. It is possible that the suppression of the processing of the distractors are supported by a specific connectivity between VWFA and V1, and between VWFA and higher order regions. In particular, an anti-phase relationship or a decrease of the connectivity in the alpha-band could be implemented (Bonnefond et al.,

2017). In addition, It has been shown that the strength of feedback connectivity, for low frequency oscillations, between FFA and V1 predicted the upcoming percept but also the strength of post-stimulus neural activity (Rassi et al., 2019). In line with this result, we can also hypothesize the face-name task, an increased connectivity in the alpha band between FFA and V1 in the pre-stimulus period in the attend-face condition and, between VWFA and V1 in the attend-name condition. Furthermore, the coupling of alpha and gamma oscillations band could be altered in the VWFA in the attend-face condition (see Pascucci et al., 2018; Bonnefond et al., 2017).

Furthermore, we hope to be able to get laminar-level (two compartments) resolution of the source localization in the face-name task using specific source localization tools and taking advantage of the individual headcasts (which limit head movements) we used in this experiment (Bonaiuto et al., 2018; Meyer et al., 2017). Our analysis, based on the paper of Bonaiuto and collaborators (2020), will further use the link vectors between the pial and white matter surfaces to approximate the orientation of cortical columns and increase precision (Bonaiuto et al., 2020; see annexes). This type of analysis will provide information regarding the laminar profile of alpha oscillations in our task. For instance, we hypothesize that we will find a predominance of alpha increase in the infragranular layer in the VWFA. Possibly the connectivity of the superficial alpha and of the deep alpha will be different. Bonnefond et al. (2017) hypothesized that alpha in the superficial layers, which exhibit a receptive field connectivity specificity at the anatomical level, might allow to implement communication between regions while alpha oscillations in the less specific deep layers might be associated with the local inhibition of groups of neurons processing irrelevant information.

Regarding future investigations, as mentioned above, we should design tasks that manipulate independently the different factors (perceptual load and/or distractor salience) that might be involved in modulating posterior alpha oscillations. For instance, using on our task with faces and names we could, as Gutteling et al. (2021), vary the target load and the salience of the distractors. For example, we could manipulate the familiarity of the words used as it has been shown that familiarity impacts the speed of words processing (Juphard et al., 2011) and therefore should impact their distracting salience. To complete on the role of alpha it will be interesting to see the effect of modulation of alpha. Becoming older is linked to gradual changes in the brain oscillations' frequency and strength (Klimesch, 1999). Perhaps the frequency band most impacted by aging is alpha, with alpha oscillations at rest in healthy older persons being much lower in amplitude and slower in frequency than those in younger adults (Babiloni et al., 2006; Klimesch, 1997). We would continue to use our face-name task, as this lends well to the link that seems quite clear between alpha and distractor inhibition. So, by having young and old subjects do the task described above, we could see the impact of the decrease in alpha power in its inhibitory role but also see if the brain sets up a complementary system to achieve the task. Finally, we could complete this study with transcranial stimulation. This part would have two distinct goals. The first would be to stimulate at the alpha rhythm in young subjects at the occipito-temporal and/or parietal level

in order to see if we can induce inhibition in these areas. The second one is to see if this stimulation on old subjects could allow the recovery of a "normal" alpha and that it would allow the recovery of performances closer to those of young people. This study would bring more information about the role of alpha either by its decrease or by its increase.

References

Aboitiz, F., Ossandon, T., Zamorano, F., Palma, B., & Carrasco, X. (2014). Irrelevant stimulus processing in ADHD : Catecholamine dynamics and attentional networks. *Frontiers in Psychology*, *5*. https://doi.org/10.3389/fpsyg.2014.00183

Adamantidis, A. R., Gutierrez Herrera, C., & Gent, T. C. (2019). Oscillating circuitries in the sleeping brain. *Nature Reviews Neuroscience*, *20*(12), 746-762. https://doi.org/10.1038/s41583-019-0223-4

Alexander, K. E., Estepp, J. R., & Elbasiouny, S. M. (2020). Effects of Neuronic Shutter Observed in the EEG Alpha Rhythm. *eNeuro*, *7*(5), ENEURO.0171-20.2020. https://doi.org/10.1523/ENEURO.0171-20.2020

Alves, P. N., Foulon, C., Karolis, V., Bzdok, D., Margulies, D. S., Volle, E., & Thiebaut de Schotten, M. (2019). An improved neuroanatomical model of the default-mode network reconciles previous neuroimaging and neuropathological findings. *Communications Biology*, *2*(1), 1-14. https://doi.org/10.1038/s42003-019-0611-3

Angelucci, A., & Bullier, J. (2003). Reaching beyond the classical receptive field of V1 neurons : Horizontal or feedback axons? *Journal of Physiology-Paris*, *97*(2), 141-154. https://doi.org/10.1016/j.jphysparis.2003.09.001

Antonov, P. A., Chakravarthi, R., & Andersen, S. K. (2020). Too little, too late, and in the wrong place : Alpha band activity does not reflect an active mechanism of selective attention. *NeuroImage*, *219*, 117006. https://doi.org/10.1016/j.neuroimage.2020.117006

Archer, K., Pammer, K., & Vidyasagar, T. (2020). A Temporal Sampling Basis for Visual Processing in Developmental Dyslexia. *Frontiers in Human Neuroscience*, *14*. https://doi.org/10.3389/fnhum.2020.00213

Augustinova, M., & Ferrand, L. (2014). Automaticity of Word Reading : Evidence From the Semantic Stroop Paradigm. *Current Directions in Psychological Science*, *23*(5), 343-348. https://doi.org/10.1177/0963721414540169

Babiloni, C., Binetti, G., Cassarino, A., Dal Forno, G., Del Percio, C., Ferreri, F., Ferri, R., Frisoni, G., Galderisi, S., Hirata, K., Lanuzza, B., Miniussi, C., Mucci, A., Nobili, F., Rodriguez, G., Luca Romani, G., & Rossini, P. M. (2006). Sources of cortical rhythms in adults during physiological aging : A multicentric EEG study. *Human Brain Mapping*, *27*(2), 162-172. https://doi.org/10.1002/hbm.20175

Baillet, S., Mosher, J. C., & Leahy, R. M. (2001). Electromagnetic brain mapping. *IEEE Signal Processing Magazine*, *18*(6), 14-30. https://doi.org/10.1109/79.962275

Başar, E., Başar-Eroğlu, C., Karakaş, S., & Schürmann, M. (1999). Are cognitive processes manifested in event-related gamma, alpha, theta and delta oscillations in the EEG? *Neuroscience Letters*, *259*(3), 165-168. https://doi.org/10.1016/S0304-3940(98)00934-3

Başar, E., Schürmann, M., Başar-Eroglu, C., & Karakaş, S. (1997). Alpha oscillations in brain functioning : An integrative theory. *International Journal of Psychophysiology*, *26*(1), 5-29. https://doi.org/10.1016/S0167-8760(97)00753-8

Başar-Eroglu, C., Başar, E., Demiralp, T., & Schürmann, M. (1992). P300-response : Possible psychophysiological correlates in delta and theta frequency channels. A review. *International Journal of Psychophysiology*, *13*(2), 161-179. https://doi.org/10.1016/0167-8760(92)90055-G

Bastiaansen, M. C. M., & Knösche, T. R. (2000). Tangential derivative mapping of axial MEG applied to event-related desynchronization research. *Clinical Neurophysiology*, *111*(7), 1300-1305. https://doi.org/10.1016/S1388-2457(00)00272-8

Bastos, A. M., Usrey, W. M., Adams, R. A., Mangun, G. R., Fries, P., & Friston, K. J. (2012). Canonical microcircuits for predictive coding. *Neuron*, *76*(4), 695-711. https://doi.org/10.1016/j.neuron.2012.10.038

Bastos, A. M., Vezoli, J., Bosman, C. A., Schoffelen, J.-M., Oostenveld, R., Dowdall, J. R., De Weerd, P., Kennedy, H., & Fries, P. (2015). Visual Areas Exert Feedforward and Feedback Influences

through Distinct Frequency Channels. *Neuron*, *85*(2), 390-401. https://doi.org/10.1016/j.neuron.2014.12.018

Bauer, M., Stenner, M.-P., Friston, K. J., & Dolan, R. J. (2014). Attentional Modulation of Alpha/Beta and Gamma Oscillations Reflect Functionally Distinct Processes. *Journal of Neuroscience*, *34*(48), 16117-16125. https://doi.org/10.1523/JNEUROSCI.3474-13.2014

Bisley, J. W. (2011). The neural basis of visual attention. *The Journal of Physiology*, *589*(Pt 1), 49-57. https://doi.org/10.1113/jphysiol.2010.192666

Bollimunta, A., Chen, Y., Schroeder, C. E., & Ding, M. (2008). Neuronal Mechanisms of Cortical Alpha Oscillations in Awake-Behaving Macaques. *Journal of Neuroscience*, *28*(40), 9976-9988. https://doi.org/10.1523/JNEUROSCI.2699-08.2008

Bonaiuto, J. J., Afdideh, F., Ferez, M., Wagstyl, K., Mattout, J., Bonnefond, M., Barnes, G. R., & Bestmann, S. (2020). Estimates of cortical column orientation improve MEG source inversion. *NeuroImage*, *216*, 116862. https://doi.org/10.1016/j.neuroimage.2020.116862

Bonaiuto, J. J., Meyer, S. S., Little, S., Rossiter, H., Callaghan, M. F., Dick, F., Barnes, G. R., & Bestmann, S. (2018). Lamina-specific cortical dynamics in human visual and sensorimotor cortices. *eLife*, *7*, e33977. https://doi.org/10.7554/eLife.33977

Bonnefond, M., & Jensen, O. (2012). Alpha Oscillations Serve to Protect Working Memory Maintenance against Anticipated Distracters. *Current Biology*, *22*(20), 1969-1974. https://doi.org/10.1016/j.cub.2012.08.029

Bonnefond, M., & Jensen, O. (2013). The role of gamma and alpha oscillations for blocking out distraction. *Commun Integr Biol*, *6*(1), e22702. https://doi.org/10.4161/cib.22702

Bonnefond, M., Kastner, S., & Jensen, O. (2017). Communication between Brain Areas Based on Nested Oscillations. *eNeuro*, *4*(2). https://doi.org/10.1523/ENEURO.0153-16.2017

Bonnefond, M., Noveck, I., Baillet, S., Cheylus, A., Delpuech, C., Bertrand, O., Fourneret, P., & Van der Henst, J.-B. (2012). What MEG can reveal about inference making : The case of if...then sentences. *Human Brain Mapping*, n/a-n/a. https://doi.org/10.1002/hbm.21465

Bortone, D. S., Olsen, S. R., & Scanziani, M. (2014). Translaminar Inhibitory Cells Recruited by Layer 6 Corticothalamic Neurons Suppress Visual Cortex. *Neuron*, *82*(2), 474-485. https://doi.org/10.1016/j.neuron.2014.02.021

Bosman, C. A., Schoffelen, J.-M., Brunet, N., Oostenveld, R., Bastos, A. M., Womelsdorf, T., Rubehn, B., Stieglitz, T., De Weerd, P., & Fries, P. (2012). Attentional Stimulus Selection through Selective Synchronization between Monkey Visual Areas. *Neuron*, *75*(5), 875-888. https://doi.org/10.1016/j.neuron.2012.06.037

Brookshire, G. (2022). Putative rhythms in attentional switching can be explained by aperiodic temporal structure. *Nature Human Behaviour*. https://doi.org/10.1038/s41562-022-01364-0

Buchanan, K. A., Blackman, A. V., Moreau, A. W., Elgar, D., Costa, R. P., Lalanne, T., Tudor Jones, A. A., Oyrer, J., & Sjöström, P. J. (2012). Target-Specific Expression of Presynaptic NMDA Receptors in Neocortical Microcircuits. *Neuron*, *75*(3), 451-466. https://doi.org/10.1016/j.neuron.2012.06.017

Buckner, R. L., & DiNicola, L. M. (2019). The brain's default network : Updated anatomy, physiology and evolving insights. *Nature Reviews. Neuroscience*, *20*(10), 593-608. https://doi.org/10.1038/s41583-019-0212-7

Buffalo, E. A., Fries, P., Landman, R., Buschman, T. J., & Desimone, R. (2011). Laminar differences in gamma and alpha coherence in the ventral stream. *Proceedings of the National Academy of Sciences*, *108*(27), 11262-11267. https://doi.org/10.1073/pnas.1011284108

Burra, N., Baker, S., & George, N. (2017). Processing of gaze direction within the N170/M170 time window : A combined EEG/MEG study. *Neuropsychologia*, *100*, 207-219. https://doi.org/10.1016/j.neuropsychologia.2017.04.028

Busch, N. A., Dubois, J., & VanRullen, R. (2009). The Phase of Ongoing EEG Oscillations Predicts Visual Perception. *Journal of Neuroscience*, *29*(24), 7869-7876. https://doi.org/10.1523/JNEUROSCI.0113-09.2009

Busch, N. A., & VanRullen, R. (2010). Spontaneous EEG oscillations reveal periodic sampling of visual attention. *Proceedings of the National Academy of Sciences*, *107*(37), 16048-16053. https://doi.org/10.1073/pnas.1004801107

Buzsáki, G., & Wang, X.-J. (2012). Mechanisms of Gamma Oscillations. *Annual Review of Neuroscience*, *35*(1), 203-225. https://doi.org/10.1146/annurev-neuro-062111-150444

Capilla, A., Schoffelen, J.-M., Paterson, G., Thut, G., & Gross, J. (2014). Dissociated α-Band Modulations in the Dorsal and Ventral Visual Pathways in Visuospatial Attention and Perception. *Cerebral Cortex*, *24*(2), 550-561. https://doi.org/10.1093/cercor/bhs343

Carlos, B. J., Hirshorn, E. A., Durisko, C., Fiez, J. A., & Coutanche, M. N. (2019). Word inversion sensitivity as a marker of visual word form area lateralization : An application of a novel multivariate measure of laterality. *NeuroImage*, *191*, 493-502. https://doi.org/10.1016/j.neuroimage.2019.02.044

Cohen, D. (1968). Magnetoencephalography : Evidence of Magnetic Fields Produced by Alpha-Rhythm Currents. *Science*. https://doi.org/10.1126/science.161.3843.784

Cohen, L., LeheÂricy, S., Chochon, F., Lemer, C., Rivaud, S., & Dehaene, S. (2002). *Language-specific tuning of visual cortex ? Functional properties of the Visual Word Form Area*. 16.

Cohen, M. X., & Donner, T. H. (2013). Midfrontal conflict-related theta-band power reflects neural oscillations that predict behavior. *Journal of Neurophysiology*, *110*(12), 2752-2763. https://doi.org/10.1152/jn.00479.2013

Cole, M. W., & Schneider, W. (2007). The cognitive control network : Integrated cortical regions with dissociable functions. *NeuroImage*, *37*(1), 343-360. https://doi.org/10.1016/j.neuroimage.2007.03.071

Cole, M. W., Yarkoni, T., Repovš, G., Anticevic, A., & Braver, T. S. (2012). Global Connectivity of Prefrontal Cortex Predicts Cognitive Control and Intelligence. *Journal of Neuroscience*, *32*(26), 8988-8999. https://doi.org/10.1523/JNEUROSCI.0536-12.2012

Corbetta, M., Patel, G., & Shulman, G. L. (2008). The reorienting system of the human brain : From environment to theory of mind. *Neuron*, *58*(3), 306-324. https://doi.org/10.1016/j.neuron.2008.04.017

Corbetta, M., & Shulman, G. L. (2002). Control of goal-directed and stimulus-driven attention in the brain. *Nature Reviews Neuroscience*, *3*(3), 201-215. https://doi.org/10.1038/nrn755

Dale, A. M., Liu, A. K., Fischl, B. R., Buckner, R. L., Belliveau, J. W., Lewine, J. D., & Halgren, E. (2000). *Mapping : Combining fMRI and MEG for High-Resolution Imaging of Cortical Activity*. 13.

Davis, H., Davis, P. A., Loomis, A. L., Harvey, E. N., & Hobart, G. (1937). Changes in Human Brain Potentials During the Onset of Sleep. *Science*, *86*(2237), 448-450. https://doi.org/10.1126/science.86.2237.448

Dehaene, S., & Cohen, L. (2011). The unique role of the visual word form area in reading. *Trends in Cognitive Sciences*, *15*(6), 254-262. https://doi.org/10.1016/j.tics.2011.04.003

Dombrowe, I., & Hilgetag, C. C. (2014). Occipitoparietal alpha-band responses to the graded allocation of top-down spatial attention. *Journal of Neurophysiology*, *112*(6), 1307-1316. https://doi.org/10.1152/jn.00654.2013

Dou, W., Morrow, A., Iemi, L., & Samaha, J. (2021). Prestimulus Alpha Phase Gates Afferent Visual Cortex Responses. *Journal of Vision*, *21*(9), 2075. https://doi.org/10.1167/jov.21.9.2075

Dugue, L., Marque, P., & VanRullen, R. (2011). The Phase of Ongoing Oscillations Mediates the Causal Relation between Brain Excitation and Visual Perception. *Journal of Neuroscience*, *31*(33), 11889-11893. https://doi.org/10.1523/JNEUROSCI.1161-11.2011

Emmerich, D. S. (1967). *Signal Detection Theory and Psychophysics*. David M. Green , John A. Swets. *The Quarterly Review of Biology*, *42*(4), 578-578. https://doi.org/10.1086/405615

Fakche, C., VanRullen, R., Marque, P., & Dugué, L. (2022). α Phase-Amplitude Tradeoffs Predict Visual Perception. *ENeuro*, *9*(1). https://doi.org/10.1523/ENEURO.0244-21.2022

Ferez, M., Luther, L., Ole, J., & Mathilde, B. (submitted). *Alpha-Beta oscillations implement the inhibition of the Ventral attention and default mode networks during an attentional task*. 15.

Fiebelkorn, I. C., Pinsk, M. A., & Kastner, S. (2018). A Dynamic Interplay within the Frontoparietal Network Underlies Rhythmic Spatial Attention. *Neuron*, *99*(4), 842-853.e8. https://doi.org/10.1016/j.neuron.2018.07.038

Foster, J. J., & Awh, E. (2019). The role of alpha oscillations in spatial attention : Limited evidence for a suppression account. *Current Opinion in Psychology*, *29*, 34-40. https://doi.org/10.1016/j.copsyc.2018.11.001

Fox, K. C. R., Spreng, R. N., Ellamil, M., Andrews-Hanna, J. R., & Christoff, K. (2015). The wandering brain : Meta-analysis of functional neuroimaging studies of mind-wandering and related spontaneous thought processes. *NeuroImage*, *111*, 611-621. https://doi.org/10.1016/j.neuroimage.2015.02.039

Foxe, J. J., & Snyder, A. C. (2011). The Role of Alpha-Band Brain Oscillations as a Sensory Suppression Mechanism during Selective Attention. *Frontiers in Psychology*, *2*. https://doi.org/10.3389/fpsyg.2011.00154

Fries, P. (2005). A mechanism for cognitive dynamics : Neuronal communication through neuronal coherence. *Trends Cogn Sci*, *9*(10), 474-480. https://doi.org/10.1016/j.tics.2005.08.011

Fries, P. (2009). Neuronal Gamma-Band Synchronization as a Fundamental Process in Cortical Computation. *Annual Review of Neuroscience*, *32*(1), 209-224. https://doi.org/10.1146/annurev.neuro.051508.135603

Fries, P. (2015). Rhythms For Cognition : Communication Through Coherence. *Neuron*, *88*(1), 220-235. https://doi.org/10.1016/j.neuron.2015.09.034

Fries, P., Womelsdorf, T., Oostenveld, R., & Desimone, R. (2008). The Effects of Visual Stimulation and Selective Visual Attention on Rhythmic Neuronal Synchronization in Macaque Area V4. *Journal of Neuroscience*, *28*(18), 4823-4835. https://doi.org/10.1523/JNEUROSCI.4499-07.2008

Friston, K. (2005). A theory of cortical responses. *Philosophical Transactions of the Royal Society B: Biological Sciences*, *360*(1456), 815-836. https://doi.org/10.1098/rstb.2005.1622

Friston, K. J. (2019). Waves of prediction. *PLOS Biology*, *17*(10), e3000426. https://doi.org/10.1371/journal.pbio.3000426

Froesel, M., Cappe, C., & Ben Hamed, S. (2021). A multisensory perspective onto primate pulvinar functions. *Neuroscience & Biobehavioral Reviews*, *125*, 231-243. https://doi.org/10.1016/j.neubiorev.2021.02.043

Gerrits, R., Van der Haegen, L., Brysbaert, M., & Vingerhoets, G. (2019). Laterality for recognizing written words and faces in the fusiform gyrus covaries with language dominance. *Cortex*, *117*, 196-204. https://doi.org/10.1016/j.cortex.2019.03.010

Gomez-Ramirez, M., Kelly, S. P., Molholm, S., Sehatpour, P., Schwartz, T. H., & Foxe, J. J. (2011). Oscillatory Sensory Selection Mechanisms during Intersensory Attention to Rhythmic Auditory and Visual Inputs : A Human Electrocorticographic Investigation. *Journal of Neuroscience*, *31*(50), 18556-18567. https://doi.org/10.1523/JNEUROSCI.2164-11.2011

Gould, I. C., Rushworth, M. F., & Nobre, A. C. (2011). Indexing the graded allocation of visuospatial attention using anticipatory alpha oscillations. *Journal of Neurophysiology*, *105*(3), 1318-1326. https://doi.org/10.1152/jn.00653.2010

Green, J. J., Boehler, C. N., Roberts, K. C., Chen, L.-C., Krebs, R. M., Song, A. W., & Woldorff, M. G. (2017). Cortical and Subcortical Coordination of Visual Spatial Attention Revealed by Simultaneous EEG–fMRI Recording. *The Journal of Neuroscience*, *37*(33), 7803-7810. https://doi.org/10.1523/JNEUROSCI.0326-17.2017

Grent-'t-Jong, T., Boehler, C. N., Kenemans, J. L., & Woldorff, M. G. (2011). Differential functional roles of slow-wave and oscillatory-α activity in visual sensory cortex during anticipatory visual-spatial attention. *Cerebral Cortex (New York, N.Y.: 1991)*, *21*(10), 2204-2216. https://doi.org/10.1093/cercor/bhq279

Gross, J., Kujala, J., Hamalainen, M., Timmermann, L., Schnitzler, A., & Salmelin, R. (2001). Dynamic imaging of coherent sources : Studying neural interactions in the human brain. *Proceedings*

of the National Academy of Sciences of the United States of America, *98*(2), 694-699. https://doi.org/10.1073/pnas.98.2.694

Gross, J., Schmitz, F., Schnitzler, I., Kessler, K., Shapiro, K., Hommel, B., & Schnitzler, A. (2004). Modulation of long-range neural synchrony reflects temporal limitations of visual attention in humans. *Proceedings of the National Academy of Sciences*, *101*(35), 13050-13055. https://doi.org/10.1073/pnas.0404944101

Gundlach, C., Moratti, S., Forschack, N., & Müller, M. M. (2020). Spatial Attentional Selection Modulates Early Visual Stimulus Processing Independently of Visual Alpha Modulations. *Cerebral Cortex*, *30*(6), 3686-3703. https://doi.org/10.1093/cercor/bhz335

Gutteling, T., Sillekens, L., Lavie, N., & Jensen, O. (2021). *Alpha oscillations reflect suppression of distractors with increased perceptual load* [Preprint]. Neuroscience. https://doi.org/10.1101/2021.04.13.439637

Haegens, S., Barczak, A., Musacchia, G., Lipton, M. L., Mehta, A. D., Lakatos, P., & Schroeder, C. E. (2015). Laminar Profile and Physiology of the Rhythm in Primary Visual, Auditory, and Somatosensory Regions of Neocortex. *Journal of Neuroscience*, *35*(42), 14341-14352. https://doi.org/10.1523/JNEUROSCI.0600-15.2015

Haegens, S., Händel, B. F., & Jensen, O. (2011). Top-Down Controlled Alpha Band Activity in Somatosensory Areas Determines Behavioral Performance in a Discrimination Task. *Journal of Neuroscience*, *31*(14), 5197-5204. https://doi.org/10.1523/JNEUROSCI.5199-10.2011

Haegens, S., Luther, L., & Jensen, O. (2012). Somatosensory Anticipatory Alpha Activity Increases to Suppress Distracting Input. *Journal of Cognitive Neuroscience*, *24*(3), 677-685. https://doi.org/10.1162/jocn_a_00164

Hämäläinen, M., Hari, R., Ilmoniemi, R. J., Knuutila, J., & Lounasmaa, O. V. (1993). Magnetoencephalography—Theory, instrumentation, and applications to noninvasive studies of the working human brain. *Reviews of Modern Physics*, *65*(2), 413-497. https://doi.org/10.1103/RevModPhys.65.413

Hämäläinen, M. S., & Ilmoniemi, R. J. (1994). Interpreting magnetic fields of the brain : Minimum norm estimates. *Medical & Biological Engineering & Computing*, *32*(1), 35-42. https://doi.org/10.1007/BF02512476

Händel, B. F., Haarmeier, T., & Jensen, O. (2011). Alpha Oscillations Correlate with the Successful Inhibition of Unattended Stimuli. *Journal of Cognitive Neuroscience*, *23*(9), 2494-2502. https://doi.org/10.1162/jocn.2010.21557

Hansen, P. C., Kringelbach, M. L., & Salmelin, R. (Éds.). (2010). *MEG : An introduction to methods*. Oxford University Press.

Harris, A. M., Dux, P. E., & Mattingley, J. B. (2018). Detecting Unattended Stimuli Depends on the Phase of Prestimulus Neural Oscillations. *Journal of Neuroscience*, *38*(12), 3092-3101. https://doi.org/10.1523/JNEUROSCI.3006-17.2018

Harris, R. J., Rice, G. E., Young, A. W., & Andrews, T. J. (2016). Distinct but Overlapping Patterns of Response to Words and Faces in the Fusiform Gyrus. *Cerebral Cortex*, *26*(7), 3161-3168. https://doi.org/10.1093/cercor/bhv147

Hildesheim, F. E., Debus, I., Kessler, R., Thome, I., Zimmermann, K. M., Steinsträter, O., Sommer, J., Kamp-Becker, I., Stark, R., & Jansen, A. (2020). The Trajectory of Hemispheric Lateralization in the Core System of Face Processing : A Cross-Sectional Functional Magnetic Resonance Imaging Pilot Study. *Frontiers in Psychology*, *11*, 507199. https://doi.org/10.3389/fpsyg.2020.507199

Howard, M. W. (2003). Gamma Oscillations Correlate with Working Memory Load in Humans. *Cerebral Cortex*, *13*(12), 1369-1374. https://doi.org/10.1093/cercor/bhg084

Huettel, S. A., Song, A. W., & McCarthy, G. (2008). *Functional magnetic resonance imaging* (2nd ed). Sinauer Associates.

Hughes, S., Lőrincz, M., Turmaine, M., & Crunelli, V. (2011). Thalamic Gap Junctions Control Local Neuronal Synchrony and Influence Macroscopic Oscillation Amplitude during EEG Alpha Rhythms. *Frontiers in Psychology*, *2*, 193. https://doi.org/10.3389/fpsyg.2011.00193

Hughes, S. W., & Crunelli, V. (2005). Thalamic Mechanisms of EEG Alpha Rhythms and Their Pathological Implications. *The Neuroscientist*, *11*(4), 357-372. https://doi.org/10.1177/1073858405277450

Iemi, L., Chaumon, M., Crouzet, S. M., & Busch, N. A. (2017). Spontaneous Neural Oscillations Bias Perception by Modulating Baseline Excitability. *The Journal of Neuroscience*, *37*(4), 807-819. https://doi.org/10.1523/JNEUROSCI.1432-16.2016

Ikkai, A., Dandekar, S., & Curtis, C. E. (2016). Lateralization in Alpha-Band Oscillations Predicts the Locus and Spatial Distribution of Attention. *PLOS ONE*, *11*(5), e0154796. https://doi.org/10.1371/journal.pone.0154796

James, K. H., James, T. W., Jobard, G., Wong, A. C. N., & Gauthier, I. (2005). Letter processing in the visual system : Different activation patterns for single letters and strings. *Cognitive, Affective, & Behavioral Neuroscience*, *5*(4), 452-466. https://doi.org/10.3758/CABN.5.4.452

Jensen, O., Bonnefond, M., & VanRullen, R. (2012). An oscillatory mechanism for prioritizing salient unattended stimuli. *Trends in Cognitive Sciences*, *16*(4), 200-206. https://doi.org/10.1016/j.tics.2012.03.002

Jensen, O., & Mazaheri, A. (2010). Shaping Functional Architecture by Oscillatory Alpha Activity : Gating by Inhibition. *Frontiers in Human Neuroscience*, *4*. https://doi.org/10.3389/fnhum.2010.00186

Jensen, O., & Tesche, C. D. (2002). Frontal theta activity in humans increases with memory load in a working memory task : Frontal theta increases with memory load. *European Journal of Neuroscience*, *15*(8), 1395-1399. https://doi.org/10.1046/j.1460-9568.2002.01975.x

Jokisch, D., & Jensen, O. (2007). Modulation of Gamma and Alpha Activity during a Working Memory Task Engaging the Dorsal or Ventral Stream. *Journal of Neuroscience*, *27*(12), 3244-3251. https://doi.org/10.1523/JNEUROSCI.5399-06.2007

Jongen, E. M. M., Smulders, F. T. Y., & van Breukelen, G. J. P. (2006). Varieties of attention in neutral trials : Linking RT to ERPs and EEG frequencies. *Psychophysiology*, *43*(1), 113-125. https://doi.org/10.1111/j.1469-8986.2006.00375.x

Juphard, A., Vidal, J., Perrone-Bertolotti, M., Minotti, L., Kahane, P., Lachaux, J.-P., & Baciu, M. (2011). Direct Evidence for Two Different Neural Mechanisms for Reading Familiar and Unfamiliar Words : An Intra-Cerebral EEG Study. *Frontiers in Human Neuroscience*, *5*. https://www.frontiersin.org/article/10.3389/fnhum.2011.00101

Kaiser, J., Iliopoulos, P., Steinmassl, K., & Schütz-Bosbach, S. (2022). Preparing for Success : Neural Frontal Theta and Posterior Alpha Dynamics during Action Preparation Predict Flexible Resolution of Cognitive Conflicts. *Journal of cognitive neuroscience*, 1-20. https://doi.org/10.1162/jocn_a_01846

Kelly, S. P., Gomez-Ramirez, M., & Foxe, J. J. (2009). The strength of anticipatory spatial biasing predicts target discrimination at attended locations : A high-density EEG study. *European Journal of Neuroscience*, *30*(11), 2224-2234. https://doi.org/10.1111/j.1460-9568.2009.06980.x

Kelly, S. P., Lalor, E. C., Reilly, R. B., & Foxe, J. J. (2006). Increases in Alpha Oscillatory Power Reflect an Active Retinotopic Mechanism for Distracter Suppression During Sustained Visuospatial Attention. *Journal of Neurophysiology*, *95*(6), 3844-3851. https://doi.org/10.1152/jn.01234.2005

Kim, J., Gulati, T., & Ganguly, K. (2019). Competing Roles of Slow Oscillations and Delta Waves in Memory Consolidation versus Forgetting. *Cell*, *179*(2), 514-526.e13. https://doi.org/10.1016/j.cell.2019.08.040

Klimesch, W. (1997). EEG-alpha rhythms and memory processes. *International Journal of Psychophysiology*, *26*(1-3), 319-340. https://doi.org/10.1016/S0167-8760(97)00773-3

Klimesch, W. (1999). EEG alpha and theta oscillations reflect cognitive and memory performance : A review and analysis. *Brain Research Reviews*, *29*(2-3), 169-195. https://doi.org/10.1016/S0165-0173(98)00056-3

Klimesch, W., Sauseng, P., & Hanslmayr, S. (2007). EEG alpha oscillations : The inhibition–timing hypothesis. *Brain Research Reviews*, *53*(1), 63-88. https://doi.org/10.1016/j.brainresrev.2006.06.003

Knecht, S., Deppe, M., Dräger, B., Bobe, L., Lohmann, H., Ringelstein, E.-B., & Henningsen, H. (2000). Language lateralization in healthy right-handers. *Brain*, *123*(1), 74-81. https://doi.org/10.1093/brain/123.1.74

Krawczyk, D. C., Michelle McClelland, M., & Donovan, C. M. (2011). A hierarchy for relational reasoning in the prefrontal cortex. *Cortex*, *47*(5), 588-597. https://doi.org/10.1016/j.cortex.2010.04.008

Lakatos, P., Karmos, G., Mehta, A. D., Ulbert, I., & Schroeder, C. E. (2008). Entrainment of Neuronal Oscillations as a Mechanism of Attentional Selection. *Science*, *320*(5872), 110-113. https://doi.org/10.1126/science.1154735

Landau, A. N., & Fries, P. (2012). Attention Samples Stimuli Rhythmically. *Current Biology*, *22*(11), 1000-1004. https://doi.org/10.1016/j.cub.2012.03.054

Landau, A. N., Schreyer, H. M., van Pelt, S., & Fries, P. (2015). Distributed Attention Is Implemented through Theta-Rhythmic Gamma Modulation. *Current Biology*, *25*(17), 2332-2337. https://doi.org/10.1016/j.cub.2015.07.048

Laufs, H., Holt, J. L., Elfont, R., Krams, M., Paul, J. S., Krakow, K., & Kleinschmidt, A. (2006). Where the BOLD signal goes when alpha EEG leaves. *NeuroImage*, *31*(4), 1408-1418. https://doi.org/10.1016/j.neuroimage.2006.02.002

Lavie, N. (2005). Distracted and confused? : Selective attention under load. *Trends Cogn Sci*, *9*(2), 75-82. https://doi.org/10.1016/j.tics.2004.12.004

Lega, B. C., Jacobs, J., & Kahana, M. (2012). Human hippocampal theta oscillations and the formation of episodic memories. *Hippocampus*, *22*(4), 748-761. https://doi.org/10.1002/hipo.20937

Levy, J., Vidal, J. R., Oostenveld, R., FitzPatrick, I., Démonet, J.-F., & Fries, P. (2013). Alpha-band suppression in the visual word form area as a functional bottleneck to consciousness. *NeuroImage*, *78*, 33-45.

Little, S., Bonaiuto, J., Barnes, G., & Bestmann, S. (2019). Human motor cortical beta bursts relate to movement planning and response errors. *PLOS Biology*, *17*(10), e3000479. https://doi.org/10.1371/journal.pbio.3000479

Logothetis, N. K., & Sheinberg, D. L. (1996). *Visual Object Recognition*. 45.

Lorincz, M. L., Crunelli, V., & Hughes, S. W. (2008). Cellular Dynamics of Cholinergically Induced (8 13 Hz) Rhythms in Sensory Thalamic Nuclei In Vitro. *Journal of Neuroscience*, *28*(3), 660-671. https://doi.org/10.1523/JNEUROSCI.4468-07.2008

Lorincz, M. L., Kékesi, K. A., Juhász, G., Crunelli, V., & Hughes, S. W. (2009). Temporal Framing of Thalamic Relay-Mode Firing by Phasic Inhibition during the Alpha Rhythm. *Neuron*, *63*(5), 683-696. https://doi.org/10.1016/j.neuron.2009.08.012

Lukashevich, I. P., & Sazonova, O. B. (1996). [The effect of lesions of different parts of the optic thalamus on the nature of the bioelectrical activity of the human brain. *Zhurnal vysshei nervnoi deiatelnosti imeni I P Pavlova*, *46*(5), 866-874.

Macmillan, N. A., & Creelman, C. D. (2005). *Detection theory : A user's guide* (2nd ed). Lawrence Erlbaum Associates.

Maris, E., & Oostenveld, R. (2007). Nonparametric statistical testing of EEG- and MEG-data. *J Neurosci Methods*, *164*(1), 177-190. https://doi.org/10.1016/j.jneumeth.2007.03.024

Markov, N. T., Vezoli, J., Chameau, P., Falchier, A., Quilodran, R., Huissoud, C., Lamy, C., Misery, P., Giroud, P., Ullman, S., Barone, P., Dehay, C., Knoblauch, K., & Kennedy, H. (2014). Anatomy of hierarchy : Feedforward and feedback pathways in macaque visual cortex. *Journal of Comparative Neurology*, *522*(1), 225-259. https://doi.org/10.1002/cne.23458

Marshall, T. R., Bergmann, T. O., & Jensen, O. (2015). Frontoparietal Structural Connectivity Mediates the Top-Down Control of Neuronal Synchronization Associated with Selective Attention. *PLOS Biology*, *13*(10), e1002272. https://doi.org/10.1371/journal.pbio.1002272

Mathewson, K. E., Gratton, G., Fabiani, M., Beck, D. M., & Ro, T. (2009). To See or Not to See : Prestimulus α Phase Predicts Visual Awareness. *Journal of Neuroscience*, *29*(9), 2725-2732. https://doi.org/10.1523/JNEUROSCI.3963-08.2009

Mathewson, K., Lleras, A., Beck, D., Fabiani, M., Ro, T., & Gratton, G. (2011). Pulsed Out of Awareness : EEG Alpha Oscillations Represent a Pulsed-Inhibition of Ongoing Cortical Processing. *Frontiers in Psychology*, *2*, 99. https://doi.org/10.3389/fpsyg.2011.00099

Matsumoto, K., & Tanaka, K. (2004). Conflict and Cognitive Control. *Science*, *303*(5660), 969-970. https://doi.org/10.1126/science.1094733

Mazaheri, A., Coffey-Corina, S., Mangun, G. R., Bekker, E. M., Berry, A. S., & Corbett, B. A. (2010). Functional Disconnection of Frontal Cortex and Visual Cortex in Attention-Deficit/Hyperactivity Disorder. *Biological Psychiatry*, *67*(7), 617-623. https://doi.org/10.1016/j.biopsych.2009.11.022

Mazaheri, A., Nieuwenhuis, I. L. C., van Dijk, H., & Jensen, O. (2009). Prestimulus alpha and mu activity predicts failure to inhibit motor responses. *Human Brain Mapping*, *30*(6), 1791-1800. https://doi.org/10.1002/hbm.20763

Mazaheri, A., van Schouwenburg, M. R., Dimitrijevic, A., Denys, D., Cools, R., & Jensen, O. (2014). Region-specific modulations in oscillatory alpha activity serve to facilitate processing in the visual and auditory modalities. *NeuroImage*, *87*, 356-362. https://doi.org/10.1016/j.neuroimage.2013.10.052

Meyer, S. S., Bonaiuto, J., Lim, M., Rossiter, H., Waters, S., Bradbury, D., Bestmann, S., Brookes, M., Callaghan, M. F., Weiskopf, N., & Barnes, G. R. (2017). Flexible head-casts for high spatial precision MEG. *Journal of Neuroscience Methods*, *276*, 38-45. https://doi.org/10.1016/j.jneumeth.2016.11.009

Michalareas, G., Vezoli, J., van Pelt, S., Schoffelen, J. M., Kennedy, H., & Fries, P. (2016). Alpha-Beta and Gamma Rhythms Subserve Feedback and Feedforward Influences among Human Visual Cortical Areas. *Neuron*, *89*(2), 384-397. https://doi.org/10.1016/j.neuron.2015.12.018

Mishkin, M., & Ungerleider, L. G. (1983). *Object vision and spatial vision:two cortical pathhways*. 4.

Mo, J., Schroeder, C. E., & Ding, M. (2011). Attentional Modulation of Alpha Oscillations in Macaque Inferotemporal Cortex. *Journal of Neuroscience*, *31*(3), 878-882. https://doi.org/10.1523/JNEUROSCI.5295-10.2011

Montgomery, S. M., Sirota, A., & Buzsaki, G. (2008). Theta and Gamma Coordination of Hippocampal Networks during Waking and Rapid Eye Movement Sleep. *Journal of Neuroscience*, *28*(26), 6731-6741. https://doi.org/10.1523/JNEUROSCI.1227-08.2008

Moorselaar, D. van, & Slagter, H. A. (2019). Learning What Is Irrelevant or Relevant : Expectations Facilitate Distractor Inhibition and Target Facilitation through Distinct Neural Mechanisms. *Journal of Neuroscience*, *39*(35), 6953-6967. https://doi.org/10.1523/JNEUROSCI.0593-19.2019

Nolte, G. (2003). The magnetic lead field theorem in the quasi-static approximation and its use for magnetoencephalography forward calculation in realistic volume conductors. *Physics in Medicine and Biology*, *48*(22), 3637-3652. https://doi.org/10.1088/0031-9155/48/22/002

Noonan, M. P., Adamian, N., Pike, A., Printzlau, F., Crittenden, B. M., & Stokes, M. G. (2016). Distinct Mechanisms for Distractor Suppression and Target Facilitation. *Journal of Neuroscience*, *36*(6), 1797-1807. https://doi.org/10.1523/JNEUROSCI.2133-15.2016

Noonan, M. P., Crittenden, B. M., Jensen, O., & Stokes, M. G. (2018). Selective inhibition of distracting input. *Behavioural Brain Research*, *355*, 36-47. https://doi.org/10.1016/j.bbr.2017.10.010

Okayasu, M., Inukai, T., Tanaka, D., Tsumura, K., Hosono, M., Shintaki, R., Takeda, M., Nakahara, K., & Jimura, K. (2022). *An excitatory-inhibitory fronto-cerebellar loop resolves the Stroop effect* (p. 2022.01.18.476551). bioRxiv. https://doi.org/10.1101/2022.01.18.476551

O'Keefe, J., & Recce, M. L. (1993). Phase relationship between hippocampal place units and the EEG theta rhythm. *Hippocampus*, *3*(3), 317-330. https://doi.org/10.1002/hipo.450030307

Oldfield, R. C. (1971). The assessment and analysis of handedness : The Edinburgh inventory. *Neuropsychologia*, *9*(1), 97-113. https://doi.org/10.1016/0028-3932(71)90067-4

Olsen, S. R., Bortone, D. S., Adesnik, H., & Scanziani, M. (2012). Gain control by layer six in cortical circuits of vision. *Nature*, *483*(7387), 47-52. https://doi.org/10.1038/nature10835

Oostenveld, R., Fries, P., Maris, E., & Schoffelen, J. M. (2011). FieldTrip : Open source software for advanced analysis of MEG, EEG, and invasive electrophysiological data. *Comput Intell Neurosci*, *2011*, 156869. https://doi.org/10.1155/2011/156869

Oostenveld, R., Fries, P., Maris, E., & Schoffelen, J.-M. (2010). FieldTrip : Open Source Software for Advanced Analysis of MEG, EEG, and Invasive Electrophysiological Data. *Computational Intelligence and Neuroscience*, *2011*, e156869. https://doi.org/10.1155/2011/156869

Ossandon, T., Jerbi, K., Vidal, J. R., Bayle, D. J., Henaff, M.-A., Jung, J., Minotti, L., Bertrand, O., Kahane, P., & Lachaux, J.-P. (2011). Transient Suppression of Broadband Gamma Power in the Default-Mode Network Is Correlated with Task Complexity and Subject Performance. *Journal of Neuroscience*, *31*(41), 14521-14530. https://doi.org/10.1523/JNEUROSCI.2483-11.2011

Palomero-Gallagher, N., & Zilles, K. (2019). Cortical layers : Cyto-, myelo-, receptor- and synaptic architecture in human cortical areas. *NeuroImage*, *197*, 716-741. https://doi.org/10.1016/j.neuroimage.2017.08.035

Palva, S., & Palva, J. M. (2007). New vistas for α-frequency band oscillations. *Trends in Neurosciences*, *30*(4), 150-158. https://doi.org/10.1016/j.tins.2007.02.001

Paneri, S., & Gregoriou, G. G. (2017). Top-Down Control of Visual Attention by the Prefrontal Cortex. Functional Specialization and Long-Range Interactions. *Frontiers in Neuroscience*, *11*. https://www.frontiersin.org/article/10.3389/fnins.2017.00545

Park, H., Lee, D. S., Kang, E., Kang, H., Hahm, J., Kim, J. S., Chung, C. K., & Jensen, O. (2014). Blocking of irrelevant memories by posterior alpha activity boosts memory encoding. *Hum Brain Mapp*, *35*(8), 3972-3987. https://doi.org/10.1002/hbm.22452

Pascual-Marqui, R. D., Michel, C. M., & Lehmann, D. (1994). Low resolution electromagnetic tomography : A new method for localizing electrical activity in the brain. *International Journal of Psychophysiology*, *18*(1), 49-65. https://doi.org/10.1016/0167-8760(84)90014-X

Pascucci, D., Hervais-Adelman, A., & Plomp, G. (2018). Gating by induced A-Γ asynchrony in selective attention. *Human Brain Mapping*, *39*(10), 3854-3870. https://doi.org/10.1002/hbm.24216

Payne, L., Guillory, S., & Sekuler, R. (2013). Attention-modulated Alpha-band Oscillations Protect against Intrusion of Irrelevant Information. *Journal of Cognitive Neuroscience*, *25*(9), 1463-1476. https://doi.org/10.1162/jocn_a_00395

Peitz, G. W., Wilde, E. A., & Grandhi, R. (2021). Magnetoencephalography in the Detection and Characterization of Brain Abnormalities Associated with Traumatic Brain Injury : A Comprehensive Review. *Medical Sciences*, *9*(1), 7. https://doi.org/10.3390/medsci9010007

Pfurtscheller, G., & Lopes da Silva, F. H. (1999). Event-related EEG/MEG synchronization and desynchronization : Basic principles. *Clinical Neurophysiology*, *110*(11), 1842-1857. https://doi.org/10.1016/S1388-2457(99)00141-8

Pfurtscheller, G., Stancák, A., & Neuper, Ch. (1996). Event-related synchronization (ERS) in the alpha band — an electrophysiological correlate of cortical idling : A review. *International Journal of Psychophysiology*, *24*(1-2), 39-46. https://doi.org/10.1016/S0167-8760(96)00066-9

Pizzo, F., Roehri, N., Villalon, S. M., Trébuchon, A., Chen, S., Lagarde, S., Carron, R., Gavaret, M., Giusiano, B., McGonigal, A., Bartolomei, F., Badier, J. M., & Bénar, C. G. (2021). Author Correction : Deep brain activities can be detected with magnetoencephalography. *Nature Communications*, *12*, 2566. https://doi.org/10.1038/s41467-021-23215-8

Poldrack, R. A., Wagner, A. D., Prull, M. W., Desmond, J. E., Glover, G. H., & Gabrieli, J. D. E. (1999). Functional Specialization for Semantic and Phonological Processing in the Left Inferior Prefrontal Cortex. *NeuroImage*, *10*(1), 15-35. https://doi.org/10.1006/nimg.1999.0441

Polk, T. A., Drake, R. M., Jonides, J. J., Smith, M. R., & Smith, E. E. (2008). Attention Enhances the Neural Processing of Relevant Features and Suppresses the Processing of Irrelevant Features in Humans : A Functional Magnetic Resonance Imaging Study of the Stroop Task. *Journal of Neuroscience*, *28*(51), 13786-13792. https://doi.org/10.1523/JNEUROSCI.1026-08.2008

Popov, T., Kastner, S., & Jensen, O. (2017). FEF-Controlled Alpha Delay Activity Precedes Stimulus-Induced Gamma-Band Activity in Visual Cortex. *The Journal of Neuroscience*, *37*(15), 4117-4127. https://doi.org/10.1523/JNEUROSCI.3015-16.2017

Prado, J., & Noveck, I. A. (2006). How reaction time measures elucidate the matching bias and the way negations are processed. *Thinking & Reasoning*, *12*(3), 309-328. https://doi.org/10.1080/13546780500371241

Prado, J., & Noveck, I. A. (2007). Overcoming Perceptual Features in Logical Reasoning : A Parametric Functional Magnetic Resonance Imaging Study. *Journal of Cognitive Neuroscience*, *19*(4), 642-657. https://doi.org/10.1162/jocn.2007.19.4.642

Raghavachari, S., Kahana, M. J., Rizzuto, D. S., Caplan, J. B., Kirschen, M. P., Bourgeois, B., Madsen, J. R., & Lisman, J. E. (2001). Gating of Human Theta Oscillations by a Working Memory Task. *Journal of Neuroscience*, *21*(9), 3175-3183. https://doi.org/10.1523/JNEUROSCI.21-09-03175.2001

Raichle, M. E. (2015). *The Brain's Default Mode Network*. 17.

Rao, R., & Ballard, D. (1999). Predictive Coding in the Visual Cortex : A Functional Interpretation of Some Extra-classical Receptive-field Effects. *Nature neuroscience*, *2*, 79-87. https://doi.org/10.1038/4580

Rassi, E., Wutz, A., Müller-Voggel, N., & Weisz, N. (2019). Prestimulus feedback connectivity biases the content of visual experiences. *Proceedings of the National Academy of Sciences*, *116*(32), 16056-16061. https://doi.org/10.1073/pnas.1817317116

Remmelzwaal, L. A., Mishra, A. K., & Ellis, G. F. R. (2020). CTNN : Corticothalamic-inspired neural network. *ArXiv:1910.12492 [Cs, q-Bio]*. http://arxiv.org/abs/1910.12492

Rihs, T. A., Michel, C. M., & Thut, G. (2007). Mechanisms of selective inhibition in visual spatial attention are indexed by alpha-band EEG synchronization. *Eur J Neurosci*, *25*(2), 603-610. https://doi.org/10.1111/j.1460-9568.2007.05278.x

Rihs, T. A., Michel, C. M., & Thut, G. (2009). A bias for posterior α-band power suppression versus enhancement during shifting versus maintenance of spatial attention. *NeuroImage*, *44*(1), 190-199. https://doi.org/10.1016/j.neuroimage.2008.08.022

Romei, V., Rihs, T., Brodbeck, V., & Thut, G. (2008). Resting electroencephalogram alpha-power over posterior sites indexes baseline visual cortex excitability. *NeuroReport*, *19*(2), 203-208. https://doi.org/10.1097/WNR.0b013e3282f454c4

Saalmann, Y. B., & Kastner, S. (2011). Cognitive and Perceptual Functions of the Visual Thalamus. *Neuron*, *71*(2), 209-223. https://doi.org/10.1016/j.neuron.2011.06.027

Saalmann, Y. B., Pinsk, M. A., Wang, L., Li, X., & Kastner, S. (2012). The Pulvinar Regulates Information Transmission Between Cortical Areas Based on Attention Demands. *Science*. https://doi.org/10.1126/science.1223082

Samaha, J., Bauer, P., Cimaroli, S., & Postle, B. R. (2015). Top-down control of the phase of alpha-band oscillations as a mechanism for temporal prediction. *Proceedings of the National Academy of Sciences*, *112*(27), 8439-8444. https://doi.org/10.1073/pnas.1503686112

Samaha, J., Iemi, L., Haegens, S., & Busch, N. A. (2020). Spontaneous Brain Oscillations and Perceptual Decision-Making. *Trends in Cognitive Sciences*, *24*(8), 639-653. https://doi.org/10.1016/j.tics.2020.05.004

Samaha, J., Iemi, L., & Postle, B. R. (2017). Prestimulus alpha-band power biases visual discrimination confidence, but not accuracy. *Consciousness and Cognition*, *54*, 47-55. https://doi.org/10.1016/j.concog.2017.02.005

Samaha, J., & Postle, B. R. (2015). The Speed of Alpha-Band Oscillations Predicts the Temporal Resolution of Visual Perception. *Current Biology*, *25*(22), 2985-2990. https://doi.org/10.1016/j.cub.2015.10.007

Sauseng, P., Klimesch, W., Gerloff, C., & Hummel, F. C. (2009). Spontaneous locally restricted EEG alpha activity determines cortical excitability in the motor cortex. *Neuropsychologia*, *47*(1), 284-288. https://doi.org/10.1016/j.neuropsychologia.2008.07.021

Sauseng, P., Klimesch, W., Heise, K. F., Gruber, W. R., Holz, E., Karim, A. A., Glennon, M., Gerloff, C., Birbaumer, N., & Hummel, F. C. (2009). Brain oscillatory substrates of visual short-term memory capacity. *Curr Biol*, *19*(21), 1846-1852. https://doi.org/10.1016/j.cub.2009.08.062

Sauseng, P., Klimesch, W., Stadler, W., Schabus, M., Doppelmayr, M., Hanslmayr, S., Gruber, W. R., & Birbaumer, N. (2005). A shift of visual spatial attention is selectively associated with human EEG alpha activity. *Eur J Neurosci*, *22*(11), 2917-2926. https://doi.org/10.1111/j.1460-9568.2005.04482.x

Schaum, M., Pinzuti, E., Sebastian, A., Lieb, K., Fries, P., Mobascher, A., Jung, P., Wibral, M., & Tüscher, O. (2021). Right inferior frontal gyrus implements motor inhibitory control via beta-band oscillations in humans. *eLife*, *10*, e61679. https://doi.org/10.7554/eLife.61679

Scheeringa, R., Fries, P., Petersson, K. M., Oostenveld, R., Grothe, I., Norris, D. G., Hagoort, P., & Bastiaansen, M. C. (2011). Neuronal dynamics underlying high- and low-frequency EEG oscillations contribute independently to the human BOLD signal. *Neuron*, *69*(3), 572-583. https://doi.org/10.1016/j.neuron.2010.11.044

Schönbrodt, F. D., & Perugini, M. (2013). At what sample size do correlations stabilize? *Journal of Research in Personality*, *47*(5), 609-612. https://doi.org/10.1016/j.jrp.2013.05.009

Schroeder, C. E., & Lakatos, P. (2009). Low-frequency neuronal oscillations as instruments of sensory selection. *Trends in Neurosciences*, *32*(1), 9-18. https://doi.org/10.1016/j.tins.2008.09.012

Seager, M. A., Johnson, L. D., Chabot, E. S., Asaka, Y., & Berry, S. D. (2002). Oscillatory brain states and learning : Impact of hippocampal theta-contingent training. *Proceedings of the National Academy of Sciences*, *99*(3), 1616-1620. https://doi.org/10.1073/pnas.032662099

Sedley, W., Gander, P. E., Kumar, S., Kovach, C. K., Oya, H., Kawasaki, H., Howard, I., Matthew A., & Griffiths, T. D. (2016). Neural signatures of perceptual inference. *eLife*, *5*, e11476. https://doi.org/10.7554/eLife.11476

Senoussi, M., Moreland, J. C., Busch, N. A., & Dugué, L. (2019). Attention explores space periodically at the theta frequency. *Journal of Vision*, *19*(5), 22. https://doi.org/10.1167/19.5.22

Siegel, M., Donner, T. H., Oostenveld, R., Fries, P., & Engel, A. K. (2008). Neuronal Synchronization along the Dorsal Visual Pathway Reflects the Focus of Spatial Attention. *Neuron*, *60*(4), 709-719. https://doi.org/10.1016/j.neuron.2008.09.010

Snyder, A. C., & Foxe, J. J. (2010). Anticipatory attentional suppression of visual features indexed by oscillatory alpha-band power increases : A high-density electrical mapping study. *J Neurosci*, *30*(11), 4024-4032. https://doi.org/10.1523/JNEUROSCI.5684-09.2010

Solís-Vivanco, R., Jensen, O., & Bonnefond, M. (2018). Top–Down Control of Alpha Phase Adjustment in Anticipation of Temporally Predictable Visual Stimuli. *Journal of Cognitive Neuroscience*, *30*(8), 1157-1169. https://doi.org/10.1162/jocn_a_01280

Solís-Vivanco, R., Jensen, O., & Bonnefond, M. (2021). New insights on the ventral attention network : Active suppression and involuntary recruitment during a bimodal task. *Human Brain Mapping*, *42*(6), 1699-1713. https://doi.org/10.1002/hbm.25322

Sperling, R. A., Bates, J. F., Cocchiarella, A. J., Schacter, D. L., Rosen, B. R., & Albert, M. S. (2001). Encoding novel face-name associations : A functional MRI study. *Human Brain Mapping*, *14*(3), 129-139. https://doi.org/10.1002/hbm.1047

Steriade, M. (2006). Grouping of brain rhythms in corticothalamic systems. *Neuroscience*, *137*(4), 1087-1106. https://doi.org/10.1016/j.neuroscience.2005.10.029

Stolk, A., Todorovic, A., Schoffelen, J.-M., & Oostenveld, R. (2013). Online and offline tools for head movement compensation in MEG. *NeuroImage*, *68*, 39-48. https://doi.org/10.1016/j.neuroimage.2012.11.047

Stoll, F. M., Wilson, C. R. E., Faraut, M. C. M., Vezoli, J., Knoblauch, K., & Procyk, E. (2016). The Effects of Cognitive Control and Time on Frontal Beta Oscillations. *Cerebral Cortex*, *26*(4), 1715-1732. https://doi.org/10.1093/cercor/bhv006

Stroop, J. R. (1935). STUDIES OF INTERFERENCE IN SERIAL VERBAL REACTIONS. *J Exp Psychol*, *18:643–662.*, 20.

Tamura, H., Kaneko, H., Kawasaki, K., & Fujita, I. (2004). Presumed Inhibitory Neurons in the Macaque Inferior Temporal Cortex : Visual Response Properties and Functional Interactions With Adjacent Neurons. *Journal of Neurophysiology*, *91*(6), 2782-2796. https://doi.org/10.1152/jn.01267.2003

Taylor, K., Mandon, S., Freiwald, W. A., & Kreiter, A. K. (2005). Coherent Oscillatory Activity in Monkey Area V4 Predicts Successful Allocation of Attention. *Cerebral Cortex*, *15*(9), 1424-1437. https://doi.org/10.1093/cercor/bhi023

Thut, G., Nietzel, A., Brandt, S. A., & Pascual-Leone, A. (2006). α-Band Electroencephalographic Activity over Occipital Cortex Indexes Visuospatial Attention Bias and Predicts Visual Target Detection. *The Journal of Neuroscience*, *26*(37), 9494-9502. https://doi.org/10.1523/JNEUROSCI.0875-06.2006

Trenner, M. U., Heekeren, H. R., Bauer, M., Rössner, K., Wenzel, R., Villringer, A., & Fahle, M. (2008). What Happens in Between? Human Oscillatory Brain Activity Related to Crossmodal Spatial Cueing. *PLoS ONE*, *3*(1), e1467. https://doi.org/10.1371/journal.pone.0001467

Tzourio-Mazoyer, N., Landeau, B., Papathanassiou, D., Crivello, F., Etard, O., Delcroix, N., Mazoyer, B., & Joliot, M. (2002). Automated anatomical labeling of activations in SPM using a

macroscopic anatomical parcellation of the MNI MRI single-subject brain. *NeuroImage*, *15*(1), 273-289. https://doi.org/10.1006/nimg.2001.0978

Van Der Werf, J., Jensen, O., Fries, P., & Medendorp, W. P. (2010). Neuronal synchronization in human posterior parietal cortex during reach planning. *J Neurosci*, *30*(4), 1402-1412. https://doi.org/10.1523/JNEUROSCI.3448-09.2010

Van Veen, B. D., Van Drongelen, W., Yuchtman, M., & Suzuki, A. (1997). Localization of brain electrical activity via linearly constrained minimum variance spatial filtering. *IEEE Transactions on Biomedical Engineering*, *44*(9), 867-880. https://doi.org/10.1109/10.623056

van Diepen, R. M., Cohen, M. X., Denys, D., & Mazaheri, A. (2015). Attention and Temporal Expectations Modulate Power, Not Phase, of Ongoing Alpha Oscillations. *Journal of Cognitive Neuroscience*, *27*(8), 1573-1586. https://doi.org/10.1162/jocn_a_00803

van Diepen, R. M., & Mazaheri, A. (2017). Cross-sensory modulation of alpha oscillatory activity : Suppression, idling, and default resource allocation. *The European Journal of Neuroscience*, *45*(11), 1431-1438. https://doi.org/10.1111/ejn.13570

van Dijk, H., Schoffelen, J.-M., Oostenveld, R., & Jensen, O. (2008). Prestimulus Oscillatory Activity in the Alpha Band Predicts Visual Discrimination Ability. *Journal of Neuroscience*, *28*(8), 1816-1823. https://doi.org/10.1523/JNEUROSCI.1853-07.2008

van Kerkoerle, T., Self, M. W., Dagnino, B., Gariel-Mathis, M. A., Poort, J., van der Togt, C., & Roelfsema, P. R. (2014). Alpha and gamma oscillations characterize feedback and feedforward processing in monkey visual cortex. *Proc Natl Acad Sci U S A*. https://doi.org/10.1073/pnas.1402773111

van Moorselaar, D., & Slagter, H. A. (2020). Inhibition in selective attention. *Annals of the New York Academy of Sciences*, *1464*(1), 204-221. https://doi.org/10.1111/nyas.14304

VanRullen, R. (2016). Perceptual Cycles. *Trends in Cognitive Sciences*, *20*(10), 723-735. https://doi.org/10.1016/j.tics.2016.07.006

VanRullen, R., Busch, N. A., Drewes, J., & Dubois, J. (2011). Ongoing EEG Phase as a Trial-by-Trial Predictor of Perceptual and Attentional Variability. *Frontiers in Psychology*, *2*. https://doi.org/10.3389/fpsyg.2011.00060

Vatterott, D. B., & Vecera, S. P. (2012). Experience-dependent attentional tuning of distractor rejection. *Psychonomic Bulletin & Review*, *19*(5), 871-878. https://doi.org/10.3758/s13423-012-0280-4

Vertes, R. P., Albo, Z., & Viana Di Prisco, G. (2001). Theta-rhythmically firing neurons in the anterior thalamus : Implications for mnemonic functions of Papez's circuit. *Neuroscience*, *104*(3), 619-625. https://doi.org/10.1016/S0306-4522(01)00131-2

Vidal, J., Ossandón, T., Jerbi, K., Dalal, S., Minotti, L., Ryvlin, P., Kahane, P., & Lachaux, J.-P. (2010). Category-Specific Visual Responses : An Intracranial Study Comparing Gamma, Beta, Alpha, and ERP Response Selectivity. *Frontiers in Human Neuroscience*, *4*. https://www.frontiersin.org/article/10.3389/fnhum.2010.00195

Voytek, B., Samaha, J., Rolle, C. E., Greenberg, Z., Gill, N., Porat, S., Kader, T., Rahman, S., Malzyner, R., & Gazzaley, A. (2017). Preparatory Encoding of the Fine Scale of Human Spatial Attention. *Journal of Cognitive Neuroscience*, *29*(7), 1302-1310. https://doi.org/10.1162/jocn_a_01124

Wang, C., Rajagovindan, R., Han, S.-M., & Ding, M. (2016). Top-Down Control of Visual Alpha Oscillations : Sources of Control Signals and Their Mechanisms of Action. *Frontiers in Human Neuroscience*, *10*. https://doi.org/10.3389/fnhum.2016.00015

Watrous, A. J., Lee, D. J., Izadi, A., Gurkoff, G. G., Shahlaie, K., & Ekstrom, A. D. (2013). A comparative study of human and rat hippocampal low-frequency oscillations during spatial navigation : Comparison of Human and Rodent Theta. *Hippocampus*, *23*(8), 656-661. https://doi.org/10.1002/hipo.22124

Wildegger, T., van Ede, F., Woolrich, M., Gillebert, C. R., & Nobre, A. C. (2017). Preparatory α-band oscillations reflect spatial gating independently of predictions regarding target identity. *Journal of Neurophysiology*, *117*(3), 1385-1394. https://doi.org/10.1152/jn.00856.2016

Winson, J. (1974). Patterns of hippocampal theta rhythm in the freely moving rat. *Electroencephalography and Clinical Neurophysiology*, *36*, 291-301. https://doi.org/10.1016/0013-4694(74)90171-0

Worden, M. S., Foxe, J. J., Wang, N., & Simpson, G. V. (2000). Anticipatory biasing of visuospatial attention indexed by retinotopically specific alpha-band electroencephalography increases over occipital cortex. *J Neurosci*, *20*(6), RC63.

Wöstmann, M., Alavash, M., & Obleser, J. (2019). Alpha Oscillations in the Human Brain Implement Distractor Suppression Independent of Target Selection. *Journal of Neuroscience*, *39*(49), 9797-9805. https://doi.org/10.1523/JNEUROSCI.1954-19.2019

Wöstmann, M., Störmer, V. S., Obleser, J., Addleman, D. A., Andersen, S. K., Gaspelin, N., Geng, J. J., Luck, S. J., Noonan, M. P., Slagter, H. A., & Theeuwes, J. (2022). Ten simple rules to study distractor suppression. *Progress in Neurobiology*, *213*, 102269. https://doi.org/10.1016/j.pneurobio.2022.102269

Wyart, V., & Tallon-Baudry, C. (2008). Neural Dissociation between Visual Awareness and Spatial Attention. *Journal of Neuroscience*, *28*(10), 2667-2679. https://doi.org/10.1523/JNEUROSCI.4748-07.2008

Wyart, V., & Tallon-Baudry, C. (2009). How Ongoing Fluctuations in Human Visual Cortex Predict Perceptual Awareness : Baseline Shift versus Decision Bias. *Journal of Neuroscience*, *29*(27), 8715-8725. https://doi.org/10.1523/JNEUROSCI.0962-09.2009

Yamagishi, N., Callan, D. E., Anderson, S. J., & Kawato, M. (2008). Attentional changes in pre-stimulus oscillatory activity within early visual cortex are predictive of human visual performance. *Brain Research*, *1197*, 115-122. https://doi.org/10.1016/j.brainres.2007.12.063

Yamagishi, N., Goda, N., Callan, D. E., Anderson, S. J., & Kawato, M. (2005). Attentional shifts towards an expected visual target alter the level of alpha-band oscillatory activity in the human calcarine cortex. *Cognitive Brain Research*, *25*(3), 799-809. https://doi.org/10.1016/j.cogbrainres.2005.09.006

Zanto, T. P., & Gazzaley, A. (2009). Neural Suppression of Irrelevant Information Underlies Optimal Working Memory Performance. *Journal of Neuroscience*, *29*(10), 3059-3066. https://doi.org/10.1523/JNEUROSCI.4621-08.2009

Zanto, T. P., Rubens, M. T., Bollinger, J., & Gazzaley, A. (2010). Top-down modulation of visual feature processing : The role of the inferior frontal junction. *Neuroimage*, *53*(2), 736-745. https://doi.org/10.1016/j.neuroimage.2010.06.012

Zhigalov, A., & Jensen, O. (2020). Alpha oscillations do not implement gain control in early visual cortex but rather gating in parieto-occipital regions. *Human Brain Mapping*, *41*(18), 5176-5186. https://doi.org/10.1002/hbm.25183

Annexes

NeuroImage 216 (2020) 116862

Contents lists available at ScienceDirect

NeuroImage

journal homepage: www.elsevier.com/locate/neuroimage

Estimates of cortical column orientation improve MEG source inversion

James J. Bonaiuto [a,b,*], Fardin Afdideh [b,c], Maxime Ferez [b,c], Konrad Wagstyl [d,e], Jérémie Mattout [b,c], Mathilde Bonnefond [b,c], Gareth R. Barnes [e,1], Sven Bestmann [e,f,1]

[a] Institut des Sciences Cognitives Marc Jeannerod, CNRS UMR5229, Bron, France
[b] Université Claude Bernard Lyon 1, Université de Lyon, France
[c] Lyon Neuroscience Research Center, CRNL, Brain Dynamics and Cognition Team, INSERM U1028, CNRS UMR5292, Lyon, France
[d] University of Cambridge, Department of Psychiatry, Cambridge, CB2 0SZ, UK
[e] Wellcome Centre for Human Neuroimaging, UCL Queen Square Institute of Neurology, University College London (UCL), London, WC1N 3AR, UK
[f] Dept of Clinical and Movement Neuroscience, UCL Queen Square Institute of Neurology, University College London (UCL), London, WC1N 3BG, UK

ARTICLE INFO

Keywords:
Source inversion
Dipole orientation
Cortical columns
Cortical surface
High precision MEG

ABSTRACT

Determining the anatomical source of brain activity non-invasively measured from EEG or MEG sensors is challenging. In order to simplify the source localization problem, many techniques introduce the assumption that current sources lie on the cortical surface. Another common assumption is that this current flow is orthogonal to the cortical surface, thereby approximating the orientation of cortical columns. However, it is not clear which cortical surface to use to define the current source locations, and normal vectors computed from a single cortical surface may not be the best approximation to the orientation of cortical columns. We compared three different surface location priors and five different approaches for estimating dipole vector orientation, both in simulations and visual and motor evoked MEG responses. We show that models with source locations on the white matter surface and using methods based on establishing correspondences between white matter and pial cortical surfaces dramatically outperform models with source locations on the pial or combined pial/white surfaces and which use methods based on the geometry of a single cortical surface in fitting evoked visual and motor responses. These methods can be easily implemented and adopted in most M/EEG analysis pipelines, with the potential to significantly improve source localization of evoked responses.

1. Introduction

Non-invasive measures of brain activity such as magnetoencephalography (MEG) and electroencephalography (EEG) are powerful tools for generating insights into human brain function with millisecond-scale temporal resolution. However, determining the current distribution that gives rise to the signals measured from EEG and MEG sensors is challenging (Baillet et al., 2001; Darvas et al., 2004; Fukushima et al., 2012; Haufe et al., 2011; Mattout et al., 2006). In order to simplify the source localization problem, many techniques introduce constraints to the dimensionality of source space. These constraints embody assumptions about how the brain generates the signals which we can measure from outside of the head.

One of these assumptions is that signals measured by M/EEG sensors are predominantly generated by large pyramidal neurons in deep cortical layers, which are arranged in parallel columns so that their cumulative activity produces a measurable extracranial signal (Baillet, 2017; Buzsáki et al., 2012; Murakami and Okada, 2006; Okada et al., 1997). Two commonly used source localization constraints based on this assumption are that the locations of source dipoles are restricted to locations on a mesh of the white matter surface as is it is closest to the deep cortical layers (Dale and Sereno, 1993; Henson et al., 2009; Hillebrand and Barnes, 2003, 2002; Mattout et al., 2007), and that the orientation of dipoles is orthogonal to this surface (Hämäläinen and Ilmoniemi, 1984, 1994; Henson et al., 2009; Hillebrand and Barnes, 2003; Lin et al., 2006; Salmelin et al., 1995), thereby approximating the orientation of cortical columns (Nunez and Srinivasan, 2006; Okada et al., 1997).

Using vectors orthogonal to the cortical surface may not be the best approximation to the orientation of cortical columns. Cortical folding patterns may result in curved cortical columns, and therefore their orientation with respect to the cortical surface could be different along the gray/white matter (white matter surface) and CSF/gray matter (pial

* Corresponding author. Institut des Sciences Cognitives Marc Jeannerod, CNRS UMR, 5229, Bron, France.
E-mail address: james.bonaiuto@isc.cnrs.fr (J.J. Bonaiuto).
[1] joint last author.

https://doi.org/10.1016/j.neuroimage.2020.116862
Received 21 October 2019; Received in revised form 7 April 2020; Accepted 14 April 2020
Available online 16 April 2020

surface) boundaries. Moreover, induced activity in low and high frequency bands can predominate in deep or superficial cortical layers (Bastos et al., 2015; Bonaiuto et al., 2018a; Buffalo et al., 2011; Haegens et al., 2015; Maier et al., 2010; Spaak et al., 2012; van Kerkoerle et al., 2014), and therefore the white matter surface may not be the optimal source location model. In the past, however, the contribution of inaccuracies in dipole location and orientation constraints to source localization error has likely been insignificant in the face of within-session participant movement, co-registration error, and the relatively low resolution of cortical surface reconstructions. However, the recent development of techniques for high precision MEG (Bonaiuto et al., 2018b, 2018a; Meyer et al., 2017; Troebinger et al., 2014b, 2014a) allow us to compare competing current-flow orientation models in more detail.

Here, we set out to determine a better way to estimate the location and orientation of source dipoles based on MRI-derived cortical surfaces. We tested three different cortical surfaces for determining dipole locations: 1) white matter, 2) pial, and 3) combined white matter/pial, and five different methods for computing dipole orientations: 1) downsampled surface normals, 2) cortical patch statistics, 3) original surface normals, 4) link vectors, and 5) variational vector fields. The most commonly used method, downsampled surface normals (Dale and Sereno, 1993; Fuchs et al., 1994; Hämäläinen and Hari, 2002; Hillebrand and Barnes, 2003; Lin et al., 2006), involves downsampling (decimating) the original cortical surface, and then computing the normal vector at each vertex as the mean of the normal vectors of each surface face it is connected to. While surface decimation increases the computational tractability of source inversion, it distorts the surface faces and therefore biases the surface normal vector estimates. The cortical patch statistics method was therefore designed to compute normal vectors by averaging the individual normal vectors from vertices adjacent to the nearest vertex in the original (down-sampled) mesh (Lin et al., 2006). The original surface normals method takes advantage of the fact that the surface decimation algorithm used here maintains a correspondence between the downsampled and original surface meshes, and uses the normal vectors of the corresponding vertices from the original cortical surface. These three methods involve computation of dipole orientation based on the geometry of a single cortical mesh: the white matter *or* pial surface. In contrast, the link vectors (Dale et al., 1999) and variational vector field (Fischl and Sereno, 2018) approaches establish correspondences between the white matter and pial surface meshes. The link vectors approach simply uses the vectors connecting each vertex on the white matter surface with the corresponding vertex on the pial surface (Dale et al., 1999). The variational vector field method constructs a field of correspondence vectors between the original white matter and pial surfaces which are constrained to be approximately normal to each cortical surface and parallel to each other (Fischl and Sereno, 2018).

We first compared the resulting orientation vectors from each method in terms of the angular difference at each surface vertex. We then ran simulations of single dipoles at a given orientation, and subsequently performed source reconstruction using various dipole orientations, noise levels, and co-registration error magnitudes. Finally, we compared the methods using evoked visual and motor responses in MEG data from human participants.

2. Methods

Data from eight healthy, right-handed, volunteers with normal or corrected-to-normal vision and no history of neurological or psychiatric disorders was used for our analyses (six male, aged 28.5 $\pm$ 8.52 years; Bonaiuto et al., 2018a; Little et al., 2018). The study protocol was in accordance with the Declaration of Helsinki, and all participants gave written informed consent which was approved by the UCL Research Ethics Committee (reference number 5833/001). All analysis code is available at https://github.com/jbonaiuto/dipole_orientation.

2.1. MRI acquisition

Prior to MEG scanning, two MRI scans were acquired with a 3T whole body MR system (Magnetom TIM Trio, Siemens Healthcare, Erlangen, Germany) using the body coil for radio-frequency (RF) transmission and a standard 32-channel RF head coil for reception. The first was a standard T1 for individual head-cast creation (Meyer et al., 2017), and the other was a high resolution, quantitative multiple parameter map (MPM; Weiskopf et al., 2013) for MEG source location.

The first protocol used a T1-weighted 3D spoiled fast low angle shot (FLASH) sequence with 1 mm isotropic image resolution, field-of view set to 256, 256, and 192 mm along the phase (anterior-posterior, A–P), read (head-foot, H–F), and partition (right-left, R–L) directions, respectively. The repetition time was 7.96 ms and the excitation flip angle was 12°. After each excitation, a single echo was acquired to yield a single anatomical image. A high readout bandwidth (425 Hz/pixel) was used to preserve brain morphology and no significant geometric distortions were observed in the images. Acquisition time was 3min 42s. A 12 channel head coil was used for signal reception without using either padding or headphones.

The second, MPM, protocol consisted of acquisition of three differentially-weighted, RF and gradient spoiled, multi-echo 3D fast low angle shot (FLASH) acquisitions and two additional calibration sequences to correct for inhomogeneities in the RF transmit field (Callaghan et al., 2015; Lutti et al., 2012, 2010), with whole-brain coverage at 800 μm isotropic resolution.

The FLASH acquisitions had predominantly proton density (PD), T1 or magnetization transfer saturation (MT) weighting. The flip angle was 6° for the PD- and MT-weighted volumes and 21° for the T1 weighted acquisition. MT-weighting was achieved through the application of a Gaussian RF pulse 2 kHz off resonance with 4 ms duration and a nominal flip angle of 220° prior to each excitation. The field of view was 256 mm head-foot, 224 mm anterior-posterior (AP), and 179 mm right-left (RL). Gradient echoes were acquired with alternating readout gradient polarity at eight equidistant echo times ranging from 2.34 to 18.44 ms in steps of 2.30 ms using a readout bandwidth of 488 Hz/pixel. Only six echoes were acquired for the MT-weighted acquisition in order to maintain a repetition time (TR) of 25 ms for all FLASH volumes. To accelerate the data acquisition, partially parallel imaging using the GRAPPA algorithm was employed with a speed-up factor of 2 in each phase-encoded direction (AP and RL) with forty integrated reference lines.

To maximize the accuracy of the measurements, inhomogeneity in the transmit field was mapped by acquiring spin echoes and stimulated echoes across a range of nominal flip angles following the approach described in Lutti et al. (2010), including correcting for geometric distortions of the EPI data due to B0 field inhomogeneity. Total acquisition time for all MRI scans was less than 30 min.

Quantitative maps of proton density (PD), longitudinal relaxation rate ($R1 = 1/T1$), MT and effective transverse relaxation rate ($R2^* = 1/T2^*$) were subsequently calculated according to the procedure described in Weiskopf et al. (2013).

2.2. FreeSurfer surface extraction

FreeSurfer (v5.3.0; Fischl, 2012) was used to extract cortical surfaces from the MPMs for MEG source localization. We used a custom FreeSurfer surface reconstruction procedure to process MPM volumes, using the PD and T1 volumes as inputs (Carey et al., 2017), resulting in surface meshes representing the pial surface (adjacent to the cerebro-spinal fluid, CSF), and the white/gray matter boundary (Fig. 1). FreeSurfer creates the pial surface by expanding the white matter surface outward to the cortex/CSF boundary. This is done by minimizing an energy functional which includes terms promoting surface smoothness and regularity as well as an intensity-based term designed to determine the cortex/CSF boundary based on local volume intensity contrast (Dale et al., 1999). Because this process involves moving the vertices of the white matter

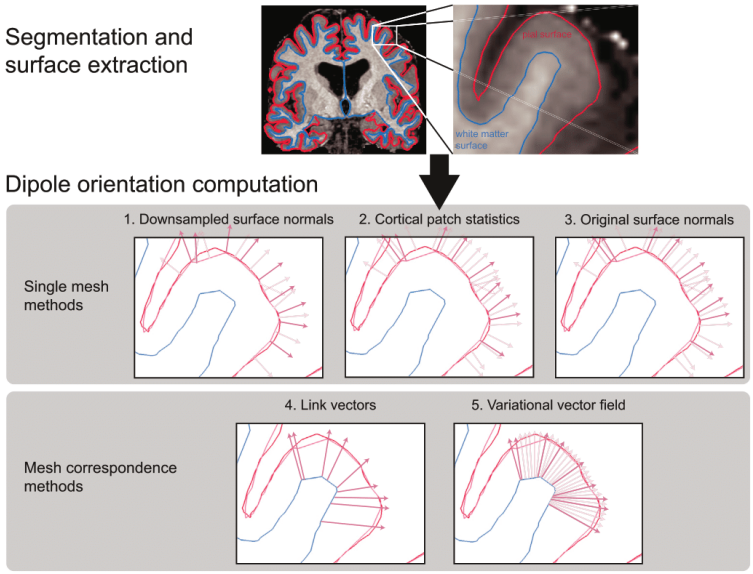

Fig. 1. Dipole orientation models. Pial and white matter surfaces are extracted from proton density and T1 weighted quantitative maps obtained from a multi-parameter mapping MRI protocol. Dipole orientation vectors are computed from these surfaces using five different methods. The downsampled surface normal and original surface normal methods compute vectors at each vertex (dark red) as the mean of the normal vectors of the surface faces they are connected to (light red). The cortical patch statistics method computes the mean of the normal vertices adjacent to the corresponding vertices in the original mesh. The link vectors method computes vectors which link corresponding vertices on the white matter and pial surfaces. The variational vector field method constructs a field of vectors which are approximately parallel to each other and orthogonal to the pial surface (shown in light red for the original surfaces and dark red for the subset of vertices in the downsampled surfaces).

surface based on the gradient of the energy functional, the result is a one-to-one correspondence between white matter and pial surface vertices. We used a custom routine to downsample each of these surfaces by a factor of 10 while maintaining this correspondence. This involved using MATLAB's reducepatch function to remove vertices from, and re-tesselate the pial surface, and then removing the same vertices from the white matter surface and copying the edge structure from the pial surface. This yielded two meshes of the same size (same number of vertices and edges), comprising about 30,000 vertices each (M = 30, 094.75, SD = 2,665.45 over participants).

2.3. Dipole orientation computation methods

The downsampled surface normal method computes, at each vertex of the decimated mesh, the average of the normal vectors of each adjacent face (Fig. 1). This method was implemented using the spm_mesh_normals function in SPM12. The cortical patch statistics method computes, at each vertex of the decimated mesh, the average surface normal vector over all vertices in the original, non-decimated mesh which are adjacent to the corresponding original mesh vertex (Fig. 1). The original surface normal method is implemented in the same way as the downsampled surface normals method, but is applied to the original, non-decimated mesh (Fig. 1). Because our decimation procedure only removed vertices from the original surface, the resulting vectors can then be mapped onto the vertices of the decimated mesh used for source localization. The link vectors method takes advantage of the fact that our decimation routine maintains the correspondence between white matter and pial surface vertices, and for each vertex on the pial surface, uses the vector linking it to the corresponding vertex on the white matter surface ($\mathbf{v_i} = \mathbf{w_i} - \mathbf{p_i}$, for the ith white matter vertex, w_i, and pial vertex p_i; Fig. 1). The variational vector field method constructs a vector field linking the white matter and pial surfaces, by using gradient descent to minimize an energy functional that encourages vectors to approximate surface normals and to be parallel to each other (Fischl and Sereno, 2018) (Fig. 1). The angular difference between any two vectors, v_1 and v_2, was computed using the formula: atan2 ($||\mathbf{v_1} \times \mathbf{v_2}||$, $\mathbf{v_1} \cdot \mathbf{v_2}$).

Vectors obtained from each method were used to construct the lead field matrix of the forward model used for source inversion of the simulated or experimental data. The models constructed using each method were compared to each other based on relative Bayesian model evidence, as approximated by differences in free energy:

$$\Delta F_{i,j} = F_i - F_j$$

where F_i and F_j are the free energy values of models i and j, respectively. Free energy is a parametric metric rewards fit accuracy and penalizes model complexity (Bonaiuto et al., 2018b; Friston et al., 2008, 2007; Henson et al., 2009; López et al., 2014; Wipf and Nagarajan, 2009):

$$F_i = Accuracy(i) - Complexity(i)$$

The first term is the log model evidence: the log of the probability of the data, given the model and parameters, and the second term is the Kullback-Liebler divergence between the true posterior density and an approximate posterior density. Because the second term is always positive, free energy provides a lower bound on the model evidence (Penny et al., 2010).

The best overall dipole orientation method and source space surface model was determined using random effects family level Bayesian inference (Penny et al., 2010) as implemented by the spm_compare_families method in SPM12. This method groups models based on visual ERFs 1 and 2 and the motor ERF in all participants into 'families', and then combines the evidence of models from the same family and computes the exceedance probability for each family. The exceedance probability corresponds to the belief that a particular model family is more likely than the other model families tested, given the data from all participants. We first grouped models into families based on dipole orientation method/source space surface model combinations (e.g. downsampled surface normals/pial surface) to determine the best combination over all ERFs and participants. We then grouped models based on dipole orientation method, and finally based on source space surface model.

2.4. Simulations

All simulations were based on a single dataset acquired from one human participant. This dataset was only used to determine the sensor layout, sampling rate (1200 Hz, downsampled to 250 Hz), number of trials (515), and number of samples (251) for the simulations. All simulations and analyses were implemented using the SPM12 software package (http://www.fil.ion.ucl.ac.uk/spm/software/spm12/).

In each simulation, we specified spatially distributed source activity centered at a single vertex on the pial surface. We simulated a Gaussian activity time course in this vertex, centered within the epoch, with a width of 25 ms and a magnitude of 10 nA m. We then spatially smoothed this simulated dipole time course with a Gaussian kernel (FWHM = 5 mm), to obtain a patch of spatially distributed activity. Within this patch, the orientation of each vertex differed, but was specified by the same rule using the link vectors method. We then used a single shell forward model (Nolte, 2003) to generate a synthetic dataset from the simulated source activity. We simulated sources at 100 random vertices on the pial surface, and ran two sets of simulations: one varying the level of noise in the simulated data and the other varying the magnitude of co-registration error.

Typical per-trial SNR levels for MEG data range from −40 to −20 dB (Goldenholz et al., 2009), and therefore Gaussian white noise was added to the simulated data and scaled in order to yield per-trial amplitude SNR levels (averaged over all sensors) of −50, −40, −30, −20, −10, or 0 dB to generate synthetic datasets across a range of realistic SNRs. Source reconstruction was performed using 10 different models. The reference model used the original link vectors as dipole orientation priors, and the remaining 9 models used vectors with angular differences from the original link vectors ranging from 7 to 63° (in increments of 7°). The orientation of the 9 additional vectors was determined by taking random points on the edge of a cone defined by the reference vector and the angular distance. In these simulations, the co-registration error was 0 mm. Within each SNR level, the free energy metric was compared between each model and the reference model.

Within-session head movement and between-session co-registration error commonly combine to introduce a typical magnitude of ~5 mm (or more) of uncertainty concerning the relative location of the brain and the MEG sensors in traditional MEG recordings (Adjamian et al., 2004; Gross et al., 2013; Ross et al., 2011; Singh et al., 1997; Stolk et al., 2013; Whalen et al., 2008). To simulate between-session co-registration error, we therefore introduced a linear transformation of the fiducial coil locations in random directions (0 mm translation - 0° rotation, 2 mm - 2°, 4 mm - 4°, 6 mm - 6°, 8 mm - 8°, or 10 mm - 10°) prior to source inversion. As in the SNR simulations, source reconstruction was performed using a reference model with the original link vectors as orientation priors, and 9 models using vectors rotated in random directions with angular differences from the original vectors from 7 to 63°. In these simulations, the per-trial amplitude SNR was set to 0 dB. Within each level of co-registration error, we compared the free energy between each model and the reference model.

2.5. Head-cast construction

From an MRI-extracted image of the scalp, a head-cast that fit between the participant's scalp and the MEG dewar was constructed (Bonaiuto et al., 2018a; Meyer et al., 2017; Troebinger et al., 2014b). Scalp surfaces were first extracted from the T1-weighted MRI scans acquired in the first MRI protocol using SPM12 (http://www.fil.ion.ucl.ac.uk/spm/). This tessellated surface, along with 3D models of fiducial coils placed on the nasion and the left and right pre-auricular points, was used to create a virtual 3D model, which was then placed inside a virtual version of the scanner dewar in order to minimize the distance to the sensors while ensuring that the participant's vision was not obstructed. The model (including spacing elements and ficudial coil protrusions) was printed using a Zcorp 3D printer (Zprinter 510). The 3D printed model was then placed inside a replica of the MEG dewar and polyurethane foam was poured in between the surfaces to create the participant-specific head-cast. The protrusions in the 3D model for fiducial coils therefore become indentations in the foam head-cast, into which the fiducial coils can be placed scanning. The locations of anatomical landmarks used for co-registration are thus unchanged over repeated scans, allowing combination of data from multiple sessions (Bonaiuto et al., 2018a; Meyer et al., 2017).

2.6. Behavioral task

Participants completed a visually cued action decision making task in which they responded to visual instruction cue projected on a screen by pressing one of two buttons using the index and middle finger of their right hand (Bonaiuto et al., 2018a). After a baseline period of fixation, a random dot kinematogram (RDK) was displayed for 2s with coherent motion either to the left or to the right. Following a delay period, an instruction cue (an arrow pointing either to the left or the right), prompted participants to press either the left or right button. The level of motion coherence in the RDK and the congruence between the RDK motion direction and instruction cue varied from trial to trial, but for the purposes of the present study, we analyzed the main effect of visual stimulus onset and button press responses. For a full description of the paradigm and task structure, see Bonaiuto et al. (2018a).

Each block contained 180 trials in total. Participants completed three blocks per session, and 1–5 sessions on different days, resulting in 540–2700 trials per participant (M = 1822.5, SD = 813.21). The task was implemented in MATLAB (The MathWorks, Inc., Natick, MA) using the Cogent 2000 toolbox (http://www.vislab.ucl.ac.uk/cogent.php).

2.7. MEG acquisition and preprocessing

MEG data were acquired using a 275-channel Canadian Thin Films (CTF) MEG system with superconducting quantum interference device (SQUID)-based axial gradiometers (VSM MedTech, Vancouver, Canada) in a magnetically shielded room. A projector was used to display visual stimuli on a screen (~50 cm from the participant), and a button box was used for participant responses. The data collected were digitized continuously at a sampling rate of 1200 Hz. MEG data preprocessing and analyses were performed using SPM12 (http://www.fil.ion.ucl.ac.uk/spm/) using MATLAB R2014a. The data were filtered (5th order Butterworth bandpass filter: 2–100 Hz, Notch filter: 50 Hz) and downsampled to 250 Hz. Eye blink artifacts were removed using multiple source eye correction (Berg and Scherg, 1994). Trials were then epoched from 1s before RDK onset to 1.5s after instruction cue onset for analysis of visual responses, and from 2s before the participant's response to 2s after for analysis of movement-evoked responses. Blocks within each session were merged, and trials whose variance exceeded 2.5 standard deviations from the mean were excluded from analysis. The epoched data were then averaged over trials using robust averaging, a form of general linear modeling (Wager et al., 2005) used to reduce the influence of outliers on the mean by iteratively computing a weighting factor for each sample according to how far it is from the mean. Preprocessing code is available at http://github.com/jbonaiuto/meg-laminar.

2.8. Source reconstruction

Source inversion was performed using the empirical Bayesian beamformer algorithm (EBB; Belardinelli et al., 2012; López et al., 2014) as implemented in SPM12. The source inversion was applied to a 100 ms time window, centered on the event of interest (the peak of the simulated signal, 100 ms following the onset of visual stimuli, or the button press response). These data were projected into 274 orthogonal spatial (lead field) modes and 4 temporal modes. Singular value decomposition (SVD) was used to reduce the sensor data to 274 orthogonal spatial (lead field) modes, each with 4 temporal modes (weighting the dominant modes of

temporal variation across the window). For uninformative priors, the maximum-likelihood solution to the inverse problem is:

$$\hat{J} = QL^T(Q_\varepsilon + LQL^T)^{-1}Y$$

where $\hat{J}$ is the estimated current density across the source space, Y is the SVD-reduced measured data, L is the lead field matrix that can be computed from the sensor and volume conductor geometry. Q_ε is the sensor covariance and Q is the prior estimate of source covariance. We assumed the sensor level covariance (Q_ε) to be an identity matrix (see discussion). Most inversion algorithms can be differentiated by the form of Q (Friston et al., 2008; López et al., 2014). EBB uses a beamformer prior to estimate the structure of Q (Belardinelli et al., 2012; López et al., 2014) based on the sensor-level data:

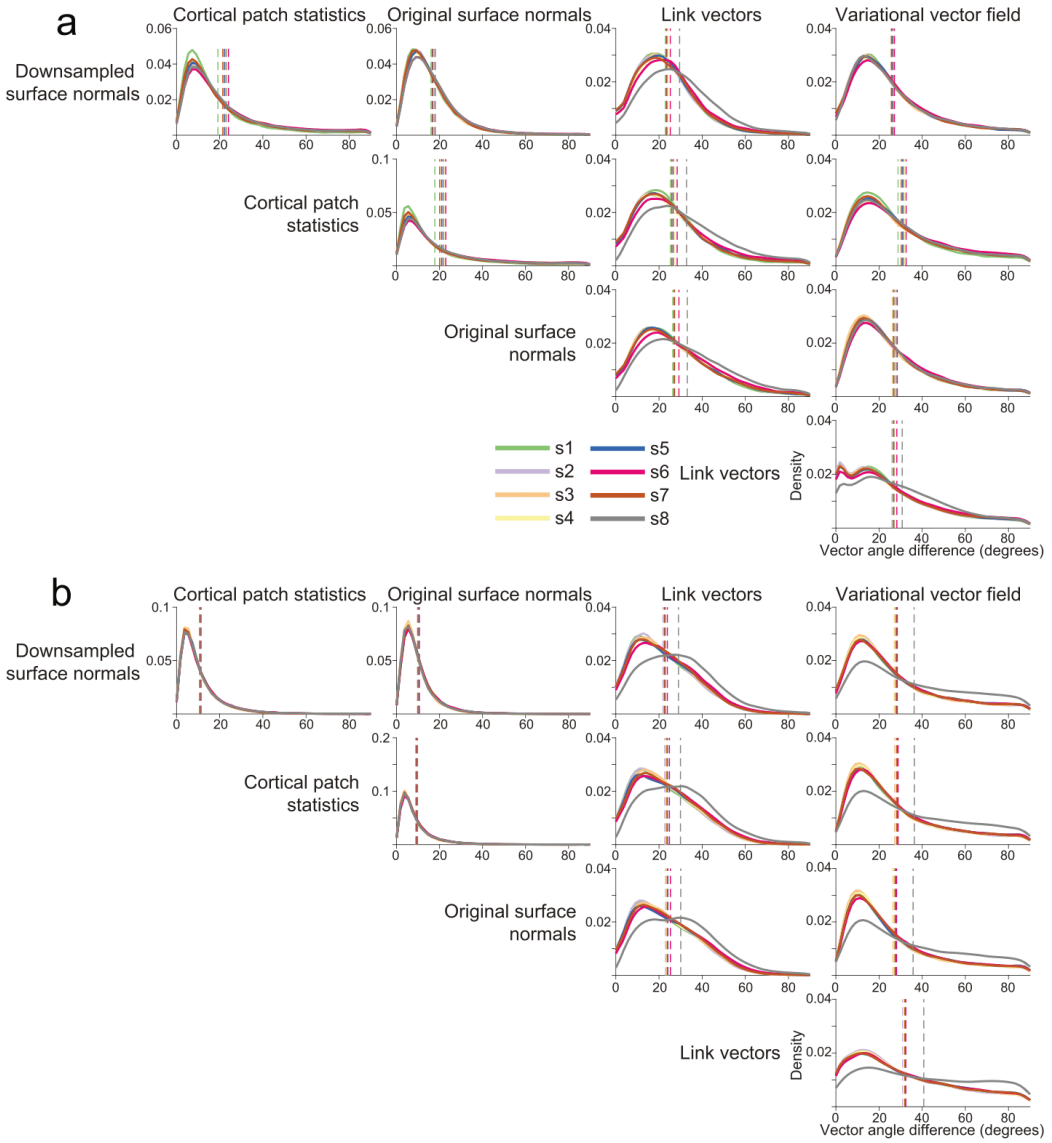

Fig. 2. Substantial discrepancy in dipole orientations across methods.
Distribution of angular difference between dipole orientations on the pial surface (**a**) and white matter surface (**b**), generated using each method for each participant. Vertical dashed lines show the mean angular difference for each participant.

$$Q(i) = \frac{1}{L_i^T L_i}\left(L_i^T (YY^T)^{-1} L_i + \lambda I\right)^{-1}$$

where each element of the diagonal $Q(i)$ corresponds to a source location i. The lead field of each source location is L_i, ^{T} denotes the transpose operator, I is an identity matrix, and λ is a regularization constant (set to 0). The prior estimates of Q_ε and Q are then re-scaled or optimally mixed using an expectation maximization scheme (Friston et al., 2008) to give an estimate of J that maximizes model evidence. All inversions used a spatial coherence prior (Friston et al., 2008) with a FWHM of 5 mm. We used the Nolte single shell head model (Nolte, 2003).

For MEG source inversion, the accuracy term of the free energy equation is defined as

$$Accuracy(i) = \frac{N_c}{2} trace\left(C_Y C_i^{-1}\right) - \frac{N_c}{2} log|C_i| - \frac{N_c N_t}{2} \log(2\pi)$$

where N_c is the number of channels, N_t is the number of samples, $C_Y = \frac{1}{N_t} YY^T$ is the data-based sampled covariance, $C_i = Q_\varepsilon + L_i Q L_i^T N_t$ is the model-based sample covariance, and $|\cdot|$ is the matrix determinant operator.

For the EBB algorithm, the complexity term of the free energy equation is dependent on hyperparameters, λ, that control the trade-off between sensor noise $Q_\varepsilon = \lambda_1 I_{N_c}$, and the beamforming prior $Q = \lambda_2 \Gamma$, where Γ is the beamforming prior:

$$Complexity(i) = \frac{1}{2}(\hat{\lambda}_i - \upsilon)^T \Pi (\hat{\lambda}_i - \upsilon) + \frac{1}{2} log|\Sigma_{\lambda_i} \Pi|$$

The prior and posterior distributions of λ, $q(\lambda_i)$ and $p(\lambda_i)$ are assumed to be Gaussian:

$$q(\lambda_i) = N\left(\lambda; \upsilon, \Pi^{-1}\right)$$

$$p(\lambda_i) = N(\hat{\lambda}_i, \Sigma_{\lambda_i})$$

where $\hat{\lambda}_i$ and Σ_{λ_i} are the posterior mean and covariance of the hyperparameters for model i. We used non-informative mean and precision (υ and Π) implemented as identity matrices scaled close to zero mean and low precision, as implemented by default in SPM.

3. Results

3.1. Different methods for estimating vector orientation yield substantial variation in dipole orientation

We first compared the dipole orientation vectors generated by each of our five methods in terms of the angular difference between vectors at the same vertex on the pial and white matter surfaces, respectively (Fig. 2). The three methods that utilize only one surface, (downsampled surface normals, cortical patch statistics, original surface normals) generated vectors which were the most similar to each other on both the pial (downsampled surface normals – cortical patch statistics individual subject mean angular difference: 19.16–23.04°; over subjects: M = 22.30°, SD = 1.51°; downsampled surface normals – original surface normals: 16.00–17.95°; over subjects: M = 16.94°, SD = 0.67°; cortical patch statistics – original surface normals: 17.80–22.89°; over subjects: M = 21.01°, SD = 1.55°) and white matter surfaces (downsampled surface normals – cortical patch statistics individual subject mean angular difference: 10.65–11.35°; over subjects: M = 10.99°, SD = 0.27°; downsampled surface normals – original surface normals: 9.64–10.57°; over subjects: M = 10.10°, SD = 0.32°; cortical patch statistics – original surface normals: 8.93–9.76°; over subjects: M = 9.34°, SD = 0.31°). Each single- and multi-surface method generated vectors with mean angular differences from each other of at least 20°, for both the pial surface (downsampled surface normals – link vectors: 22.94–29.56°, M = 24.51°, SD = 2.15°; downsampled surface normals – variational vector field: 25.52–27.13°, M = 26.05°, SD = 0.55°; cortical patch statistics – link vectors: 25.26–32.76°, M = 27.42°, SD = 2.06°; cortical patch statistics – variational vector field: 28.80–32.55°, M = 30.91°, SD = 1.11°; original surface normals – link vectors: 26.77–33.12°, M = 28.44°, SD = 2.06°; original surface normals – variational vector field: 26.18–28.43°, M = 27.06°, SD = 0.75°) and the white matter surface (downsampled surface normals – link vectors: 21.81–29.03°, M = 23.46°, SD = 2.33°; downsampled surface normals – variational vector field: 27.08–36.26°, M = 28.78°, SD = 3.06°; cortical patch statistics – link vectors: 22.64–24.82°, M = 24.48°, SD = 2.34°; cortical patch statistics – variational vector field: 27.31–36.34°, M = 29.04°, SD = 3.00°; original surface normals – link vectors: 23.38–30.09°, M = 25.00°, SD = 2.15°; original surface normals – variational vector field: 26.43–35.69°, M = 28.31°, SD = 3.08°). The two multi-surface methods, link vectors and variational vector field, generated vectors with some of the largest mean angular differences of all method pairs on each surface (pial surface: 67.41–30.74°, M = 27.71°, SD = 1.40°; white matter surface: 31.33–40.74°, M = 33.31°, SD = 3.04°). These results were comparable when using surfaces derived from more commonly used 1 mm^3 T1 scans instead of 800 μm^3 MPMs (Figure S1). Therefore, rather than being close approximations to each other, each method generates substantially different dipole orientation vectors, even within the multi-surface class of methods.

We next compared dipole orientation vectors generated by each method between the pial and white matter surfaces derived from the 800 μm^3 MPM volumes (Fig. 3) and 1 mm^3 T1 volumes (Figure S2). Because the link vectors method generates vectors that connect corresponding vertices on the pial and white matter surfaces, the resulting dipole orientations on each surface are equivalent (i.e. the link vector from a particular vertex on the pial surface points in exactly the opposite direction as the link vector from the corresponding white matter surface vertex). All three single-surface methods generated vectors with the lowest average angular difference between pial and white matter surfaces created using either the 800 μm^3 MPM volumes (downsampled surface normals: individual subject mean angular difference = 16.88–20.52°, over subjects M = 18.23°, SD = 1.13°; cortical patch statistics: 22.66–27.81°, M = 25.70°, SD = 1.67°; original surface normals: 22.90–26.81°, M = 24.46°, SD = 1.26°) or the 1 mm^3 T1 volumes (downsampled surface normals: 17.89–19.49°, M = 18.66°, SD = 0.56°; cortical patch statistics: 25.10–27.23°, M = 26.23°, SD = 0.70°; original surface normals: 24.10–28.80°, M = 25.45°, SD = 1.46°). The variational vector field method generated dipole orientation vectors that differed the most between the pial and white matter surface (MPM: 37.47–43.54°, M = 38.80°, SD = 1.99°; T1: 37.07–40.28°, M = 39.10°, SD = 1.00°). Aside from the link vectors method, there is therefore at least as much variation in dipole orientations between the pial and white matter surfaces within a method as there is between methods for one surface.

3.2. With high precision MEG data, getting the orientation right matters

Having established that each method yields substantially different orientation vectors, we next sought to determine the minimum angular difference between dipole orientations distinguishable by source inversion model comparison, and how this is affected by typical levels of SNR and co-registration error. We therefore simulated dipoles at 100 random source locations on the pial surface and created synthetic datasets with varying SNR and co-registration error levels. We then performed source inversion on the synthetic datasets, using a reference model in which the dipole orientations exactly match those of the simulated dipole, and 9 other models in which the dipole orientations were rotated with respect to simulated dipole orientation. We then compared each of these models to the reference model in terms of the relative free energy, using a significance threshold of ±3 for the free energy difference (indicating that one model is approximately twenty times more likely than the other).

At lower SNR levels (−50 dB), each model was indistinguishable from the reference model (magnitude of relative free energy less than 3). However, as SNR increased, models with an angular error as low as 15°

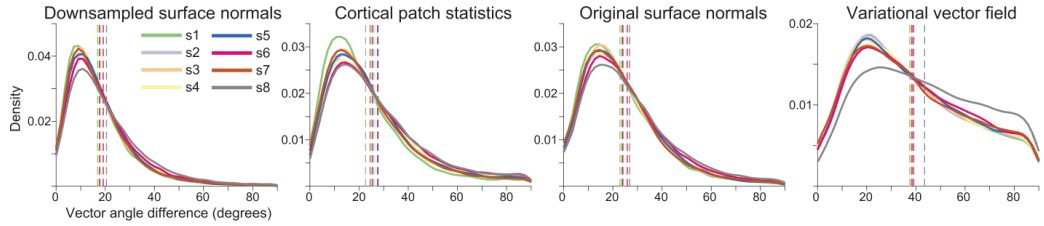

Fig. 3. Substantial discrepancy in dipole orientations between pial and white matter surfaces. Distribution of angular difference between dipole orientations at corresponding vertices on the pial and white matter surfaces, generated using the 800 μm^3 MPM volumes. The link vectors method is not shown because this method generates identical dipole orientations for the pial and white matter surfaces. Each solid line shows the distribution for a single participant. Vertical dashed lines show the mean angular difference for each participant.

relative to the reference model started to become differentiable (i.e., a relative free energy difference of >3; Fig. 4a). Relative model evidence was less dependent on co-registration error, and at all levels tested models with an angular error of at least 15° could be differentiated from the reference model (Fig. 4b). This angular error is well within the range of the angular differences between vectors generated by each of the methods considered here (Fig. 2). In other words, given sufficient SNR and co-registration accuracy, one should be able to determine the best method to use with human data based on source inversion model comparison.

3.3. Comparing surface models with empirical head-cast data

We next compared orientation models based on three different evoked responses from human participants. We performed source inversion, and compared the resulting model fits in terms of relative free energy compared to that of the downsampled surface normal model (the current most commonly used method). This was repeated using source space models restricted to the pial surface, white matter surface, and combined pial – white matter surface (Bonaiuto et al., 2018a, 2018b). In this case the combined pial-white model had double the number of sources and these sources could be arranged with identical orientations on each surface (link vectors); or different orientations (cortical patch statistics, downsampled surface normals, original surface normals, and variational vector field).

The evoked response fields (ERFs) were the visually-evoked response to the RDK (visual ERF 1) and instruction cue (visual ERF 2), and the motor-evoked response during the button press (motor ERF). When running the source inversion over the full time course of each ERF, each orientation model yielded slightly different peak cortical locations (Fig. 5a and b), with the original surface normals and variational vector field methods giving the closest peak coordinates (M = 4.88 mm, SD = 2.93 mm), and the cortical patch statistics and link vectors methods yielding coordinates furthest away from each other (M = 13.96 mm, SD = 12.76 mm). At each peak location identified by the downsampled surface normals method, the source space ERFs given by the downsampled surface normals, cortical patch statistics, and variational vector field methods, respectively, were most similar to each other, whilst the link vectors methods yielded an ERF with a larger amplitude, and the original surface normals method yielded an ERF with inverted polarity (RMSE<0.1; Fig. 5c and d). However, at the peak coordinate identified by each method the ERFs were very similar (RMSE<0.05; Fig. 5e and f).

We then compared each method in terms of model fit. The link vectors method achieved a significantly better model fit than the downsampled surface normal method in 7/8 subjects for visual ERFs 1 and 2 and the motor ERF using the pial surface, 7/8 subjects for visual ERF 1 and the motor ERF and 8/8 subjects for visual ERF 2 using the white matter surface, and 7/8 subjects for visual ERFs 1 and 2 and the motor ERF using the two-layer surface (Fig. 6b). The variational vector field method had significantly better model fit than the downsampled surface normal method in 6/8 subjects for visual ERF 1 and 4/8 subjects for visual ERF 2, but only 2/8 subjects for the motor ERF using the pial surface, 1/8

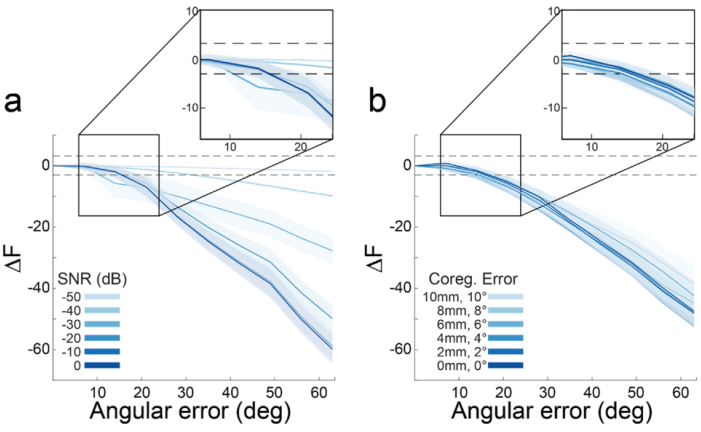

Fig. 4. With high precision MEG data, model evidence decreases with dipole orientation error. **a** Each line shows the change in model evidence (ΔF) as the orientation of the dipole used for inversion is rotated away from the true orientation at different SNR levels (co-registration error = 0 mm). The shaded regions represent the standard error of ΔF over all 100 simulations at each angular error value tested. The lower dotted line (at ΔF = −3) show the point at which the imperfect model is 20 times less likely than the true model. The differences between models become more apparent at higher SNR. **b** As in a, for different magnitudes of co-registration error (SNR = 0 dB). Co-registration error has a smaller impact than SNR on discriminating between models with different dipole orientations.

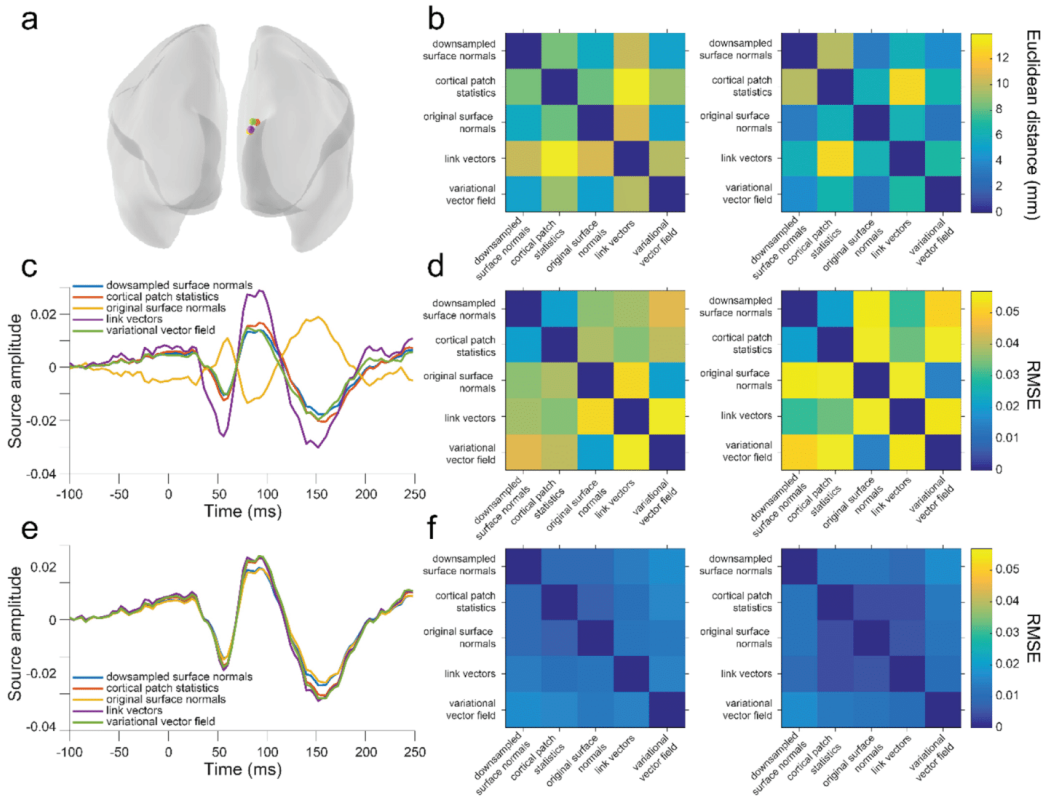

Fig. 5. Variation in source localization across methods.
a Peak source locations on the pial surface for visual ERF 1, for each dipole orientation method, in a single subject. **b** Mean (left) and standard deviation (right) of the Euclidean distance between peak source locations for each method, using the pial surface, over subjects and ERFs. **c** Time course of source activity for visual ERF 1 for the different methods, at the peak pial source location identified using the downsampled surface normals method, for a single subject. **d** Mean (left) and standard deviation (right) of the RMSE between source activity time courses at the peak source location identified using the downsampled surface normals method, for each method, using the pial surface, over subjects and ERFs. **e** Time course of source activity for visual ERF 1 at the peak pial source location identified from each method, for a single subject. **f** Mean (left) and standard deviation (right) of the RMSE between source activity time courses at the peak source location identified using each method with the pial surface, over subjects and ERFs.

subjects for visual ERF 1 and the motor ERF and 4/8 subjects for visual ERF 2 using the white matter surface, and 5/8 subjects for visual ERFs 1 and 2 and 1/8 subjects for the motor ERF using the two-layer surface. The original surface normal method was most similar to the downsampled surface normal method, only being significantly better in 4/8 subjects for visual ERF 1, 5/8 subjects for visual ERF 2, and 0/8 subjects for the motor ERF using the pial surface, 0/8 subjects for visual ERFs 1 and 2 and the motor ERF using the white matter surface, and 1/8 subjects for visual ERF 1, 3/8 subjects for visual ERF 2, and 0/8 subjects for the motor ERF using the two-layer surface. The cortical patch statistics method was significantly better than the downsampled surface normals method in 3/8 subjects for visual ERF 1, 6/8 subjects for visual ERF 2, and 2/8 subjects for the motor ERF using the pial surface, 0/8 subjects for visual ERFs 1 and 2 and the motor ERF using the white matter surface, and 2/8 subjects for visual ERF 1, 4/8 subjects for visual ERF 2, and 0/8 subjects for the motor ERF.

While the cortical patch statistics and original surface normal methods are an improvement on the widely used downsampled surface normal method, multi-surface methods such as link vectors and variational vector fields achieve better model fits overall, using either single- or two-layer cortical surface models (Fig. 6b). These results were comparable when using surfaces derived from more commonly used 1 mm^3 T1 scans instead of 800 μm^3 MPMs, with the exception of the variational vector field method, which performed significantly worse than the downsampled surface normal method in 6/8 subjects for the motor ERF using the pial surface (Figure S3).

3.4. Interaction between orientation and source space models

We next sought to establish how the orientation models interacted with the different possible choices of source space, specifically the cortical surface used to define source locations and the surface used to compute dipole orientations. We fit the empirical evoked response data, using source space location models based on the white matter, pial, or combined white matter/pial surfaces, and for each orientation model using the white matter, pial, or combined white matter/pial surfaces

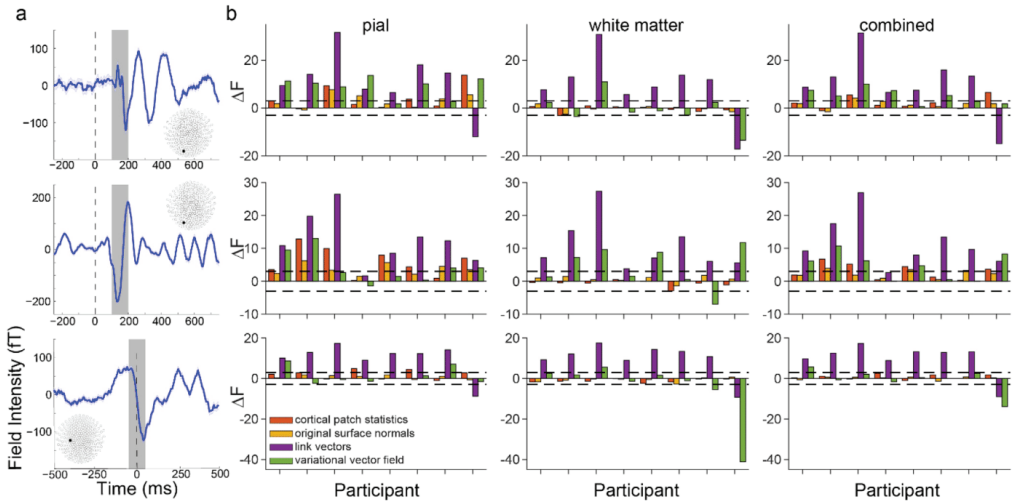

Fig. 6. Surface correspondence-based methods yield the best model fit.
a Trial-averaged event-related fields (ERFs) aligned to the onset of visual stimulus 1 (the random dot kinematogram; top), visual stimulus 2 (the instruction cue; middle), and to the participant's response (button press; bottom). Data shown are for a single representative participant. The inlays show the MEG sensor layout with filled circles denoting the sensor from which the ERFs are recorded. Each shaded region represents the time window over which source inversion was performed. **b** Change in free energy (relative to the downsampled surface normals model) for each method tested for each participant for visual ERF 1 (top), visual ERF 2 (middle), and the motor ERF (bottom) using vectors derived from 800 μm^3 MPM volumes and source space models based on the pial (left), white matter (center), and combined pial/white matter surfaces (right).

(with the exception of the combined surface source space orientation model which can only be used with the combined surface source space location model).

To compare source space surface location and orientation models, we used random effects family level Bayesian inference (Penny et al., 2010) over the results from visual ERFs 1 and 2 and the motor ERF in all participants. This method groups models into 'families', and then combines the evidence of models from the same family to compute the exceedance

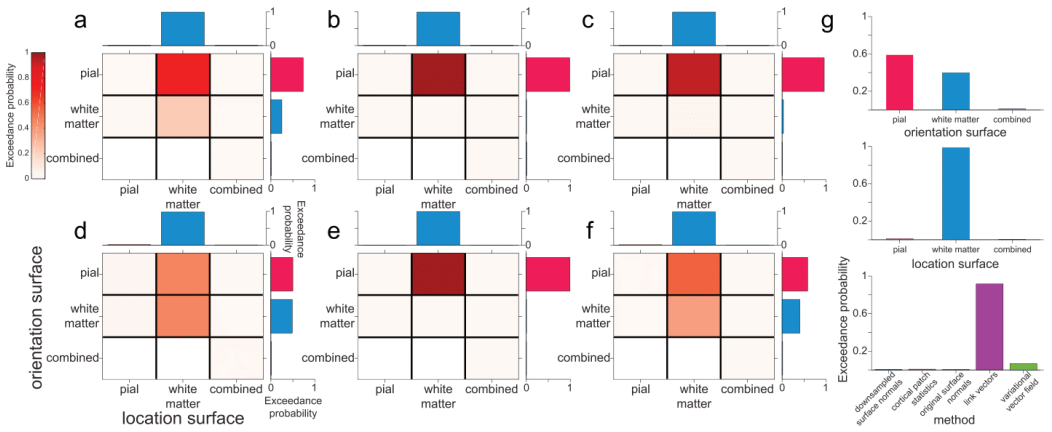

Fig. 7. Source inversion using the pial surface and surface correspondence-based methods yield the best model fit overall.
a-e Exceedance probabilities for each combination of source space orientation (pial, white matter, and combined) and location (pial, white matter, and combined) models for each dipole orientation vector method tested (**a** downsampled surface normals, **b** cortical patch statistics, **c** original surface normals, **d** link vectors, **e** variational vector field) using surfaces derived from 800 μm^3 MPM volumes. In each panel the top and right plots show exceedance probabilities for models grouped by source space location or orientation model alone. **f** As in **a-e**, for each source space orientation and location models over all dipole orientation vector methods. **g** Exceedance probabilities for each source space orientation model over all source space location models and dipole orientation vector methods (top), for each source space location model over all source space orientation models and dipole orientation vector methods (middle), and for each dipole orientation vector method over all source space orientation and location models (bottom).

probability (EP) for each model family. This corresponds to the belief that a particular model family is more likely than the other model families tested, given the data from all participants. We first compared combinations of source space location and orientation surface models within each method, and found that for most dipole orientation methods (downsampled surface normals, cortical patch statistics, original surface normals, and variational vector field), the best source orientation space model was the pial surface and the best source space location model was the white matter surface (downsampled surface normals EP = 0.708, cortical patch statistics EP = 0.968, original surface normals EP = 0.924, variational vector field EP = 0.975; Fig. 7a–c,e). For the link vectors method, the best source space location model was the white matter surface, and the pial and white matter source space orientation models were nearly indistinguishable (pial orientation model EP = 0.458, white matter orientation model EP = 0.468; Fig. 7d). This was not unexpected because the orientation vectors generated from these surfaces using the link vectors method are exactly 180° to each other. Over all dipole orientation methods, the best source space orientation surface was the pial surface and the best source space location model was the white matter surface (EP = 0.654; Fig. 7f). We then grouped models into families based on the source space surface used for orientation and location. This confirmed that the models using the pial surface to compute dipole orientation provided the best model fit, with an EP of 0.608 (white matter surface EP = 0.379), and models using the white matter surface to define source space locations outperformed the others, with an EP of 0.985 (Fig. 7g). Finally, we grouped models based on the method used to compute dipole orientation vectors and confirmed that the link vectors and variational vector field methods were the best overall, with EPs of 0.918 and 0.064, respectively (Fig. 7g). Using surfaces obtained from 1 mm^3 T1 volumes yielded the same results (Figure S4).

4. Discussion

In this paper we show that methods for computing dipole orientation which are based on establishing correspondences between white matter and pial cortical surfaces dramatically outperform methods based on the geometry of a single cortical surface in fitting evoked visual and motor responses. To this end, we compared five different approaches for estimating dipole vector orientation, both in simulations and visual and motor evoked MEG responses.

Our results show substantial variation in dipole vector orientation across the different methods. This indicates that the choice of method is likely to significantly impact the quality of source estimation. At low SNR levels and with head movements commonly observed in conventional MEG recordings, this influence is small or non-detectable. However, with the increased SNR and reduced head movements afforded by high-precision MEG (Meyer et al., 2017; Troebinger et al., 2014b), these differences become distinguishable when average angular errors between methods vary by around 15°. These small orientation errors put a hard limit on any possible improvements in non-invasive estimates of cortical current flow. For example Hillebrand and Barnes (2003) showed that small orientation errors resulted in localization errors which increased monotonically with SNR.

This means that with higher precision MEG recordings, accurate estimation of the dipole orientation becomes increasingly important. Consequently, conventional approaches which estimate vector orientation from a single (downsampled) surface, and based on lower resolution MRI volumes, are likely to offer limited accuracy in source estimation, at least for evoked fields, as analyzed here. By contrast, methods that utilize link vectors between pial and white matter surfaces constructed from higher resolution structural images perform significantly better in explaining observed evoked responses.

The average angular differences between the five methods compared here were substantial, with means of 18–30°, both in high-resolution MPMs and in commonly used T1-weighted structural images with 1 mm^3 spatial resolution. We do not know the ground truth of current flow orientation in the brain, but we show here that the average angular difference between methods is within the range distinguishable in simulated data with SNR and co-registration error levels achievable with high precision MEG. We were therefore able to compare these methods in terms of how well they fit human MEG data, leveraging the free energy metric, in order to determine which method best estimates true dipole orientations.

We were surprised by the large variation in orientation estimates from the same anatomy using different methods. The typical expected orientation differences between methods was ~20–30°. This in turn led to differences in estimated source location of ~5–14 mm. In this study we sought to minimize head-movement and co-registration errors by using head-casts, but in typical MEG studies such additional errors will only add to this variation. Based on these estimates it would seem that if precise anatomical information (e.g. from high resolution MRI volumes) is not available then an approach using some form of loose orientation constraint is advisable (Lin et al., 2006). However, one advantage of being able to exploit anatomical information is to use the sensitivity of MEG to cortical orientation to refine the source localization.

While the family of source space location models based on the white matter surface yielded the highest exceedance probability, the results of the surface comparison varied by evoked response and dipole orientation computation method. Evoked responses can be broken down into temporally dynamic components and therefore may be the result of a complex temporal pattern of signals in both deep and superficial cortical layers. We here used the same 100 ms time window for source inversion in all participants and therefore this analysis did not take into account between-participant differences in the timing of evoked responses and could not track the time course of laminar activity. The inherent differences between induced and evoked responses may therefore explain the more variable attribution of the evoked response to pial and white matters surfaces, compared to the bias of high- and low frequency signals towards deep and superficial cortical laminae, respectively (Bonaiuto et al., 2018a). Future extensions of this work could utilize source inversion in successive time bins to address this limitation and generate temporally resolved estimates of laminar activity.

We assumed the sensor level covariance matrix to be diagonal. However, an independent sensor dataset recorded during a similar time period in an empty room, showed off-diagonal structure (Figure S5). Importantly, the same pattern of model comparison results was obtained when using a sensor covariance matrix based on these noise measurements (Figure S6, S7).

In this work, we used free energy as our metric of model fit but we would expect these findings to generalize across other metrics. For example, we have previously shown that for model comparison problems of the type utilized in this study, free energy is very highly correlated with nonparametric cross validation error measures of model fit (Bonaiuto et al., 2018b).

The present findings do not just impact high SNR MEG recordings obtained with cryogenic sensors, but also for new generations of cryogen-free MEG sensors (optically-pumped magnetometers; OPMs). These sensors can be worn on the head and permit long-duration recordings without head-to-sensor movement, with accurate knowledge of each sensor's position with respect to the brain (Boto et al., 2018, 2017; Holmes et al., 2018; Iivanainen et al., 2019, 2017; Knappe et al., 2014). Our results show that source estimation for this type of recordings is likely to benefit from methods that estimate vector orientation based on white matter – pial surface vertex correspondences, as opposed to more commonly used techniques employing a single surface.

We here assumed that straight vectors provide the best approximation of the orientation of cortical columns that generate MEG data. However, cortical columns are often curved (Bok, 1929). In future work, the curvature of cortical columns could be approximated using sequences of straight vectors computed from laminar equivolumetric surfaces (Waehnert et al., 2014; Wagstyl et al., 2018). If each vector was tangential to the

corresponding segment of the actual (curved) cortical column, this would result in a piecewise linear estimate of column shape, which may allow more precise source localization (Bonaiuto et al., 2018b, 2018a; Troebinger et al., 2014a). This development would benefit from higher resolution (e.g. 7 T) MRI scans, as well as cytoarchitectonic data from histological sections (Amunts et al., 2013; Wagstyl et al., 2018). The current paper provides a novel framework and set of baselines for *in vivo* evaluation of the impact of future columnar models on source modeling.

Our results are likely to impact other methods which require accurate estimation of cortical surfaces and the orientation of surface normal vectors. For example, current flow modelling techniques that estimate the distribution of current delivered with non-invasive brain stimulation approaches such as transcranial direct current stimulation (tDCS; Bestmann and Walsh, 2017; Bestmann and Ward, 2017) estimate the normal component of the electric field across the cortical surface, and relate this component to the observed physiological changes elicited by tDCS (e.g. Laakso et al., 2019; Seo and Jun 2019). We expect that improved surface segmentation approaches and vector estimation, as introduced in our present study, will provide more accurate estimates of these normal components. This will be relevant for explaining how current delivery via tDCS impacts on physiological and behavioral responses, and whether the normal component of the electric field is indeed important to explain these effects.

5. Conclusion

Based on the results of our model comparisons, we have shown that, for evoked responses, source inversion using source locations on the white matter surface and dipole orientation priors computed using link vectors outperforms the other source location and orientation computation methods we tested. We therefore recommend that this approach be used as the default in source inversion.

CRediT authorship contribution statement

James J. Bonaiuto: Conceptualization, Methodology, Software, Formal analysis, Investigation, Data curation, Writing - original draft, Writing - review & editing, Visualization. **Fardin Afdideh:** Methodology, Software, Validation, Formal analysis, Writing - review & editing. **Maxime Ferez:** Software, Investigation, Validation. **Konrad Wagstyl:** Conceptualization, Methodology, Software. **Jérémie Mattout:** Conceptualization, Resources, Supervision. **Mathilde Bonnefond:** Resources, Writing - review & editing, Supervision. **Gareth R. Barnes:** Conceptualization, Methodology, Writing - review & editing, Supervision. **Sven Bestmann:** Conceptualization, Methodology, Writing - review & editing, Supervision.

Acknowledgements

FA, MF, and MB were supported by the European Union's Seventh Framework Programme (FP7/2007–2013)/ERC starting grant agreement number 716862 to M. Bonnefond. KW was supported by the Wellcome Trust (215901/Z/19/Z). The Wellcome Centre for Human Neuroimaging is supported by a centre award from the Wellcome Trust (203147/Z/16/Z). The funders had no role in the preparation of the manuscript.

Appendix A. Supplementary data

Supplementary data to this article can be found online at https://doi.org/10.1016/j.neuroimage.2020.116862.

References

Adjamian, P., Barnes, G.R., Hillebrand, A., Holliday, I.E., Singh, K.D., Furlong, P.L., Harrington, E., Barclay, C.W., Route, P.J.G., 2004. Co-registration of magnetoencephalography with magnetic resonance imaging using bite-bar-based fiducials and surface-matching. Clin. Neurophysiol. 115, 691–698. https://doi.org/10.1016/j.clinph.2003.10.023.

Amunts, K., Lepage, C., Borgeat, L., Mohlberg, H., Dickscheid, T., Rousseau, M.-E., Bludau, S., Bazin, P.-L., Lewis, L.B., Oros-Peusquens, A.-M., Shah, N.J., Lippert, T., Zilles, K., Evans, A.C., 2013. BigBrain: an ultrahigh-resolution 3D human brain model. Science 340, 1472–1475. https://doi.org/10.1126/science.1235381.

Baillet, S., 2017. Magnetoencephalography for brain electrophysiology and imaging. Nat. Neurosci. 20, 327–339. https://doi.org/10.1038/nn.4504.

Baillet, S., Mosher, J.C., Leahy, R.M., 2001. Electromagnetic brain mapping. IEEE Signal Process. Mag. 18, 14–30. https://doi.org/10.1109/79.962275.

Bastos, A.M., Vezoli, J., Bosman, C.A., Schoffelen, J.-M., Oostenveld, R., Dowdall, J.R., De Weerd, P., Kennedy, H., Fries, P., 2015. Visual areas exert feedforward and feedback influences through distinct frequency channels. Neuron 85, 390–401. https://doi.org/10.1016/j.neuron.2014.12.018.

Belardinelli, P., Ortiz, E., Barnes, G.R., Noppeney, U., Preissl, H., 2012. Source reconstruction accuracy of MEG and EEG Bayesian inversion approaches. PloS One 7, e51985. https://doi.org/10.1371/journal.pone.0051985.

Berg, P., Scherg, M., 1994. A multiple source approach to the correction of eye artifacts. Electroencephalogr. Clin. Neurophysiol. 90, 229–241. https://doi.org/10.1016/0013-4694(94)90094-9.

Bestmann, S., Walsh, V., 2017. Transcranial electrical stimulation. Curr. Biol. 27, R1258–R1262. https://doi.org/10.1016/J.CUB.2017.11.001.

Bestmann, S., Ward, N., 2017. Are current flow models for transcranial electrical stimulation fit for purpose? Brain Stimul. 10, 865–866. https://doi.org/10.1016/j.brs.2017.04.002.

Bok, S., 1929. Der Einfluss in den Furchen und Windungen auftretenden Krümmungen der Grosshirnrinde auf die Rindenarchitektur. Z. für Gesamte Neurol. Psychiatr. 121, 682–750.

Bonaiuto, J., Meyer, S.S., Little, S., Rossiter, H., Callaghan, M.F., Dick, F., Barnes, G.R., Bestmann, S., 2018a. Lamina-specific cortical dynamics in human visual and sensorimotor cortices. Elife 7, 226274. https://doi.org/10.7554/eLife.33977.

Bonaiuto, J., Rossiter, H.E., Meyer, S.S., Adams, N., Little, S., Callaghan, M.F., Dick, F., Bestmann, S., Barnes, G.R., 2018b. Non-invasive laminar inference with MEG: comparison of methods and source inversion algorithms. Neuroimage 167, 372–383. https://doi.org/10.1016/j.neuroimage.2017.11.068.

Boto, E., Holmes, N., Leggett, J., Roberts, G., Shah, V., Meyer, S.S., Muñoz, L.D., Mullinger, K.J., Tierney, T.M., Bestmann, S., Barnes, G.R., Bowtell, R., Brookes, M.J., 2018. Moving magnetoencephalography towards real-world applications with a wearable system. Nature 555, 657–661. https://doi.org/10.1038/nature26147.

Boto, E., Meyer, S.S., Shah, V., Alem, O., Knappe, S., Kruger, P., Fromhold, T.M., Lim, M., Glover, P.M., Morris, P.G., Bowtell, R., Barnes, G.R., Brookes, M.J., 2017. A new generation of magnetoencephalography: room temperature measurements using optically-pumped magnetometers. Neuroimage 149, 404–414. https://doi.org/10.1016/j.neuroimage.2017.01.034.

Buffalo, E.A., Fries, P., Landman, R., Buschman, T.J., Desimone, R., 2011. Laminar differences in gamma and alpha coherence in the ventral stream. Proc. Natl. Acad. Sci. U.S.A. 108, 11262–11267. https://doi.org/10.1073/pnas.1011284108.

Buzsáki, G., Anastassiou, C.A., Koch, C., 2012. The origin of extracellular fields and currents — EEG , ECoG. LFP and spikes 13, 407–420. https://doi.org/10.1038/nrn3241.

Callaghan, M.F., Josephs, O., Herbst, M., Zaitsev, M., Todd, N., Weiskopf, N., 2015. An evaluation of prospective motion correction (PMC) for high resolution quantitative MRI. Front. Neurosci. 9, 97. https://doi.org/10.3389/fnins.2015.00097.

Carey, D., Caprini, F., Allen, M., Lutti, A., Weiskopf, N., Rees, G., Callaghan, M.F., Dick, F., 2017. Quantitative MRI provides markers of intra-, inter-regional, and age-related differences in young adult cortical microstructure. bioRxiv. https://doi.org/10.1101/139568.

Dale, A.M., Fischl, B., Sereno, M.I., 1999. Cortical surface-based analysis: I. Segmentation and surface reconstruction. Neuroimage 9, 179–194. https://doi.org/10.1006/nimg.1998.0395.

Dale, A.M., Sereno, M.I., 1993. Improved localizadon of cortical activity by combining EEG and MEG with MRI cortical surface reconstruction: a linear approach. J. Cognit. Neurosci. 5, 162–176. https://doi.org/10.1162/jocn.1993.5.2.162.

Darvas, F., Pantazis, D., Kucukaltun-Yildirim, E., Leahy, R.M., 2004. Mapping human brain function with MEG and EEG: methods and validation. Neuroimage 23, S289–S299. https://doi.org/10.1016/J.NEUROIMAGE.2004.07.014.

Fischl, B., 2012. FreeSurfer. Neuroimage 62, 774–781. https://doi.org/10.1016/j.neuroimage.2012.01.021.

Fischl, B., Sereno, M.I., 2018. Microstructural parcellation of the human brain. Neuroimage 182, 219–231. https://doi.org/10.1016/J.NEUROIMAGE.2018.01.036.

Friston, K., Harrison, L., Daunizeau, J., Kiebel, S., Phillips, C., Trujillo-Barreto, N., Henson, R., Flandin, G., Mattout, J., 2008. Multiple sparse priors for the M/EEG inverse problem. Neuroimage 39, 1104–1120.

Friston, K., Mattout, J., Trujillo-Barreto, N., Ashburner, J., Penny, W., 2007. Variational free energy and the Laplace approximation. Neuroimage 34, 220–234. https://doi.org/10.1016/j.neuroimage.2006.08.035.

Fuchs, M., Wagner, M., Wischmann, H.-A., Ottenberg, K., Dössel, O., 1994. Possibilities of functional brain imaging using a combination of MEG and MRT. In: Oscillatory Event-Related Brain Dynamics. Springer US, Boston, MA, pp. 435–457. https://doi.org/10.1007/978-1-4899-1307-4_31.

Fukushima, M., Yamashita, O., Kanemura, A., Ishii, S., Kawato, M., Sato, M., 2012. A state-space modeling approach for localization of focal current sources from MEG. IEEE Trans. Biomed. Eng. 59, 1561–1571. https://doi.org/10.1109/TBME.2012.2189713.

Goldenholz, D.M., Ahlfors, S.P., Hämäläinen, M.S., Sharon, D., Ishitobi, M., Vaina, L.M., Stufflebeam, S.M., 2009. Mapping the signal-to-noise-ratios of cortical sources in

magnetoencephalography and electroencephalography. Hum. Brain Mapp. 30, 1077–1086. https://doi.org/10.1002/hbm.20571.
Gross, J., Baillet, S., Barnes, G.R., Henson, R.N., Hillebrand, A., Jensen, O., Jerbi, K., Litvak, V., Maess, B., Oostenveld, R., Parkkonen, L., Taylor, J.R., van Wassenhove, V., Wibral, M., Schoffelen, J.-M., 2013. Good practice for conducting and reporting MEG research. Neuroimage 65, 349–363. https://doi.org/10.1016/j.neuroimage.2012.10.001.
Haegens, S., Barczak, A., Musacchia, G., Lipton, M.L., Mehta, A.D., Lakatos, P., Schroeder, C.E., 2015. Laminar profile and physiology of the α rhythm in primary visual, auditory, and somatosensory regions of neocortex. J. Neurosci. 35.
Hämäläinen, M., Hari, R., 2002. Magnetoencephalographic (MEG) characterization of dynamic brain activation. In: Toga, A., Mazziotta, J. (Eds.), Brain Mapping: the Methods. Academic Press, Amsterdam, pp. 227–254.
Hämäläinen, M., Ilmoniemi, R., 1984. Interpreting measured magnetic fields of the brain: estimates of current distributions. Tech. rep, Helsinki Univ. Technol. TKK-F-A559.
Hämäläinen, M.S., Ilmoniemi, R.J., 1994. Interpreting magnetic fields of the brain: minimum norm estimates. Med. Biol. Eng. Comput. 32, 35–42. https://doi.org/10.1007/BF02512476.
Haufe, S., Tomioka, R., Dickhaus, T., Sannelli, C., Blankertz, B., Nolte, G., Müller, K.-R., 2011. Large-scale EEG/MEG source localization with spatial flexibility. Neuroimage 54, 851–859. https://doi.org/10.1016/J.NEUROIMAGE.2010.09.003.
Henson, R.N., Mattout, J., Phillips, C., Friston, K.K.J., 2009. Selecting forward models for MEG source-reconstruction using model-evidence. Neuroimage 46, 168–176. https://doi.org/10.1016/j.neuroimage.2009.01.062.
Hillebrand, A., Barnes, G.R., 2003. The use of anatomical constraints with MEG beamformers. Neuroimage 20, 2302–2313.
Hillebrand, A., Barnes, G.R., 2002. A quantitative assessment of the sensitivity of whole-head MEG to activity in the adult human cortex. Neuroimage 16, 638–650.
Holmes, N., Leggett, J., Boto, E., Roberts, G., Hill, R.M., Tierney, T.M., Shah, V., Barnes, G.R., Brookes, M.J., Bowtell, R., 2018. A bi-planar coil system for nulling background magnetic fields in scalp mounted magnetoencephalography. Neuroimage 181, 760–774. https://doi.org/10.1016/J.NEUROIMAGE.2018.07.028.
Iivanainen, J., Stenroos, M., Parkkonen, L., 2017. Measuring MEG closer to the brain: performance of on-scalp sensor arrays. Neuroimage 147, 542–553. https://doi.org/10.1016/J.NEUROIMAGE.2016.12.048.
Iivanainen, J., Zetter, R., Grön, M., Hakkarainen, K., Parkkonen, L., 2019. On-scalp MEG system utilizing an actively shielded array of optically-pumped magnetometers. Neuroimage 194, 244–258. https://doi.org/10.1016/J.NEUROIMAGE.2019.03.022.
Knappe, S., Sander, T., Trahms, L., 2014. Optically-pumped magnetometers for MEG. In: Magnetoencephalography. Springer Berlin Heidelberg, Berlin, Heidelberg, pp. 993–999. https://doi.org/10.1007/978-3-642-33045-2_49.
Laakso, I., Mikkonen, M., Koyama, S., Hirata, A., Tanaka, S., 2019. Can electric fields explain inter-individual variability in transcranial direct current stimulation of the motor cortex? Sci. Rep. 9, 626. https://doi.org/10.1038/s41598-018-37226-x.
Lin, F.-H., Belliveau, J.W., Dale, A.M., Hämäläinen, M.S., 2006. Distributed current estimates using cortical orientation constraints. Hum. Brain Mapp. 27, 1–13. https://doi.org/10.1002/hbm.20155.
Little, S., Bonaiuto, J., Barnes, G.R., Bestmann, S., 2018. Motor cortical beta transients delay movement initiation and track errors. bioRxiv 384370. https://doi.org/10.1101/384370.
López, J.D., Litvak, V., Espinosa, J.J., Friston, K., Barnes, G.R., 2014. Algorithmic procedures for Bayesian MEG/EEG source reconstruction in SPM. Neuroimage 84, 476–487. https://doi.org/10.1016/j.neuroimage.2013.09.002.
Lutti, A., Hutton, C., Finsterbusch, J., Helms, G., Weiskopf, N., 2010. Optimization and validation of methods for mapping of the radiofrequency transmit field at 3T. Magn. Reson. Med. 64, 229–238. https://doi.org/10.1002/mrm.22421.
Lutti, A., Stadler, J., Josephs, O., Windischberger, C., Speck, O., Bernarding, J., Hutton, C., Weiskopf, N., 2012. Robust and fast whole brain mapping of the RF transmit field B1 at 7T. PloS One 7, e32379. https://doi.org/10.1371/journal.pone.0032379.
Maier, A., Adams, G.K., Aura, C., Leopold, D.A., 2010. Distinct Superficial and deep laminar domains of activity in the visual cortex during rest and stimulation. Front. Syst. Neurosci. 4 https://doi.org/10.3389/fnsys.2010.00031.
Mattout, J., Henson, R.N., Friston, K.J., 2007. Canonical source reconstruction for MEG. Comput. Intell. Neurosci. 2007, 67613. https://doi.org/10.1155/2007/67613.
Mattout, J., Phillips, C., Penny, W.D., Rugg, M.D., Friston, K.J., 2006. MEG source localization under multiple constraints: an extended Bayesian framework. Neuroimage 30, 753–767. https://doi.org/10.1016/j.neuroimage.2005.10.037.
Meyer, S.S., Bonaiuto, J., Lim, M., Rossiter, H., Waters, S., Bradbury, D., Bestmann, S., Brookes, M., Callaghan, M.F., Weiskopf, N., Barnes, G.R., 2017. Flexible head-casts for high spatial precision MEG. J. Neurosci. Methods 276, 38–45. https://doi.org/10.1016/j.jneumeth.2016.11.009.
Murakami, S., Okada, Y., 2006. Contributions of principal neocortical neurons to magnetoencephalography and electroencephalography signals. J. Physiol. 575, 925–936. https://doi.org/10.1113/jphysiol.2006.105379.
Nolte, G., 2003. The magnetic lead field theorem in the quasi-static approximation and its use for magnetoenchephalography forward calculation in realistic volume conductors. Phys. Med. Biol. 48, 3637–3652. https://doi.org/10.1088/0031-9155/48/22/002.
Nunez, P., Srinivasan, R., 2006. Electric Fields of the Brain: the Neurophysics of EEG. Oxford University Press.
Okada, Y.C., Wu, J., Kyuhou, S., 1997. Genesis of MEG signals in a mammalian CNS structure. Electroencephalogr. Clin. Neurophysiol. 103, 474–485.
Penny, W.D., Stephan, K.E., Daunizeau, J., Rosa, M.J., Friston, K.J., Schofield, T.M., Leff, A.P., 2010. Comparing families of dynamic causal models. PLoS Comput. Biol. 6, e1000709 https://doi.org/10.1371/journal.pcbi.1000709.
Ross, B., Charron, R.E.M., Jamali, S., 2011. Realignment of magnetoencephalographic data for group Analysis in the sensor domain. J. Clin. Neurophysiol. 28, 190–201. https://doi.org/10.1097/WNP.0b013e3182121843.
Salmelin, R., Hämäläinen, M., Kajola, M., Hari, R., 1995. Functional segregation of movement-related rhythmic activity in the human brain. Neuroimage 2, 237–243.
Seo, H., Jun, S.C., 2019. Relation between the electric field and activation of cortical neurons in transcranial electrical stimulation. Brain Stimul 12, 275–289. https://doi.org/10.1016/J.BRS.2018.11.004.
Singh, K.D., Holliday, I.E., Furlong, P.L., Harding, G.F.A., 1997. Evaluation of MRI-MEG/EEG co-registration strategies using Monte Carlo simulation. Electroencephalogr. Clin. Neurophysiol. 102, 81–85. https://doi.org/10.1016/S0921-884X(96)96570-4.
Spaak, E., Bonnefond, M., Maier, A., Leopold, D.A., Jensen, O., 2012. Layer-specific entrainment of γ-band neural activity by the α rhythm in monkey visual cortex. Curr. Biol. CB 22, 2313–2318. https://doi.org/10.1016/j.cub.2012.10.020.
Stolk, A., Todorovic, A., Schoffelen, J.-M., Oostenveld, R., 2013. Online and offline tools for head movement compensation in MEG. Neuroimage 68, 39–48. https://doi.org/10.1016/J.NEUROIMAGE.2012.11.047.
Troebinger, L., López, J.D., Lutti, A., Bestmann, S., Barnes, G.R., 2014a. Discrimination of cortical laminae using MEG. Neuroimage 102, 885–893. https://doi.org/10.1016/j.neuroimage.2014.07.015.
Troebinger, L., López, J.D., Lutti, A., Bradbury, D., Bestmann, S., Barnes, G.R., 2014b. High precision anatomy for MEG. Neuroimage 86, 583–591. https://doi.org/10.1016/j.neuroimage.2013.07.065.
van Kerkoerle, T., Self, M.W., Dagnino, B., Gariel-Mathis, M.-A., Poort, J., van der Togt, C., Roelfsema, P.R., 2014. Alpha and gamma oscillations characterize feedback and feedforward processing in monkey visual cortex. Proc. Natl. Acad. Sci. U.S.A. 111, 14332–14341. https://doi.org/10.1073/pnas.1402773111.
Waehnert, M.D., Dinse, J., Weiss, M., Streicher, M.N., Waehnert, P., Geyer, S., Turner, R., Bazin, P.-L., 2014. Anatomically motivated modeling of cortical laminae. Neuroimage 93, 210–220.
Wager, T.D., Keller, M.C., Lacey, S.C., Jonides, J., 2005. Increased sensitivity in neuroimaging analyses using robust regression. Neuroimage 26, 99–113. https://doi.org/10.1016/J.NEUROIMAGE.2005.01.011.
Wagstyl, K., Lepage, C., Bludau, S., Zilles, K., Fletcher, P.C., Amunts, K., Evans, A.C., 2018. Mapping cortical laminar structure in the 3D BigBrain. Cerebr. Cortex 28, 2551–2562. https://doi.org/10.1093/cercor/bhy074.
Weiskopf, N., Suckling, J., Williams, G., Correia, M.M., Inkster, B., Tait, R., Ooi, C., Bullmore, E.T., Lutti, A., 2013. Quantitative multi-parameter mapping of R1, PD(*), MT, and R2(*) at 3T: a multi-center validation. Front. Neurosci. 7, 95. https://doi.org/10.3389/fnins.2013.00095.
Whalen, C., Maclin, E.L., Fabiani, M., Gratton, G., 2008. Validation of a method for coregistering scalp recording locations with 3D structural MR images. Hum. Brain Mapp. 29, 1288–1301. https://doi.org/10.1002/hbm.20465.
Wipf, D., Nagarajan, S., 2009. A unified Bayesian framework for MEG/EEG source imaging. Neuroimage 44, 947–966. https://doi.org/10.1016/J.NEUROIMAGE.2008.02.059.